12-2011

Temporal Pier Scour Evolution under Stepped Hydrographs

Mark Schillinger
Clemson University, markschillinger@yahoo.com

TEMPORAL PIER SCOUR EVOLUTION UNDER STEPPED HYDROGRAPHS

A Thesis
Presented to
the Graduate School of
Clemson University

In Partial Fulfillment
of the Requirements for the Degree
Master of Science
Civil Engineering

---

by
Mark W. Schillinger
December 2011

Accepted by:
Dr. Abdul A. Khan, Committee Chair
Dr. Nadim M. Aziz
Dr. Firat Y. Testik

ABSTRACT

The present study was aimed at measuring the scour hole profile at bridge piers under clear water scour. Scour tests were performed under both steady state flow and under stepped hydrographs. Multiple smaller flood events were run to determine how flood history affects scour hole development. Various equilibrium scour depth equations and proposed temporal scour models were compared. The similarity of the scour hole profiles with time and flow history were evaluated.

Experiments were conducted in a 14.8 m long, 1.19 m wide, 1.22 m deep rectangular flume with a model bridge pier. A uniform sediment bed (d_{50}= 1.5 mm) was used throughout the study. Scour hole profiles were measured using a light sensor. Three steady state flow experiments with a constant flow depth and different bed shear stresses and velocities were run. These three flow conditions were later used to model eight unique stepped hydrographs.

The order of flood events was found not to effect the scour depth or scour hole shape. The scour hole maintained the same non-dimensional, longitudinal similarity regardless of flow history or time for both steady and unsteady flows. This finding indicated steady state scour evolution models can be used to model scour under stepped hydrographs.

Several equilibrium scour depth equations were evaluated and it was found the CSU equation (FHWA, 2001) was just as accurate as several proposed temporal scour models.

Best-fit power and logarithmic temporal scour depth equations were obtained from each steady state test. These equations along with models proposed by Melville and Chiew (1999) and Chang et al. (2004) were found to predict steady state temporal scour evolution with reasonable accuracy.

Using the method of superposition, these methods were used to predict scour depths under stepped hydrographs. For stepped hydrographs, the scour development for each event (or each step) followed the temporal scour evolution under steady flow conditions. It was found that the order and frequency of events did not change the scour development pattern. It was determined that the power and logarithmic function accurately predicted final scour depths (± 10% and ± 12%, respectively) and temporal scour evolution. The models proposed by Melville and Chiew (1999) and Chang et al. (2004) were found to provide no greater accuracy in predicting final scour depths than the CSU equation (FHWA, 2001). More research is needed on temporal scour evolution under steady flow conditions in order to predict scour during floods.

DEDICATION

This thesis is dedicated to my parents who have both supported me tremendously throughout my education and life. To my father Dr. William who instilled with me a great work ethic, was instrumental in me pursuing engineering and science, and was always able to give extremely useful advice throughout my research. I would also like to thank my mother Valerie for her always encouraging words and for making our arduous winter drive across the country fun and memorable.

ACKNOWLEDGMENTS

The work presented here was conducted at Clemson Hydraulics Laboratory and could have only been achieved through the collaborative effort of many individuals. I would like to foremost thank my advisor Dr. Khan who gave me the opportunity to pursue my graduate education at Clemson, suggested the topic of temporal scour evolution at piers, was a great source of research advice, and allowed me to continue my interest in physical hydraulic modeling.

I would also like to thank Danny Metz and John Cox for their tremendous support in modifications and maintenance of the laboratory and equipment and Warren Scovil for his technical advice and help on all things electrical. A special thanks also is made to Chris Shivar who worked with me moving hundred pound bags of sand in the blistering summer heat; a task that was grueling but greatly appreciated.

I would finally like to acknowledge the many friends, my girlfriend Estefanía Balda Alvarez, and my classmates I have met during my time at Clemson. They have been instrumental in making my time here enjoyable and worthwhile.

TABLE OF CONTENTS

Table of Contents (Continued)..... Page

LIST OF TABLES

LIST OF FIGURES

List of Figures (Continued)

List of Figures (Continued)

Figure Page

List of Figures (Continued)

Figure Page

CHAPTER 1

INTRODUCTION

Bridges are important means of providing passage of goods and people. Of the nearly 600,000 public bridges in the United States approximately 484,500 are over waterways (Gee, 2003). Failure of these vital structures can cause death, injury, and severe economic hardship on local communities due to high cost of replacement or repairs and increased travel times. The 2007 collapse of a bridge on I-35W in Minnesota alone took the lives of 13, injured 245, and was very costly. The Minnesota Department of Transportation spent $234 million to replace this bridge and estimated that the state's economy lost $60 million in road-user costs during this time (MnDOT, 2008).

Scour, which is the water-induced erosion of the streambed or bank material, is by far the most common cause of bridge failure in the United States. Adverse hydraulic conditions accounted for 58% of the 1502 reported bridge failures from 1966 to 2005 (NCHRP, 2009). Scour related failures include the collapse of 73 bridges in 1995 in Virginia, West Virginia, and southwest Pennsylvania; 17 bridges in New York and New England during the spring of 1987; the US 51 bridge in Tennessee that took eight lives in 1989; and the twin I-5 bridges over the Arroyo Pasejero that killed seven people in 1995 (Morris and Pagan-Ortiz, 1997). From 1980 to 1990, 11 bridges in New York failed because of scour. Estimates show that more than 5 times as much was lost by local business and industry in indirect costs than paid out through highway repair contracts (Rhodes and Trent, 1993).

Due to the high cost associated with scour related bridge failures and the civil engineer's ethical code to "hold paramount the safety, health and welfare of the public," it is imperative to accurately predict scour at bridge piers and abutments (ASCE Ethical Code, 2006). Scouring at bridge piers and abutments is a highly complex process. The flow field near these structures is highly turbulent and unsteady vortices form near the erodible bed and on the water surface. Inherently, accurate modeling of such site-specific, time-dependent processes is a challenging task.

The Federal Highway Administration (FHWA) recommends using a single event design flood such as a 100-year or 500-year storm to calculate maximum expected scour depth. Most laboratory research has been conducted under steady flow states where there is no initial scour near the pier. The tests are then run until the scour depth reaches an equilibrium state. This equilibrium scour depth is then taken as the maximum expected scour depth for a given structure. These tests are based on the assumption that peak design flow lasts an infinitely long period of time until maximum scour is developed (Totapally, 1998). During natural floods this is an unrealistic assumption as peak flow may persist only for a fraction of the total event time. Thus it is imperative to find how scour evolves during unsteady flow events to make more accurate scour depth predictions. In addition, the effects of flood order and frequency on the scour evolution need to be quantified. Current scour equations often over predict maximum scour depths in the field (Johnson, 1995) and currently there is no unifying theory of pier scour that

allows the designer to have high confidence in scour depth predictions (Raudkivi and Ettema, 1983).

In this study, a physical model is used to investigate the temporal variation of clear water scour at a circular pier for uniform, non-cohesive sediment. Steady state tests are conducted for different bed shear stresses and flow velocities. Equilibrium scour depths are recorded upstream of the pier during these tests. Simulated hydrographs, based upon the steady state events, are then used to create unsteady flow in the flume. The specific objectives of this study are:

(1) Verify if current single-event design methodologies recommended by the FHWA are the best model to predict scour at bridge piers.

(2) Determine how flood history impacts scour hole development.

(3) Determine how the order of flood events affect scour hole geometry shape (i.e. 10 yr. flood before 50 yr. or 50 yr. before 10 yr.).

(4) Compare multiple temporal scour evolution models under steady flow and stepped hydrographs.

CHAPTER 2

LITERATURE REVIEW

Local clear water scour at bridge piers and abutments occurs due to interaction of flow with the pier or abutment. The flow interaction with the pier causes a downflow due to a downward pressure gradient (Melville, 1975). This downward impinging jet erodes the sediment at the base of the structure forming a scour hole which in turn causes horseshoe vortices to develop (Melville, 1975). The flow field near these structures can become highly turbulent and unsteady vortices will form near the erodible bed and on the water surface. The size of the scour hole will depend on the strength of these vortices and the bed material properties. The rate of scour under steady flow conditions will be highest initially then decrease in a manner best described by a power or logarithmic equation (Totapally, 1998). The scouring process will continue until the vortices are not strong enough to remove sediment from the scour hole.

Types of Scour

Scour at bridges is generally classified into three categories: general scour (which includes contraction scour), long-term aggradation or degradation, and localized scour (FHWA, 2001). General scour includes erosion due to a contraction of a channel or other flow conditions such as scour that occurs on the outside of a river bend. This scour may be uniform or non-uniform across the channel width depending on local flow and sediment conditions.

Long-term aggradation and degradation of a riverbed can be caused by man-made or natural processes. Aggradation in a river reach will occur when the sediment load is higher than the transport capacity. This deposition can be caused by either human changes in the river or natural processes such as upstream river bank erosion. Degradation is the lowering or erosion of the riverbed and occurs when the sediment load is less than the transport capacity (for example, downstream of a dam).

Local scour, which is a highly turbulent, three-dimensional process, consists of erosion near man-made structures including abutments, bridge piers, spur dikes, and other flow obstructions. When a structure such as a bridge pier is placed within a channel, local velocities increase due to a reduction in flow area. In addition, an impinging downward jet causes a horseshoe vortex to develop at the upstream base of the structure and erodes the bed material. As this material is lifted off the bed it is transported downstream by the main flow (Totapally, 1998). A significant amount of this material is often found immediately downstream of piers resulting in sediment deposition downstream of the structure. The scour process is further complicated by smaller vortices that occur at the wake of the structure. These vortices are quasi-periodical and along with accelerated side flow cause wake scour (Dargahi, 1990). The primary interest in this research are the processes associated with local scour so further review will only discuss this type of scour. The horseshoe and wake vortices around a cylindrical pier are shown below in Figure 2.1.

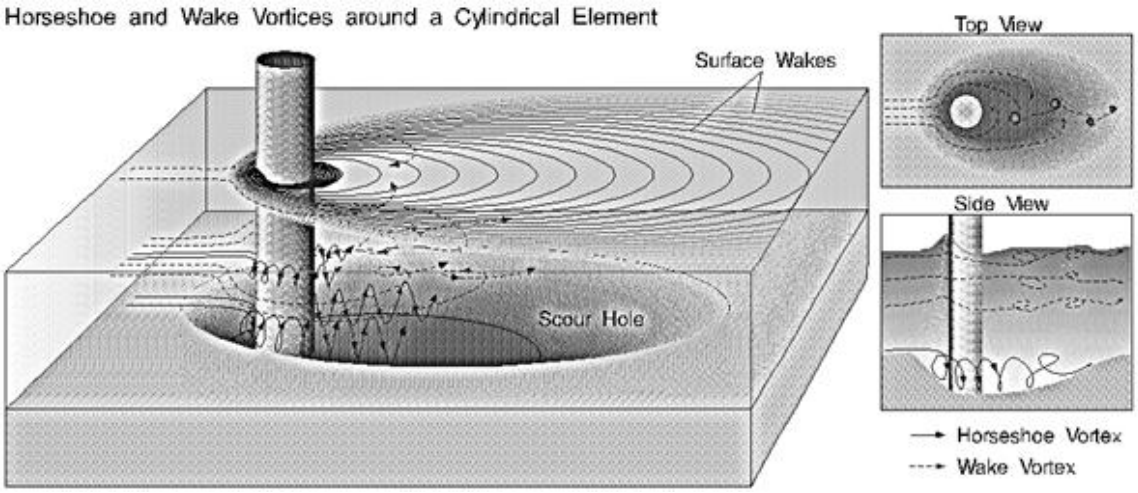

Figure 2.1: Horseshoe and Wake Vortices around a Cylindrical Element (USGS, 2011)

Classification of Local Scour

Local scour is classified depending on whether flow is loaded with sediment immediately upstream of the structure of interest. When the approach flow is continually carrying sediment into the scour hole, i.e. when the flow velocity exceeds a critical velocity for the sediment bed ($V > V_c$) over the whole river reach, the resultant erosion at a bridge pier or abutment is classified as live bed scour. Clear water scour occurs when no sediment transport is occurring in the channel, i.e., $V \leq V_c$. The maximum clear water local scour depth occurs when the flow velocity equals that of the sediment's critical velocity (Melville and Chiew, 1999).

The scour evolution for live bed and clear water scour are different as shown in Figure 2.2. During live bed scour, maximum scour depth is quickly reached due to high flow velocities and fluctuates periodically around an average depth (Melville, 1984). This

fluctuation corresponds to the bed forms migration within the scour hole. During clear water conditions, the scour depth increases until the vortices are not strong enough to remove bed material from the hole. Equilibrium scour depth can take days to develop during clear water conditions. Franzetti et al. (1989) found that it occurred after 100 hours of testing on piers, while Ballio (2000) conducted testing on abutments for several hundred hours without an equilibrium state being reached. It was concluded that the time scales for equilibrium scour are generally much greater for abutments then piers (Ballio, 2000). Designs based on predicted equilibrium scour depths can be over conservative as peak flows may only last a few hours not days during a natural flood (Melville and Chiew, 1999). Since this research is focused on processes related with clear water scour, only variables associated with clear water scour will be discussed further.

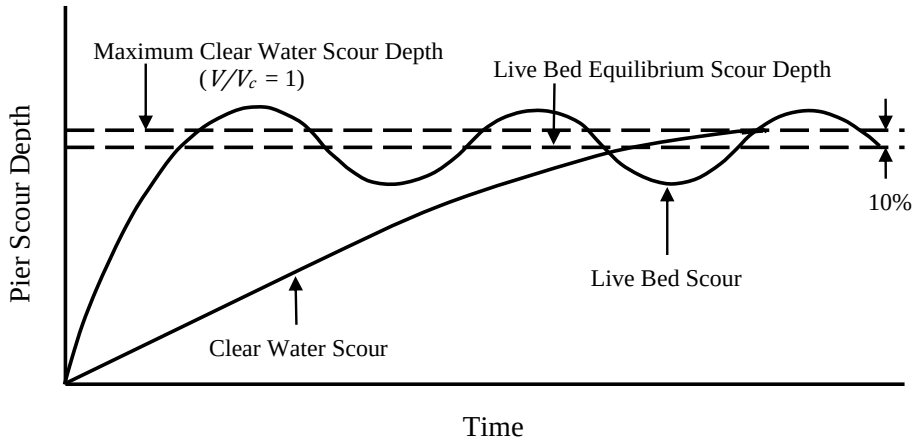

Figure 2.2: Comparison of Clear Water and Live Bed Scour as a Function of Time (after Raudkivi and Ettema, 1983)

Variables Affecting Clear Water Scour

Many factors affect scour hole development which are generally broken down into four different categories: approach flow, structural geometry and alignment, time variation of flow, and sediment characteristics. Many researchers have typically studied these variables in laboratory settings by varying the selected parameters of interest. The following sections will discuss the various research that has been conducted on the key parameters that affect scour hole development at piers.

The hydraulic and fluid properties that affect scour include the flow velocity, flow depth, bed shear stress, fluid viscosity, and density. Since testing was conducted in fresh water at roughly room temperatures, fluid properties such as the viscosity and density were not considered as variables. It is usually assumed that the fluid viscosity has minimal effect on scour development (Simmaro, 2007) and the fluid density is incorporated into dimensionless parameters such as the critical shear stress of the bed material, which is discussed later. In general, as the fluid density is increased scour depths will increase as well.

Flow Velocity and Velocity Based Dimensionless Parameters for Steady Flows

Numerous researchers have studied scour under steady flows and only relatively recently have researchers started studying the effect of unsteady flow on scour development (Kothyari et al. 1992; Totapally 1998; Chang et al. 2004, Lu et al. 2011). Due to the

relatively small amount of research on scour under unsteady flow conditions, the majority of the following literature review will be on research under steady flow unless noted otherwise. However, since flood events are unsteady in nature the importance of unsteady flow cannot be ignored during the scour process. Flow velocity is related to discharge, flow depth, and the channel width in rectangular channels, which was used to conduct this research. For a constant discharge and channel width as the depth decreases the velocity will increase. Velocity for a rectangular channel is calculated from the continuity equation below:

$$Q = VBh \tag{2.1}$$

Where Q is the flow discharge, V is the mean flow velocity, B is the channel width, and h is the flow depth. If the flow depth and other parameters remain constant any increases in flow velocity will generally result in increased scour depth. This is due to the fact that as the approach flow velocity increases the strength of vortices will increase, which in turn lead to greater scour depths.

Most researchers have incorporated the effect of flow velocity by using dimensionless numbers such as the Froude number, Fr, densimetric Froude number, $Fr_{d,}$,and/or critical shear velocity, u_{*c} as scaling parameters. The Froude number is the ratio of a fluid's characteristic velocity to a shallow water wave velocity or more simply the ratio of inertial to gravitational forces, and is expressed as $V/\sqrt{gh}$ for a rectangular channel, where g is gravitational acceleration. Garde et al. (1961), Zaghloul (1975, 1983), Rajartanam and Nwachkwu (1983), Froehlich (1989) have included the Froude number

as a scaling parameter to evaluate scour. It should be noted that Garde et al. (1961) found that it was not necessary to distinguish between clear water and live bed scour when the Froude number was used as a scaling parameter.

Based on the analysis of the field data, Johnson (1995) determined that the Froude number had very little correlation with scour depth and other parameters might be of more use in predicting scour depth in the field. Another study conducted by Mueller (1996) using United States Geological Survey (USGS) data found that the empirical methods, such as Froude number based Colorado State University (CSU) equation, over-predicted scour depths the majority of the time. Due to scour depth over-predictions by the majority of these empirical methods, there has been a general trend in finding other methods to predict scour depths with greater accuracy.

Many researchers have started to study the correlation between scour depth and the densimetric Froude number, $Fr_{d,}$ defined as:

$$Fr_d = \frac{V}{\sqrt{g'h}} \tag{2.2}$$

Where g' is the reduced gravitational acceleration calculated as:

$$g' = \big((\rho_s - \rho)/\rho\big)g = (SG_s - 1)g \tag{2.3}$$

Where SG_s is the specific gravity of sediment (approximately 2.65 for quartz sand, used in this study), ρ is the density of water, and ρ_s is the sediment density. Kohli and Hager

(2001) conducted laboratory research on vertical wall abutments in floodplains and found the densimetric Froude number had a significant effect on scour depths.

A study by Oliveto and Hager (2002) conducted about 200 laboratory experiments on clear water scour in bridge piers and abutments. They used six different types of sediment with varying uniformities and sediment specific gravity ranging from 1.42 to 2.65. Approach flow depths, velocities, and pier sizes were also systematically varied. It was concluded that the densimetric mixture Froude number, Fr_{dm} was one of three key parameters affecting temporal scour evolution. The densimetric mixture Froude number was calculated as $Fr_{dm} = Fr_d(\sigma_g)^{-1/3}$, where σ_g is the sediment gradation coefficient.

One of the most important and common parameters in analyzing scour is the shear velocity and shear stress ratios. It is a fundamental component of the scouring process with clear water and live bed scour classified based on these ratios. Shear velocity u_* is calculated as: $u_* = (\tau_o/\rho)^{0.5}$, where τ_o is the bed shear stress. The bed shear stress is calculated as: $\tau_o = \rho g R S_f$, where R is the hydraulic radius of the channel and S_f is the friction slope. Due to the difficulties in directly measuring shear stress, although it has been done, shear stress is typically calculated from measured velocity profiles.

The time averaged velocity is commonly related to the shear velocity through the following equation:

$$\frac{u(z)}{u_*} = \frac{1}{k} ln\left(\frac{z}{z_o}\right) \tag{2.4}$$

Where the variables are defined as follows:

$u(z)$ is the time averaged velocity in the direction of primary flow at a height z above the bed

k is the von Karman constant

z_o is the characteristic roughness

Nezu and Rodi (1986) conducted open channel flow experiments and found that this equation should only be used within the near-wall region, outside of this region the velocity profile deviated from the log law. They found that using a mean value 0.412 for the von Karman constant yielded shear velocities similar to those calculated from the Reynolds stress distribution. An empirical wake function, $w(\varepsilon)$, originally introduced by Coles (1956) was used to account for deviations from the log law.

The shear stress or shear velocity are usually divided by a critical shear stress (τ_{oc}) or critical shear velocity (u_{*c}), respectively, obtaining a common dimensionless parameter to evaluate sediment transport or scour. The critical shear stress and critical velocity correspond to the initiation of sediment transport. As flow velocity increases the depth of scour increases as well; reaching a maximum at approximately $V = V_c$. A common graphical method for finding the critical shear stress for given flow and sediment conditions is the use of the Shields diagram. The Shields diagram relates the critical shear

stress as a function of the shear velocity, sediment size, sediment and fluid densities, kinematic viscosity, and gravitational acceleration. The Shields function for water is expressed as:

$$\tau_{oc}\left(\rho g d(SG_s - 1)\right)^{0.5} = f\left(\frac{u_* d}{\upsilon}\right) \tag{2.8}$$

Where d is the sediment size, however due to sediment nonuniformity in natural rivers, the median sediment size d_{50} is often used as the representative particle size, and υ is the kinematic viscosity of the fluid.

The critical shear stress for sediment transport initiation cannot be found directly from the Shields diagram. Various researchers have proposed explicit equations including Melville (1997), Hager and Oliveto (2002), and Cao et al. (2006) to predict incipient motion. Melville (1997) proposed a simplified method for estimating critical shear velocity (m/s) for quartz sediments at 20°C as just a function of sediment size in millimeters. The explicit equations are given below:

for $0.1\ mm < d < 1\ mm$ $\qquad u_{*c} = 0.0115 + 0.0125 d^{1.4}$ (2.9)

for $1\ mm < d < 100\ mm$ $\qquad u_{*c} = 0.0305 d^{0.5} - 0.0065 d^{-1}$ (2.10)

Hager and Del Guidice (2000) estimated shear stress in a more generalized way then Melville (1997) by not limiting the equation to just quartz sand at a specific temperature. Their research incorporated a dimensionless grain size (d_*) and dimensionless critical shear stress (τ_{*c}), defined as:

$$d_* = d_{50}\,(g'/v^2)^{1/3}. \tag{2.11}$$

for $10 < d_* < 150$ $$\tau_{*c} = 0.026 d_*^{1/6} \tag{2.12}$$

for $d_* \geq 150$ $$\tau_{*c} = 0.060 \tag{2.13}$$

$$\tau_{*c} = \tau_{50}/((\rho_s - \rho) g d_{50} \tag{2.14}$$

τ_{50} is the calculated critical shear stress for the median sediment size (d_{50}).

This method was chosen to determine critical shear velocity and results were similar to those calculated using Melville's (1997) approach. The results are shown for both Hager and Del Guidice (2000) and Melville's (1997) methods for the sediment in Table 2.1.

Table 2.1: Critical Shear Velocity Calculations

d_{50} mm	$u_{*c}^{(1)}$ (m/s)	$u_{*c}^{(2)}$ (m/s)	$u_{*c}^{(1)}/u_{*c}^{(2)}$
1.5	0.0342	0.0331	103.3%

Notes:
1) Hager and Del Giudice (2000) Method for 22°C fresh water
2) Melville (1997) Method

Flow Depth

For a constant flow velocity, when the depth is increased, the flow rate will increase as well. This will result in a greater scour depth. However, scour depths eventually become independent of increases in flow depth/discharge. Raudkivi and Ettema (1983) found that as the ratio of flow depth (h) to pier width (b) increased, d_{se}/b increased as well but

eventually became independent of the flow depth for h/b ratio of greater than 3. Other laboratory based research suggest that this ratio may be closer to 2.4 (Melville and Sutherland, 1988) but has been found to be much lower for wide (prototype) piers. Jones and Sheppard (2000) found this ratio to be around 2.

Flow depth has been found to effect the diameter of the vortex, D_v, at circular piers, which is important to the initiation of scour. As flow depth increases, the primary (horseshoe) vortex increases in diameter as well. The increase in vortex area leads to a decrease in shear stress at the front of the pier (Hjorth 1975; Melville, 1975), reducing the rate at which scour depth increases. Kothyari et al. (1992) proposed the following equation to estimate vortex diameter as a function of pier diameter and flow depth. The equation could be assumed to be valid for piers in wide channels and was based on his experiments and data from Baker (1979), Qadar (1980), and Muzzamil et al. (1989).

$$D_v = 0.28h(b/h)^{0.85} \qquad (2.15)$$

Structural Alignment and Geometry

Structural geometry and alignment relative to the flow path are important parameters in predicting scour depths. The angle of attack, α, of the approach flow (as shown in Figure 2.3) is usually incorporated into scour depth equations as an empirically based coefficient, such as the Colorado State University (CSU) equation's coefficient K_2. Laursen and Toch (1956) found that as the angle of attack changed from zero, the

location of greatest scour changed as well, moving from the front upstream end of the pier to the area exposed to the approach flow.

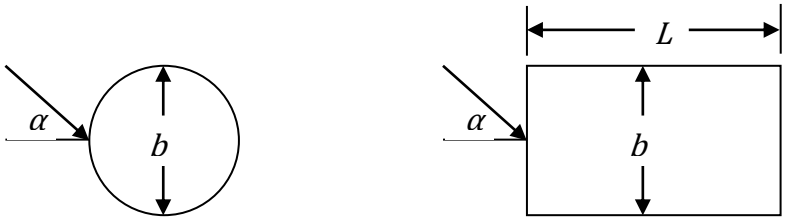

Figure 2.3: Circular and Rectangular Pier Geometry

In the CSU equation (FHWA, 2001), K_2 is defined as follows:

$$K_2 = (cos\alpha + (L/b)sin\alpha)^{0.65} \tag{2.16}$$

The effect of pier geometry is generally incorporated as another empirically based coefficient. Conceptually it is apparent that a square nosed pier, as shown in Figure 2.3, will have more resistance to flow due to increased form drag then a more streamlined structure such as a circular pier, resulting in a greater scour depth. The importance of pier geometry in relation to scour depths has been extensively studied and incorporated into equations by Breusers (1977) using Laursen and Toch's (1956) data and in the HEC-18 recommended CSU equation (FHWA, 2001). The factor K_1 in the CSU equation incorporates the shape of the pier nose and values of 1.1, 1.0, 1.0, and 0.9 are used for square nosed, round nosed, circular cylinder, and sharp nosed piers, respectively. Laursen and Toch (1956) found that the scour decreased as the body became more streamlined

and proposed different empirical coefficients. Since testing in this study was conducted using a circular pier, the shape factor can be taken as 1.

Time Variation of Flow

Until recently scour research has focused on studying the equilibrium scour depths that occur under steady flow in laboratory conditions. The Federal Highway Administration (FHWA) currently recommends using single event storms to estimate scour depths for design of bridge piers and abutments. During natural floods, peak flow may persist only for a fraction of the total event time. The determination of the equilibrium scour depth for the peak discharge during design flood is inherently flawed. Equilibrium scour depth can take days to develop during clear water conditions. Franzetti et al. (1989) found it occurred after 100 hours of testing on piers while Ballio (2000) conducted testing on abutments for several hundred hours without an equilibrium state being reached. It was concluded that the time scales for equilibrium scour are generally much greater for abutments then piers (Ballio, 2000). Since equilibrium scour depths can take days to develop and the majority of scour occurs in a short period of time, scour in laboratory tests is assumed to have reached equilibrium condition when changes in scour depth become minimal.

Designs based on equilibrium scour depths can be overly conservative as peak flows may only last a few hours not days during a natural flood (Melville and Chiew, 1999). These assumptions can lead to inaccurate scour predictions and currently there is no unifying

theory of pier scour that allows the designer to have much confidence in scour depth predictions (Raudkivi and Ettema, 1983). A study by Shatanawi et al. (2008) on abutment scour in South Carolina rivers found that at some sites the observed scour depth was greater than 100-year scour depth prediction. However, at these sites there was no evidence of a 100-year flood episode after the bridge was built. Shatanawi et al. (2008) showed that repeated occurrences of smaller frequency floods might cause scour that was greater than the 100-year return periods prediction.

Laboratory experiments conducted by Totapally (1998) on abutment scour, under varying hydrographs and flow conditions found that the rate of scour could best be described as a logarithmic equation. The correlation coefficient of the logarithmic equation was greater than that of a power equation to predict temporal scour depth. The correlation coefficient ranged from 0.94 to 0.99 compared to 0.92 to 0.98 for logarithmic and power equations, respectively. The use of the logarithmic function to describe the temporal evolution of scour is not uniformly agreed upon by hydraulic researchers. Breusers (1967) and Cunha (1975) both used power laws to describe this process.

The rate of scour under steady flow conditions was found to be highest initially then decreased in a logarithmic manner until the vortices were not strong enough to remove sediment from the scour hole. Melville and Chiew (1999) found that in just 10% of the equilibrium time (time it takes to reach equilibrium scour depth) 50% to 80% of the scour depth had occurred. Since equilibrium scour can take days or weeks to develop, this is

still a significant amount of time. Research conducted by Rouse (1965), Gill (1972), Dargahi (1990) and Oliveto and Hager (2002), among others, have also found scour depth to vary as a logarithmic function.

Totapally (1998) used the method of superposition for the stepwise hydrographs to mimic unsteady flows to calculate abutment scour depths. Varying levels of success was achieved in predicting the scour evolution during unsteady flows. Logarithmic equations were fitted to the steady state scour evolution data and were used to calculate scour under unsteady hydrographs. Totapally (1998) did not formulate a generalized equation to predict the equilibrium scour depth or the temporal scour evolution under steady state flow. It was found that scour holes were geometrically similar throughout scour hole development. Totapally (1998) approximated unsteady flow as a series of steady flows, which is common in scour research due to the inherent difficulties in replicating unsteady flow in a laboratory. This method is preferable since natural floods may take days to reach peak discharge and constant measurements and experimental adjustments would be needed to accurately replicate natural hydrographs. Totapally (1998) used method of superposition to predict scour evolution under unsteady flows (described in Chapter 5). This method was essentially the same as that proposed by Kothyari et al. (1992) for pier scour under unsteady flows.

Chang et al. (2004) conducted pier scour experiments using stepwise hydrographs. It was observed that scour depths steadily increased during the rising limb of the hydrograph

and changed minimally during the lag period. The research used empirical based equations from their own data and that of Ettema (1980) and Kothyari (1989) to calculate equilibrium scour depths and predict the unsteady and steady state temporal evolution of scour. The technique employed to predict scour under unsteady flows was similar to that proposed by Kothyari et al. (1992). Lu et. al (2011) conducted experiments to observe scour for non-uniform piers (piers with foundations) under unsteady flow. In order to predict the temporal evolution of scour under unsteady flows, the method of superposition, as discussed above, was used.

The procedure adopted by Chang et al. (2004) to determine the temporal evolution of scour for uniform sediments under steady state flow conditions is presented below:

(1) Calculate critical velocity, V_c , using the following equation from Chiew (1995), if the critical velocity is not known from direct measurements:

$$V_c/u_{*c} = 5.75\log(h/2d_{50}) + 6 \tag{2.17}$$

(2) Determine the equilibrium scour depth, d_{se}, as follows:

$$for\ 0.3 \leq V/V_c \leq 1 \qquad d_{se}/b = K_d K_h[3.77(V/V_c) - 1.13] \tag{2.18}$$

Where K_d and K_h are adjustment factors for the sediment size and flow depth effects on d_{se}, respectively. Based on the authors' criteria, the sediment was fine relative to the pier diameter ($b/d_{50} \geq 50$) and the flow depth was large relative to the pier diameter ($h/b \geq 3$). Thus both K_d and K_h can be taken as 1.

(3) A dimensionless time, T_c , corresponding to a very small initial time period, where the scour rate is assumed to be constant, is calculated as follows:

$$T_c = \{(d_{se}/b)/(0.35K_v) - 0.31\}^{-3.33} \quad (2.19)$$

Where K_v $(= V/V_c - 0.4)$ is an adjustment factor that accounts for the flow intensity.

(4) The time to reach equilibrium scour, t_e , is calculated in days using a modified equation originally from Melville and Chiew (1999):

$$t_e = A\left(\frac{b}{V}\right)K_v\left(\frac{d_{se}}{b}\right)^k\left(\frac{h}{b}\right)^m \quad (2.20)$$

Where A, m, and k are coefficients from Melville and Chiew (1999) dependent on sediment size, pier diameter, and the flow depth. The velocity, V, needs to be in units consistent with the pier diameter and in seconds.

(5) The scour depth at various dimensionless times, T $(= t/t_e$) is then calculated using the three following equations:

for $0 \leq T \leq T_c$ $$\frac{d_s}{b} = 0.08K_v{T_c}^{-1.3}T \quad (2.21)$$

for $T_c \leq T \leq 0.04$ $$\frac{d_s}{b} = \frac{d_{se}}{b} - 0.27K_v(T^{-0.3} + 0.41) \quad (2.22)$$

for $0.04 \leq T \leq 1$ $$\frac{d_s}{b} = \frac{d_{se}}{b} - 1.1K_v(T - 2.22T^{0.45} + 1.22) \quad (2.23)$$

Kothyari et al. (1992) introduced an algorithm to predict temporal pier scour depths under steady and unsteady clear water flows for uniform, non-uniform, and stratified sediments. Only the uniform sediment algorithm will be discussed further. For a steady flow, the time for a single sediment particle to be removed from the scour hole, t_*, is calculated using the shear velocity at that time, $u_{*,t}$, and the average probability of particle

movement, $p_{o,t}$, based on relationships developed by Paintal (1971). The scour depth at the new time increment is then considered to be the previous scour depth plus the size of a sediment particle. This process is repeated until the calculated shear stress at the pier nose, $\tau_{p,t}$, is lower than the critical shear stress of the bed. At this time, the algorithm is stopped and the current depth and time are considered to be equilibrium depth and time. The calculation procedure for the method proposed by Kothyari et al. (1992) for temporal scour evolution for steady flows with uniform sediment is presented below.

(1) Calculate the initial primary vortex diameter using equation 2.15 and the cross sectional area of the primary vortex at t = 0 , A_o , using the following equation:

$$A_o = \pi D_v^2/4 \tag{2.24}$$

(2) Calculate the shear stress of the approach flow as $\tau_o = \rho g R S_f$ or any other method.

(3) The cross sectional area of the primary vortex at any time, A_t, is taken as the sum of the cross sectional area of the scour hole, A_s and A_o, with A_s calculated as:

$$A_s = d_s^2/(2tan\Phi) \tag{2.25}$$

Where Φ is the angle of repose assumed to be 30^o by the authors.

(4) The shear stress at the pier nose at any time is determined using the relationship below:

$$\tau_{p,t} = C_1 \tau_o (A_o/A_t)^{C_2} \tag{2.26}$$

Where C_1 is equal to 4.0 based on the assumption that the shear stress is approximately twice as large before scouring begins and that incipient pier

scouring occurs when $\tau_o/\tau_{*c} \geq 0.5$ with the later statement being reported by multiple authors (Chabert and Engeldinger 1956; Hancu 1971; Hjorth 1975; Ettema 1980; Kothyari 1989). C_3 is a coefficient equal to 0.57 determined from experimental data.

(5) Average probability of particle movement at any time is found using the following equation (Paintal, 1971):

for $\tau_{p,t}/\rho' g d_{50} \leq 0.25$ $\quad p_{o,t} = 0.45\tau_o\left(\tau_{p,t}/\rho' g d_{50}\right)^{3.45}$ (2.27)

for $\tau_{p,t}/\rho' g d_{50} > 0.25$ $\quad p_{o,t} = 1.0$ (2.28)

(6) The time for a single particle to be removed from the scour hole is then calculated as shown:

$$t_* = C_3 d_{50}/\left(p_{o,t} u_{*,t}\right) \quad (2.29)$$

With $u_{*,t} = \sqrt{\tau_{*,t}/\rho}$ and C_3 a coefficient equal to 0.050 determined from experimental data.

(7) The new time is now $t_i = t_{i-1} + t_*$ and the new scour depth is $d_{s,i} = d_{s,i-1} + d_{50}$.

(8) Steps 3 to 7 are then repeated until $\tau_{p,t}$ becomes less than or equal to τ_c. At this point, equilibrium scour depth is reached.

Kothyari et al. (1992) found that the computed scour depths compared well with the measurements made by Chabert and Engeldinger (1956), Ettema (1980), and Kothyari (1989). Generally the computed scour had satisfactory agreement for steady state clear

water scour; although multiple runs had differences greater than 20% between observed and computed scour. Results from the two unsteady flow tests had good agreement between calculated and measured scour. Due to the limited number of tests and short hydrograph durations (1 hr and $\approx$ 7 hr tests), the method was not verified fully.

Mia and Nago (2003) conducted laboratory experiments to develop a temporal scour evolution method for clear water conditions with a uniform sediment bed and a cylindrical pier under steady flow conditions. They used their own data from experiments in a hydraulic flume and data from Chabert and Engeldinger (1956), Ettema (1980), Yanmaz and Atlinbilek (1991) to develop their model. Equilibrium scour under steady flow was assumed to have been reached when the scour rate was less than 1 mm per hour or no change in scour was observed.

The design method by Mia and Nago (2003) was based on a sediment transport theory by Yalin (1977) and incorporated equations by Kothyari et al. (1992) that related the strength of the primary horseshoe vortex with changes in the area of the scour hole. The shape of the scour hole was assumed to remain the same shape throughout testing and be similar to an inverted cone with the sediment's angle of repose equal to that of a cone's angle of frustum. The bed shear velocity at the pier nose was calculated using equation 2.26 (Kothyari et al., 1992), however, different values for C_1 and C_2 were used. A value of 3.3 for C_1 was used based on research by Chiew (1995) that suggested scouring occurs

when $\tau_o/\tau_{*c} \geq 0.3$. C_2 was determined to be 0.29 from experimental data, which was significantly different than the value of 0.57 used by Kothyari et al. (1992).

Mia and Nago (2003) found good agreement between measured and computed temporal scour data. Much lower agreement was found between the algorithm proposed by Kothyari et al. (1992) and data from Chabert and Engeldinger (1956), Ettema (1980), Yanmaz and Atlinbilek (1991), and the authors. The model by Kothyari et al. (1992) tended to substantially under predict both equilibrium scour depths and equilibrium scour time for steady flows. Comparisons between the model proposed by the authors and common empirical formulas by Hancu (1971), Breusers et al. (1977), Melville and Sutherland (1988), and the FHWA (1993) were made. The authors' model was also compared with experimental data from Chiew (1995) and Melville and Chiew (1999). Empirical formulas by Hancu (1971) and Breusers et al. (1977) underestimated scour depths at lower Froude numbers while the FHWA (1993) method had better results overall. Data from Chiew (1995) and Melville and Chiew (1999) were considered to have good agreement with the authors' method, as the majority of their data was within ± 25% of calculated scour depths.

Melville and Chiew (1999) developed an equation to determine the temporal scour development at circular bridge piers for clear water scour under steady flows for uniform sediment. Data consisted of their own laboratory measurements and measurements made by Graf (1995) and Ettema (1980). Since equilibrium scour might take days to develop,

equilibrium scour depth and time was taken as when scour changed less than 5% of the pier diameter per 24 hour period. This definition is mathematically defined below as:

$$\frac{d(d_{se})}{dt} \leq \frac{0.05b}{24\ hrs} \tag{2.30}$$

It was hypothesized and shown that d_{se} and t_e are functions of the ratio of velocity to critical velocity (V/V_c), flow shallowness (b/h), and sediment coarseness relative to the pier diameter (b/d_{50}). Equilibrium scour depths were computed using a method from Melville (1997) that was simplified due to tests being conducted only on circular piers and with uniform sediment. The equilibrium scour depth was calculated as a function of the flow intensity factor, K_i, a particle size factor, K_d, and a flow shallowness expression, K_{yd}. The procedure to calculate equilibrium scour is shown below:

(1) The flow intensity factor is defined as:

for $V/V_c < 1$ $$\mathrm{K}_i = V/V_c \tag{2.31}$$

for $V/V_c > 1$ $$\mathrm{K}_i = 1 \tag{2.32}$$

(2) The particle size factor is calculated as a function of pier diameter and particle size as:

for $b/d_{50} < 25$ $$\mathrm{K}_d = 0.57\log(2.24\ b/d_{50}) \tag{2.33}$$

for $b/d_{50} > 25$ $$\mathrm{K}_d = 1 \tag{2.34}$$

(3) The flow depth to pier diameter factor is then calculated as:

for $b/h < 0.7$ $$\mathrm{K}_{yd} = 2.4b \tag{2.35}$$

for $0.7 < b/h > 5$ $$K_{yd} = 2(bh)^{0.5} \quad (2.36)$$

for $b/h > 5$ $$K_{yd} = 4.5h \quad (2.37)$$

(4) The equilibrium scour depth is now calculated as the product of the three previous factors:

$$d_{se} = K_i K_d K_{yd} \quad (2.38)$$

(5) Once equilibrium scour depths are known, the following equations can be used to calculate the equilibrium scour time. The velocity, V, needs to be in units consistent with the pier diameter and in seconds.

for $h/b > 6$ $$t_e(days) = 48.26 \frac{b}{V}\left(\frac{V}{V_c} - 0.4\right) \quad (2.39)$$

for $h/b \leq 6$ $$t_e(days) = 30.89 \frac{b}{V}\left(\frac{V}{V_c} - 0.4\right)\left(\frac{h}{b}\right)^{0.25} \quad (2.40)$$

(6) The following temporal scour equation was developed which represented their data well, where scour depths can be calculated at any time and vice versa.

$$\frac{d_s}{d_{se}} = \exp\left\{-0.03\left|\frac{V_c}{V}\ln(t/t_e)\right|^{1.6}\right\} \quad (2.41)$$

Although the authors did not use these formulas to predict scour under stepped hydrographs, the method of superposition could theoretically be used with these equations.

A recent laboratory based study by Oliveto and Hager (2002) used six different sediments of varying size and uniformity, a wide range of flow depths, and various pier and abutment geometries under steady flow conditions to calculate local scour. From some

200 experiments, a temporal scour equation was developed that incorporated known variables that affect scour including sediment characteristics, approach flow, structural shape, and time The dimensionless scour depth, for $Fr_d > Fr_{di}$, was calculated as follows:

$$\mathrm{Z} = 0.068 N Fr_{dm} \log(T) \tag{2.42}$$

Where Fr_{di} is the densimetric Froude number that corresponds to incipient local scour, N is a shape factor calculated as 1 for circular piers, Z is the dimensionless scour given by d_s/L_R, T is a dimensionless time given by $\sigma^{1/3} t\sqrt{g' d_{50}}/L_R$, and L_R is given by $b^{2/3}h^{1/3}$.

By taking into account a wide range of parameters that affect scour depths including time variations, Oliveto and Hager (2002) found this equation to be sufficiently accurate by river engineering standards for their laboratory tests and available literature data. These equations have limited applicability for natural pier scour as this equation is only valid under the following conditions:

(1) Straight, rectangular channels

(2) The distribution of roughness is nearly uniform across the channel

(3) Fluid is water and the sediment is sand or gravel

(4) Flow is steady state

(5) The ratio of flow depth to sediment size is large enough to avoid additional effects of macroroughness

(6) Approach flow is perpendicular to pier

An independent field verification of this formula has not yet been performed and this formula is not currently used or recommended by federal agencies to calculate scour.

Sediment Characteristics

The most commonly used non-cohesive sediment parameters to model scour are the median sediment size d_{50} and sediment gradation coefficient σ_g given by:

$$\sigma_g = \sqrt{d_{84}/d_{16}} \tag{2.43}$$

This coefficient is used to measure the uniformity of the sediment and is calculated along with d_{50} from a particle size distribution.

It has been well documented (Ettema 1980; Raudkivi and Ettema 1983; Melville and Sutherland 1988; Kothyari et al. 1992; Oliveto and Hager 2002; Chang et al. 2004) that as the sediment bed becomes increasingly non-uniform, scour depths decrease due to bed armoring. As the smaller size sediments are transported out of the scour hole, the larger sediments shield the smaller sediments from becoming suspended. This process limits the transport of sediment out of the scour hole and limits the scour depth.

Various researchers have proposed different methods to incorporate the sediment gradation. For example, Oliveto and Hager (2002) introduced the densimetric mixture Froude number. Others have simply used a coefficient or correction factor to account for armoring by modifying existing equations, such as the Colorado State University (CSU).

Raudkivi and Ettema (1983) conducted laboratory experiments and found that the pier diameter relative to sediment size (b/d_{50}) was important in predicting equilibrium clear water scour depths in cohesionless soils. Four significant zones were identified and described as follows (in the following the groove refers to the bottom of the scour hole):

(1) "$b/d_{50} \geq 130$; *the sediment is fine relative to pier diameter. The sediment is entrained from the groove by the downflow and from the slope by the horseshoe vortex until equilibrium is reached.*

(2) $130 > b/d_{50} \geq 30$*; the sediment is of an intermediate size. The sediment is entrained mainly from the groove with only a limited entrainment under the horseshoe vortex. The supply of sediment to the groove is accomplished by sliding down the slope.*

(3) $30 > b/d_{50} \geq 8$; *the sediment is coarse relative to pier diameter and relative to the downflow. A significant proportion of the energy of the downflow is dissipated in the coarse bed material at the base of the scour hole.*

(4) $b/d_{50} < 8$; *the stones are so large that the erosion phase does not develop. The scour is mainly due to the entrainment of the flanks of the pier* (Raudkivi and Ettema, 1983)."

In the field, the b/d_{50} ratio tends to be quite large and the sediment size is of negligible importance in pier scour (Breusers and Raudkivi 1991; Raudkivi 1986). The equilibrium scour depth relative to pier diameter (d_{se}/b) reaches a maximum as b/d_{50}

becomes greater than approximately 25 or 50, as observed by multiple researchers (Raudkivi, 1986; Melville, 1997; Lee and Strum, 2009).

Scour Hole Geometry

The top width of the scour hole for cohesionless sediment, shown in Figure 2.4, from one side of a pier can be estimated by the following equation according to HEC-18 guidelines (FHWA, 2001):

$$W = d_s(K + cot\phi) \tag{2.44}$$

Where W is the top width of the scour hole, K is the bottom width of the scour hole, and ϕ is the angle of repose of the sediment which generally varies between 26° to 34° for sand in water.

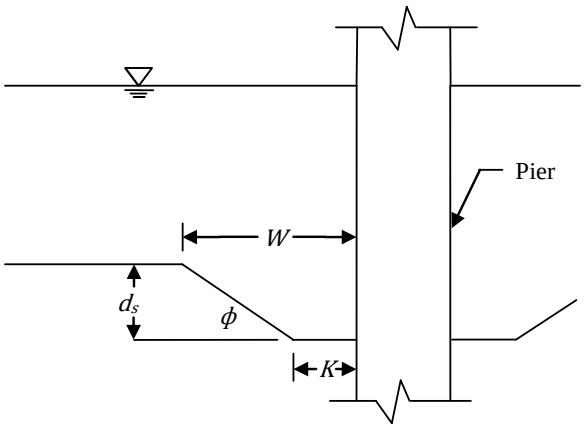

Figure 2.4: Scour Hole in Cross Stream Direction

Experimental research conducted by Yanmaz and Altinbilek (1991) on time dependent pier scour found that the shape of the scour hole is unchanged with respect to time. The increase in scour hole volume, $\forall$, decelerates as time elapses. By assuming the side slopes to be the angle of repose, the volume of the scour hole at any time around a circular pier was computed using equation 2.45. This equation was originally proposed by Carstens (1966) and Shen et al. (1969).

$$\forall = \frac{\pi}{3tan\phi}\left(\frac{d_s^3}{tan\phi} - \frac{3d_s^2 b}{2}\right) \tag{2.45}$$

This equation assumes that the downstream and upstream ends of the scour hole are symmetrical. This assumption may not be valid if substantial amounts of deposition occur downstream of the pier.

Review of Equilibrium Scour Depth Equations

Designs based on predicted equilibrium scour depths can be over conservative as peak flows may only last a few hours instead of days during a natural flood (Melville and Chiew, 1999). Various equations developed in the laboratory are currently used to calculate equilibrium scour. Currently there is no unifying theory of pier scour that allows the designer to have high confidence in scour depth predictions (Raudkivi and Ettema, 1983). This section will discuss some of these equations. The readers should refer to Johnson (1995) who compared 7 different commonly used equations with field data for more detail.

Numerous empirical equations have been developed using the Froude number as a key parameter to calculate the equilibrium scour depth. Typical variables for scour prediction equations are the flow velocity, pier diameter, and flow depth. HEC – 18 (FHWA, 2001) recommends the use of the CSU equation, where scour depth is calculated as:

$$d_{se} = 2.0hK_1K_2K_3K_4(^{b}/_{h})^{0.65}Fr^{0.43} \quad (2.46)$$

Where $K_1, K_2, K_3,$ and $K_4$are correction factors that take into account the pier nose shape, angle of attack, bed condition, and armoring by bed material size, respectively.

Mueller (1996) found that this equation was useful in design purposes as observed scour was typically less than calculated based on the United States Geological Survey (USGS) field data. Although due to over prediction, this equation does not give the designer a high degree of confidence and can make scour prevention measures more expensive than needed. Johnson (1995) also concluded that predicted scour depths were substantially larger than observed scour in the field for high Froude numbers (Fr > 0.8) but worked well for very low Froude numbers. The analysis by Johnson (1995), however, did not incorporate the correction factor K_4 as this was not part of the previous CSU equation in HEC-18 (FHWA, 1993).

Jain and Fischer (1979) also developed design equations based on laboratory data that included a Froude based parameter. The set of equations are as follows:

for $(Fr - Fr_c) > 0.2$ $\quad d_{se} = 2.0b(Fr - Fr_c)^{0.25}(^{h}/_{b})^{0.5}$ (2.47)

for $(Fr - Fr_c) < 0$ $$d_{se} = 1.85 b Fr_c^{0.25} (h/b)^{0.5} \quad (2.48)$$

for $0 < (Fr - Fr_c) < 0.2$ $$d_{se} = Max(\text{Eqn. 2.47 and Eqn. 2.48}) \quad (2.49)$$

Johnson (1995) found that this equation generally over predicted scour for h/b < 1.5 in the field. It was determined that the Froude number had very little correlation with equilibrium scour depth and other parameters may be of more importance in predicting prototype scour.

Neill (1964) developed a simple scour equation based on Laursen and Toch's (1956) design curves and calculated equilibrium scour depth as:

$$d_{se} = 1.35 b^{0.7} h^{0.3} \quad (2.50)$$

A review by Muhamed et al. (2005) using field and laboratory data found that this formula produced reasonable results when compared to laboratory data. Johnson (1995) using field data found this equation over predicted scour depths for a wide range of $Fr, h/b$, and V/V_c with greater inaccuracies reported for h/b < 1.5 and V/V_c < 0.9. Since V/V_c < 1 corresponds to clear water scour, it can be assumed this is not an ideal model for predicting equilibrium scour in clear scour conditions.

CHAPTER 3

EXPERIMENTAL SETUP AND PROCEDURES

Experiments were conducted at the Clemson Hydraulics Laboratory (CHL), Department of Civil Engineering at Clemson University, South Carolina. Details of the equipment and instruments used, the experimental setup, experiments performed, and procedure are outlined in this section.

Experimental Setup

All experiments were conducted in a 14.8 m long, 1.19 m wide, 1.22 m deep flume with clear acrylic sidewalls. The layout of the flume is shown in Figure 3.1. A 2.4 m long, 1.19 m wide, 0.88 m deep recess was built flush to the flume bed. The downstream end of the recess was 2.4 m upstream of the tail weir. All tests were conducted in this region and a 77 mm diameter acrylic model pier was placed at the center of this recess, 11.8 m downstream of the flume entrance, as shown in Figure 3.2. The clear acrylic side walls allowed for viewing of flow phenomena in the recess. A false floor was constructed in the recess 0.3 m below the floor of the flume bed. The location of the false floor was chosen to be substantially below the maximum equilibrium scour depths in the experiments. Beneath the false floor, a 51 mm diameter drain line was installed.

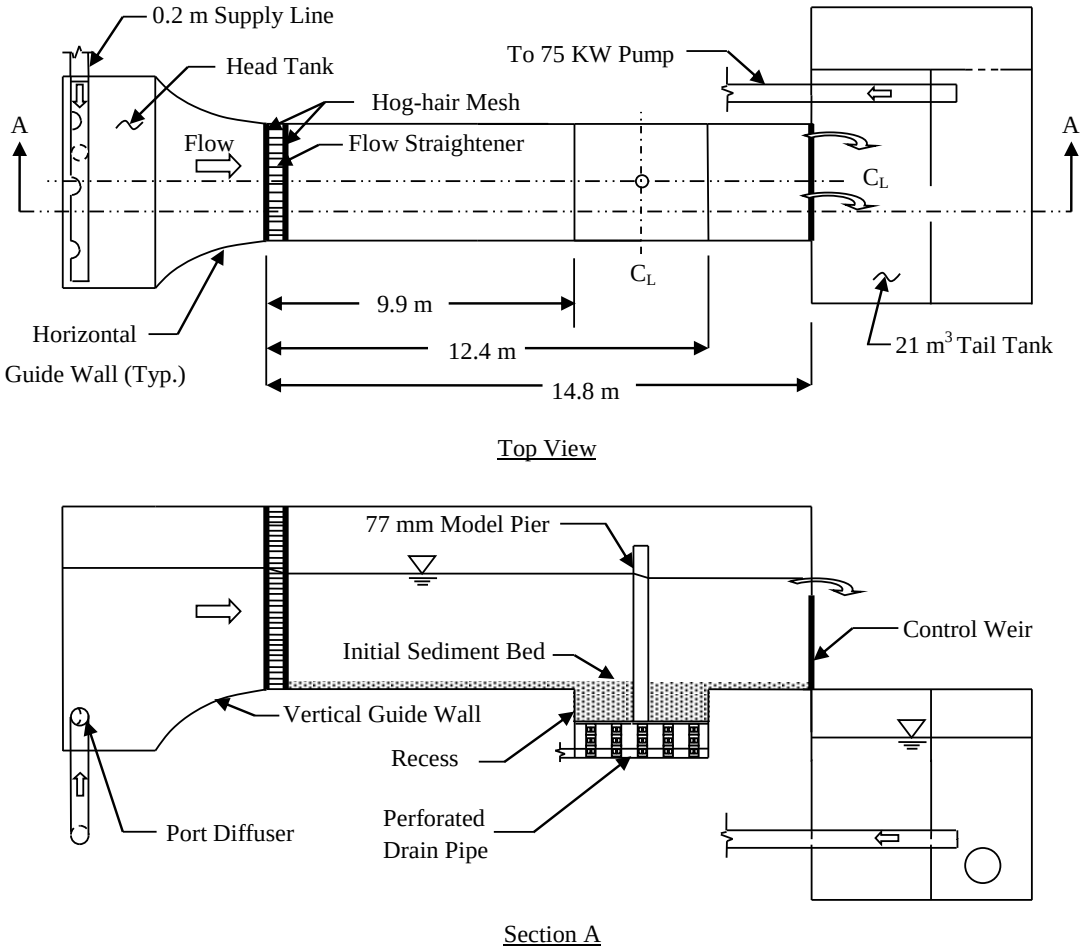

Figure 3.1: General Model Layout (Not to Scale)

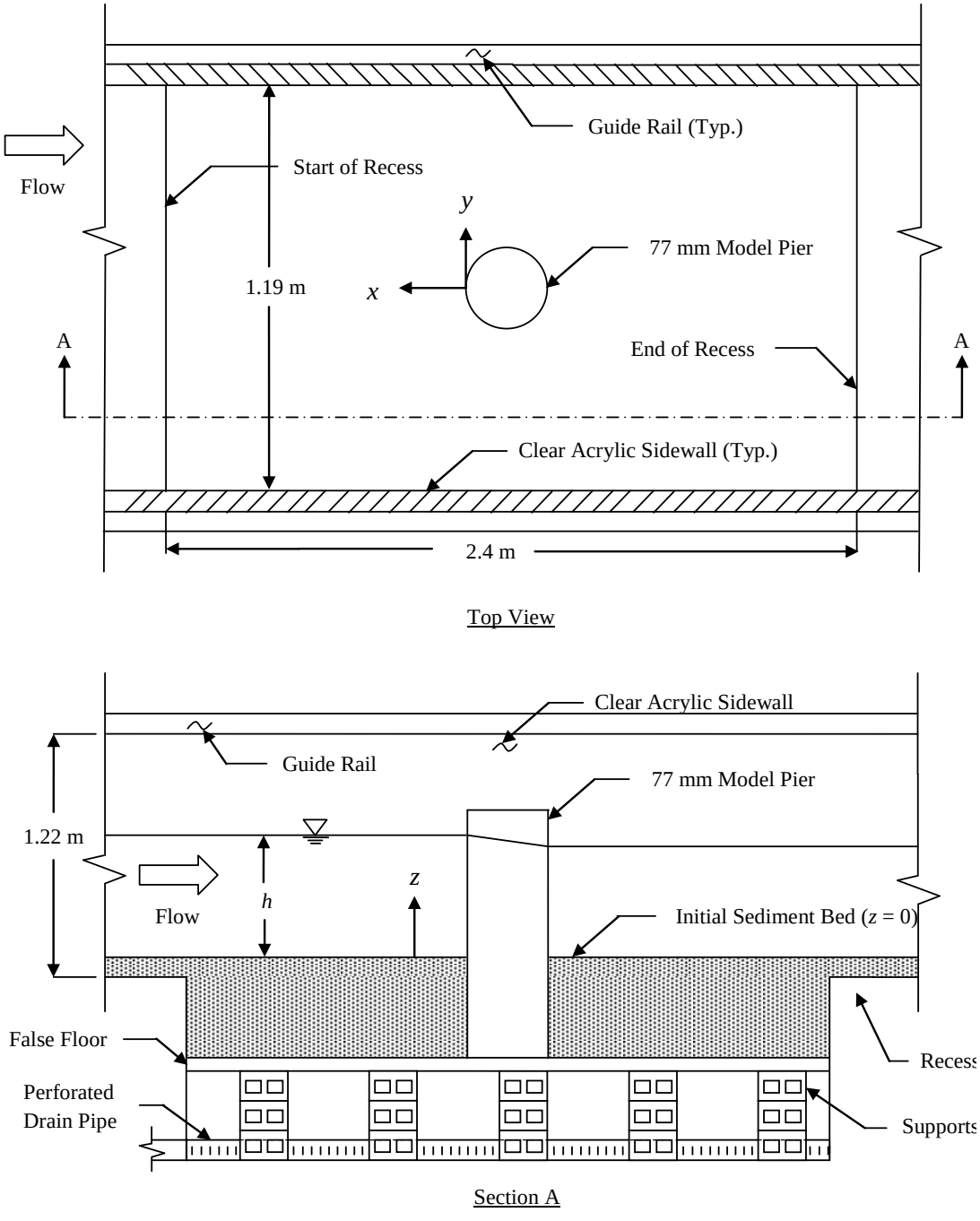

Figure 3.2: Recess and Model Pier (Not to Scale)

Water was recirculated through the system by a 75 KW variable speed pump. The flow rate was adjusted using a variable frequency drive (VFD). A 0.2 m supply line provided flow to a port diffuser which discharged into the head tank. The head tank had curved vertical and horizontal guide walls which allowed a smoother transition into the flume. At the flume inlet, a 15 cm long honey-comb shaped flow straightener was installed across the flume. Hog-hair mesh was added to both the port diffuser and flow straightener to minimize turbulence, dampen waves, and allow for a uniform approach velocity into the channel. An 80 cm thick gravel bed was added to the first 1.8 m of the channel (immediately downstream of the flow straightener) to avoid bed degradation during the boundary layer development. The gravel had a minimum size of 9 mm. This gravel size was selected since it had a critical shear velocity substantially larger than the maximum shear velocity used during testing.

At the downstream end of the flume, a thin rectangular weir was used to control flow depths. The weir was adjusted using an electrical motor. The flow then discharged into a 21 m^3 tail tank that was partitioned into three sections which dampened waves before flow entered the pump intake.

Discharge measurements were made using a magnetic flow meter installed in a 0.2 m supply pipe, 13 m downstream of the pump outlet. The magnetic flow meter outputted a pulse with a frequency of 1 KHz to a digital rate meter which converted the pulses into a discharge. LabView software was used to analyze the discharge data. All sample times

were at least one minute long (1 min = 60,000 samples). The mean discharge was then calculated. During each test, this process was repeated multiple times to check discharge and potentially make necessary adjustments to the flowrate. The final recorded flow rate for each test's flow condition was the average of several discharge measurements.

Uniform sand was obtained from a local quarry and was used throughout the experiments. The sediment bed in the channel was 80 mm thick. A particle size gradation curve based on the data provided by the sand supplier is shown in Figure 3.3. Three sieve analyses were performed and the results were found to be similar to the supplier's data. Sediment characteristics such as the median sediment size (d_{50}) and sediment gradation coefficient (σ_g) were then obtained from the gradation curve. The median sediment size was 1.50 mm and the gradation coefficient was 1.20. The critical shear velocity was calculated by the method described by Hager and Del Giudice (2000) based on the Shields diagram and shown in Table 3.1. The sediment is considered non-cohesive.

Table 3.1 : Sediment Characteristics

d_{50} (mm)	σ_g	u_{*c} (m/s)
1.50	1.20	0.0342

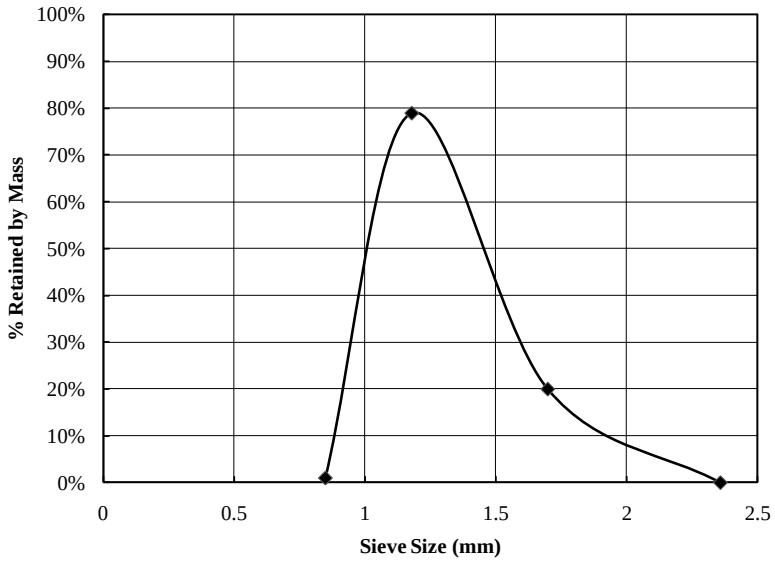

Figure 3.3: Particle Size Distribution

An Acoustic Doppler Velocimeter (ADV) and dye visualizations were used to check that the approach flow in the testing region was uniform. The ADV was able to be positioned in all three Cartesian directions. The coordinate system used in the experiments is shown in Figure 3.4. The x and y coordinates are relative to the upstream center of the pier nose. The elevation of the sediment bed before testing was considered to be $z = 0$. The ADV was mounted to a small cart within a larger rolling cart that traveled on rails atop of the flume side walls. The larger instrumentation cart could be moved across the entire length of the flume (x-direction). A pointer was attached to this cart and the location was determined by measuring the distance to a reference location. Lateral (y-direction) directions were adjusted by moving the smaller cart. Positions were then determined by measuring the distance to the flume side wall using a standard tape. Due to geometric constraints, only the inner 60% of the flume width could be traversed. This was

determined not to be of concern as flow near the side walls was outside the region where scour occurred. The vertical range (z-direction) was adjusted by rotating a threaded rod that was attached to the cart. This location was set by measuring the distance to a fixed reference point using a tape. A 10MHz ADV was used during initial calibration of the flume. A smaller 16MHz MicroADV was used during scour tests to minimize effects on flow conditions and scour. Periodically, neutrally buoyant ADV seeding material was added to the water. This allowed for more accurate data by increasing the signal to noise ratio (SNR) and correlation of the velocity data. Measurements were limited to at least 53 mm below the water surface, which corresponded to the distance from the sensor face to the MicroADV's sampling volume.

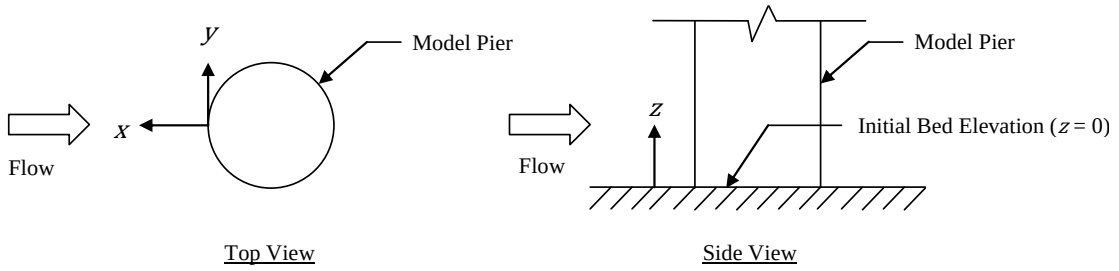

Figure 3.4: Coordinate System

Velocity measurements were taken at various depths for each steady and unsteady test at x = 1.18 m and y = 0 (flume centerline.). To assure that the velocity profile was fully developed at the pier, measurements were taken along the flume centerline at three different locations (x = -1.26 m, -38 mm, and 1.18 m) before scour testing commenced (i.e., before the installation of the pier). The flow profiles along the flume centerline and

the ADV measurement locations are shown in Figure 3.5 and 3.6, respectively. Shear velocities were calculated by fitting a logarithmic equation to the measured velocity data. The shear velocity was then determined as the logarithmic slope multiplied by a von Karman constant of 0.412 following Nezu and Rodi (1986).

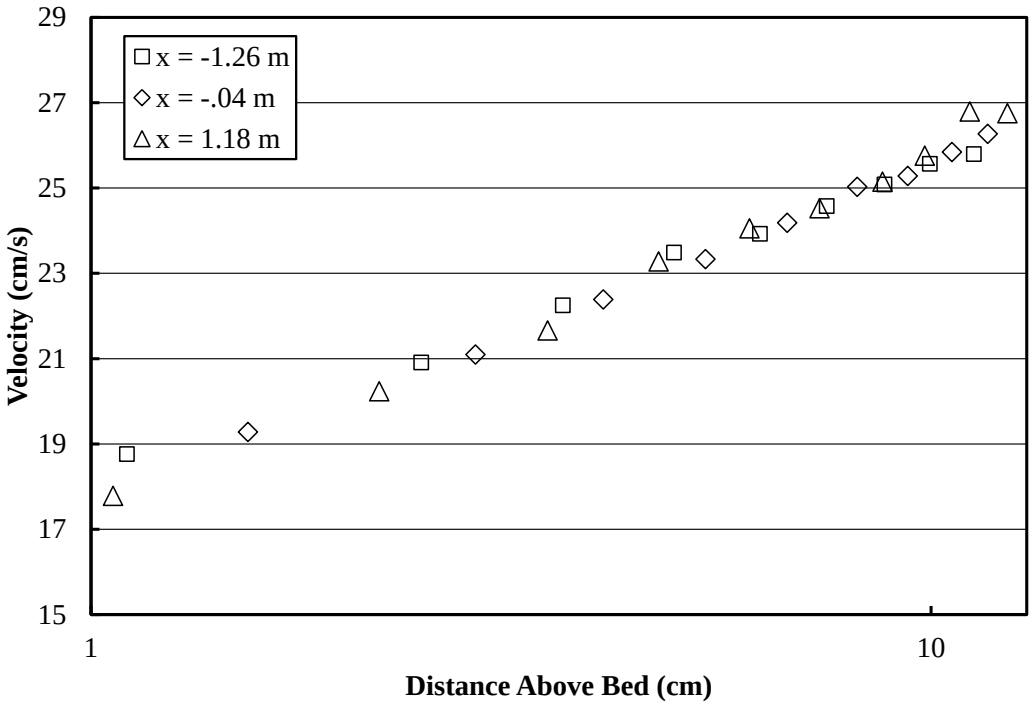

Figure 3.5: Flow Profile along Flume Centerline (V/V_c = 0.40, h = 255 mm)

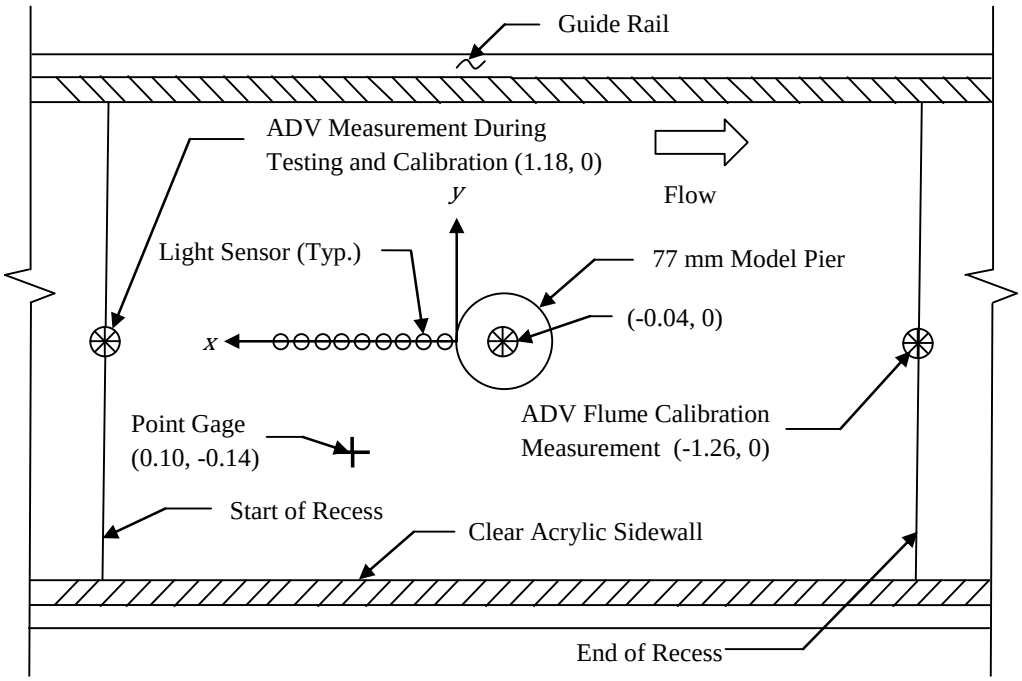

Figure 3.6: Top View of Measurement Locations (*x*, *y* denotes coordinates in meters)

A non-touch fiber optic sensor was used to measure the depth of scour. A similar system was tested and verified by Ballio and Radice (2003). The fiber optic sensor (Baumer Electric FZAM 18P6460/S14) was connected to a fiber optic cable (Baumer Electric FUE 100A1011) which was mounted on the large instrumentation cart. The tip of the fiber optic cable had a diameter of 3 mm and was mounted to an 8 mm rod that could be adjusted linearly in the vertical direction. Vertical measurements were made using a vernier height gauge that could be read to 0.1 mm accuracy. A sensing distance of 28 mm in water (measured from the tip of the cable to the sediment bed) was selected and verified for accuracy. This sensing distance was chosen to be as small as possible to

minimize the diameter of the beam spotlight. Locations in the x and y directions were determined by measuring the position from a fixed reference point on the cart with a tape.

Flow depths were measured using standard manual point gages with accuracies of ± 0.1 mm**.** All depths were measured at x = 102 mm and y = -137 mm as shown in Figure 3.6. This location was chosen as it was close to the pier, easy to access, and did not interfere with the scour measurement system. The initial distance to the sediment bed was measured along with the distance to the water surface. The difference between the two measurements was considered to be the flow depth at the pier. This was a valid assumption as the friction slope was relatively small during all tests. A summary of the instrumentation used and their respective measured quantity is shown in Table 3.2.

Table 3.2: Summary of Instrumentation Used

Measured Quantity	Instrument(s) Used
Discharge	Magnetic Flow Meter
Local Velocity	16MHz MicroADV & 10 MHz ADV(1)
Bed Level	Light Sensor & Point Gage
Water Surface	Point Gage
Scour Depth	Light Sensor

Notes:
(1) 10MHz ADV only used during flume calibration; 16MHz MicroADV used throughout rest of scour testing

Initial Calculations and Procedures

Both steady and unsteady flow experiments were conducted under clear water conditions. Testing procedures and initial calculations were the same for both steady state and simulated hydrographs. Initial procedures involved adjusting the flow depth, leveling the bed, measuring the bed elevation at multiple locations before testing, and determining the required pump speed.

The critical shear velocity was calculated from an explicit equation based on the Shields diagram provided by Hager and Del Giudice (2000). This value was compared to another explicit formulation based on the Shields diagram by Melville (1997) and was found to be similar as shown in Table 2.1. The critical velocity was calculated from Melville (1997) using the following logarithmic velocity profile equation:

$$V_c = 5.75u_{*c}\log(5.53h/d_{50}) \tag{3.1}$$

Since the flow depth, critical shear velocity, and sediment size remained the same throughout the testing, the critical velocity was always the same. Using Melville's (1997) equation the critical velocity was calculated as 0.58 m/s, however, preliminary tests showed that the observed critical velocity was 30% lower than the calculated value.

Desired discharge was calculated using the known flume geometry, flow depth, and desired mean velocities. The pump speed was set from a calibration curve and slight

adjustments were made accordingly based on the measured flowrate from the magnetic flow meter.

Flow depths were calculated using a point gage at x = 102 mm and y = -137 mm and was considered to be the difference between the water surface level and the sediment bed. This was considered accurate as the friction slope was very low throughout testing. The initial bed measurement was taken before scour testing commenced.

The sediment bed was leveled using a wooden scraper that was manually moved along the top of the flume walls. The wooden scraper allowed for a consistent sand bed depth of 8 cm in the channel. The sand bed depth was 36 cm in the recess. Near the pier (< 15 cm) the wooden scraper could not be used due to geometric constraints so the bed was carefully leveled by hand using a bubble level and flat piece of wood. After the bed was leveled, the flume was slowly filled and ran at a low flowrate to prevent scour prior to testing. During this time, multiple bed level measurements were made upstream of the pier with the light sensor. The initial elevation of the sediment bed was considered to be the average of multiple measurements upstream of the pier.

Experimental Procedures for Steady Flow Conditions

The experimental procedure was similar for both stepped hydrograph and steady experiments. During steady state conditions, the experiment was run continuously until

the scour depth changed less than 5% of the pier diameter over 24 hours. In this study that corresponded to a rate of 3.8 mm/day. This criterion is originally from Melville and Chiew (1999) who used this as a definition of equilibrium scour and is mathematically defined in equation 2.30.

The steady state testing plan is shown in Table 3.3. The steady state tests corresponded to V/V_c = 0.49, 0.57, and 0.65 and were titled as Q1, Q2, and Q3, respectively. Testing length ranged from 114 to 211 hours. Flow conditions Q2 and Q3 were run multiple times to check the repeatability of the experiments.

Table 3.3: Steady Flow Tests

Test Name	Duration hours	Discharge m^3/s	Flow Depth mm	Velocity cm/s	V/Vc	Shear Velocity cm/s
Q1	113.6	0.087	254	0.286	0.49	1.60
Q2	211.3	0.101	254	0.334	0.57	2.08
Q3	152.1	0.115	254	0.379	0.65	2.93

While the steady state flow experiments were running the flow depth, flow rate, and scour depths were checked at least daily and at a higher frequency during the first several hours. Scour profiles were taken, when changes in the scour depth were substantial, with the highest frequency during the start of testing. Since measurements could only be taken individually, the reported times for scour profiles was the mean time of all the measurements taken for each individual profile. The first measurement for each scour

profile was always taken immediately in front of the pier. Measurements were then taken moving away from the pier in the longitudinal direction ($+x$). The time to take each individual measurement was typically between thirty seconds to one minute.

A velocity profile was measured with an approximate range of 4% to 55% of the flow depth once during each test. A total of 15 to 17 measurements at various depths were made along the flume centerline (y = 0 m) at x = 1.18 m. 8 to 9 measurements were taken at 0.5 cm intervals in the bottom 20% of the flow depth. Shear velocities were calculated from the logarithmic velocity distribution from both the larger profile and the bottom 20% of the flow depth. Similar results were found using either data set as shown in Figure 3.4. Both the full velocity profile and bottom 20% profile are shown in Figures 3.7 and 3.8, respectively. Very high agreement ($R^2 > 0.97$) using a computer generated logarithmic best fit equation was found except for one smaller profile for flow condition Q1, which had slightly lower correlation ($R^2 > 0.92$) due to a single outlier.

Table 3.4: Steady Flow Shear Velocities

Test No.	All Measured Data		Data < 20% h	
	u_* (cm/s)	u_*/u_{*c}	u_* (cm/s)	u_*/u_{*c}
Q1	1.60	47%	1.68	49%
Q2	2.08	61%	1.85	54%
Q3	2.93	86%	3.01	88%

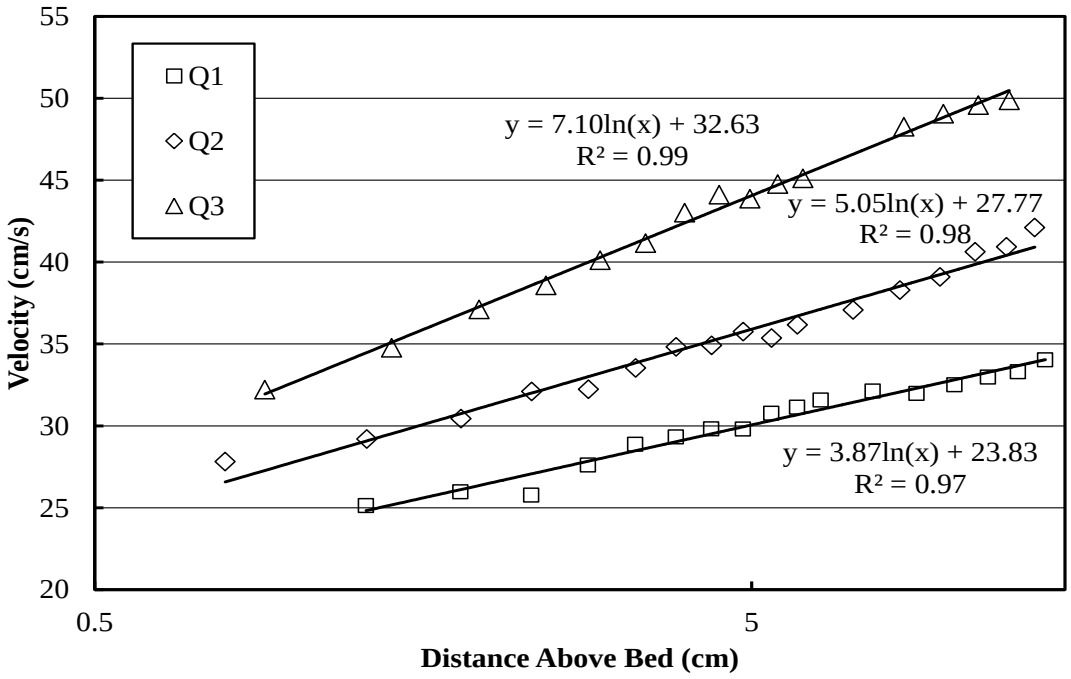

Figure 3.7: Steady Flow Velocity Profiles (All Measured Data)

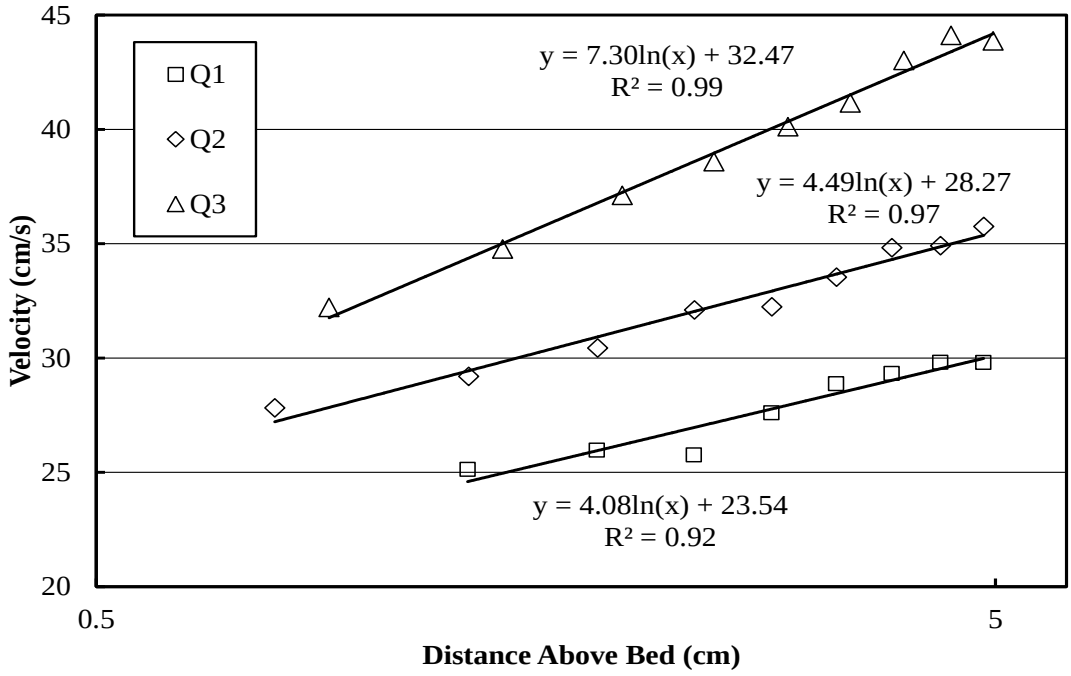

Figure 3.8: Steady Flow Velocity Profiles (Data < 20% *h*)

Maximum scour depths were measured at the highest frequency early in the experiments when the scour rate was highest and at least daily. Periodically, the scour profile was measured along with the undisturbed bed to check if bed aggradation or degradation had occurred upstream of the scour hole. The upstream bed did degrade slightly during the steady state tests at rates of 0.2, 0.5, and 0.4 mm/day for tests Q1, Q2, and Q3, respectively. This degradation was not taken into account in the calculations of scour depth as it was considered minimal relative to the equilibrium scour depth.

The naming convention for the unsteady and steady state runs is as follows. The first letters denotes the type of discharge, Q for steady and QU for unsteady, the first number denotes the test number, and a dash followed by a number indicates the trial number. Repeated trials were often done to verify data.

Experimental Procedures for Unsteady Flow Conditions

Due to the inherent difficulties in measuring and reproducing an unsteady hydrograph, simulated stepped hydrographs were used instead where each step corresponded to a previously run steady state test. This way comparison could be made between measured scour depth evolution and scour equations proposed by various researchers.

The experimental procedures for the unsteady and steady state tests were similar. The flow depth, discharge, and scour depths were all calculated in the same way as described for the steady state tests. Changes in discharge between steps were made gradually (over

an approximately one minute period) to minimize flow acceleration or deceleration. The bed was also leveled and checked using the same procedures as described previously. Typically, the scour depths and longitudinal scour profiles were measured shortly before and after changes in the flood hydrograph occurred. Additional scour depths and scour profiles measurements were made periodically within each step.

Velocity profiles were measured and shear velocities calculated in the same manner as discussed before. Velocities, however, were only measured in the bottom 20% of the flow depth in vertical increments of 0.5 cm, which corresponded to seven to eight data points. This was done to allow for more time to be devoted to taking scour measurements. During each stepped hydrograph tests, velocity profiles for the bottom 20% of the flow depth were measured for each distinct step.

Each step in the hydrograph was run for at least 3 hours. This allowed enough time to observe any substantial changes in scour hole geometry and was long enough to produce very replicable data. Occasionally longer flow steps were used as in the case of tests QU4, QU6, QU7, and QU8. During test number QU4 a base flow of Q1 was run for a longer period at the end of the test to determine if a low flow condition could increase the scour depth after a high flow episode. Tests QU6, QU7, and QU8 also had a few longer time increments for the flows of Q1 and Q2. This was done to check the influence the time period may have on the results. Flow Q3 was never run for longer periods since the rate of scour would be significant. Eight unsteady tests were conducted. A summary table

for each stepped hydrograph test along with accompanying figures is shown below in Tables 3.5 to 3.12 and Figures 3.9 to 3.16, respectively.

Table 3.5: Hydrograph No. 1

Step No.	Base Flow	Duration (hours)	Discharge (m^3/s)	Flow Depth (mm)	Velocity (cm/s)	Shear Velocity (cm/s)
1	Q1	3	0.087	254	0.286	2.18
2	Q2	3	0.101	254	0.332	2.49
3	Q3	3	0.115	254	0.381	3.12
4	Q2	3	0.101	254	0.333	2.41
5	Q1	3	0.087	254	0.287	2.17

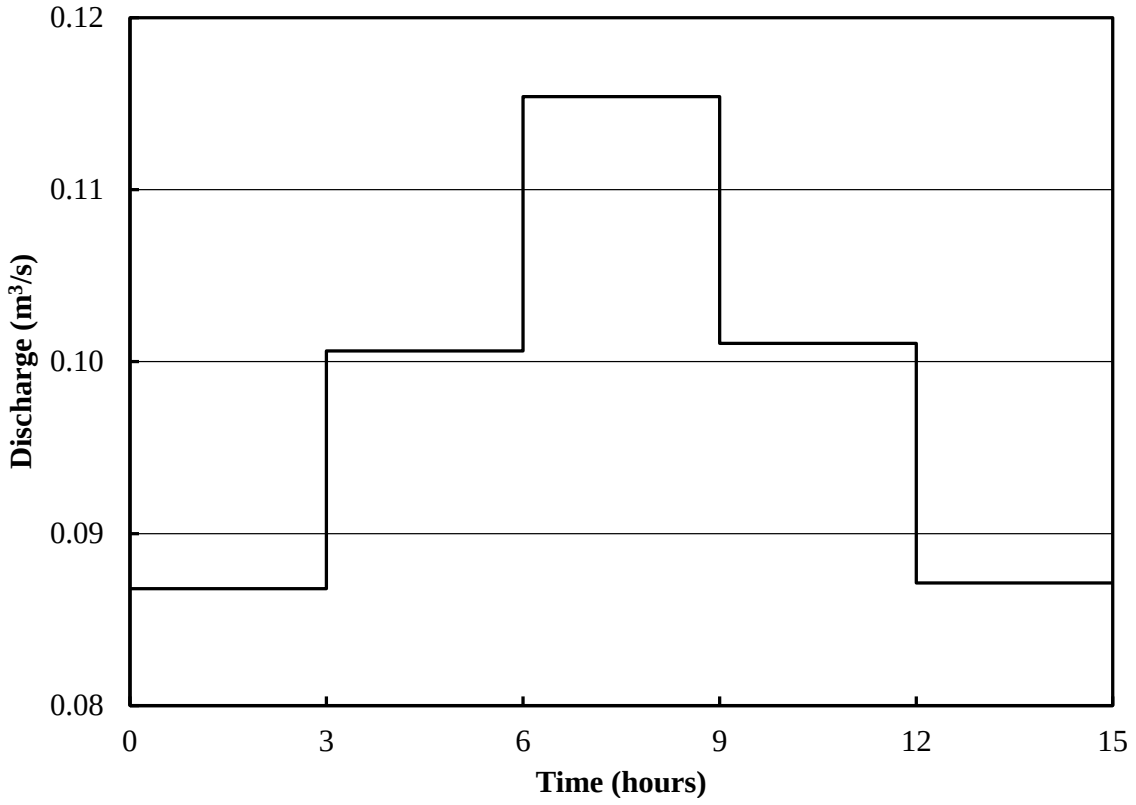

Figure 3.9: Hydrograph No. 1

Table 3.6: Hydrograph No. 2

Step No.	Base Flow	Duration (hours)	Discharge (m^3/s)	Flow Depth (mm)	Velocity (cm/s)	Shear Velocity (cm/s)
1	Q2	3	0.101	254	0.333	2.65
2	Q3	3	0.115	254	0.379	2.91
3	Q1	3	0.087	254	0.287	1.59

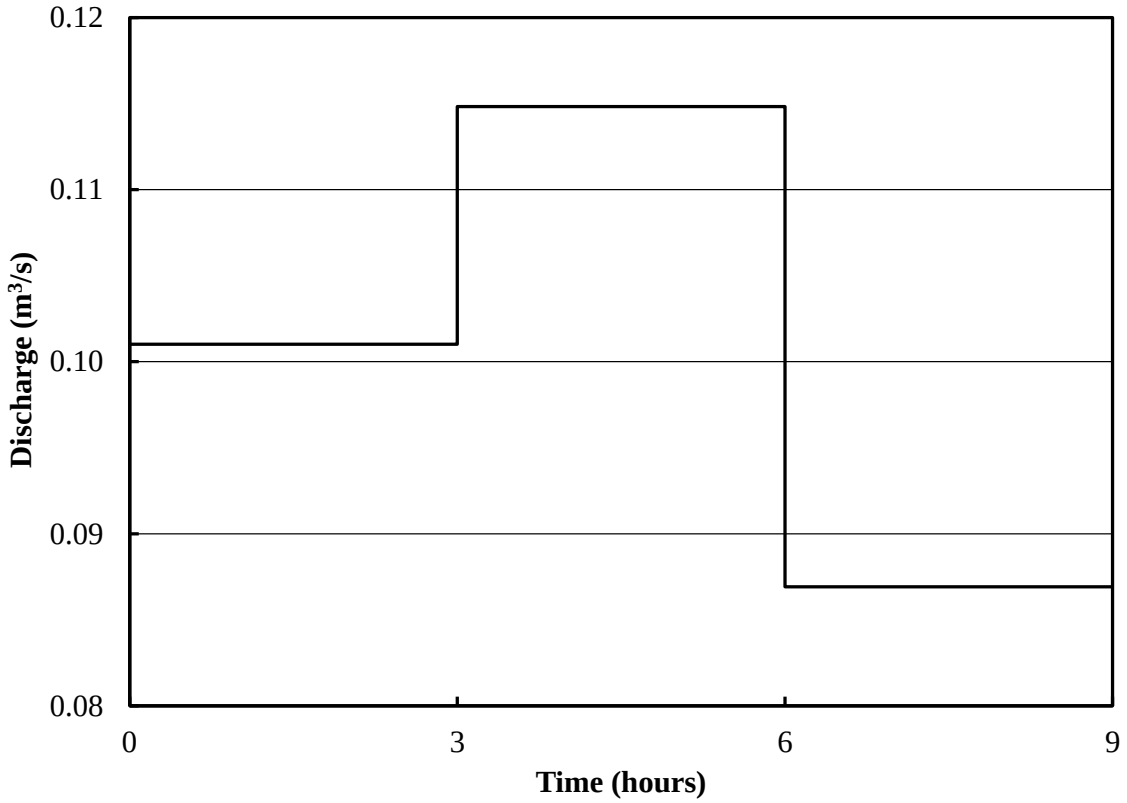

Figure 3.10: Hydrograph No. 2

Table 3.7: Hydrograph No. 3

Step No.	Base Flow	Duration (hours)	Discharge (m^3/s)	Flow Depth (mm)	Velocity (cm/s)	Shear Velocity (cm/s)
1	Q1	3	0.086	254	0.285	2.02
2	Q3	3	0.115	254	0.380	3.38
3	Q2	3	0.101	254	0.334	2.32

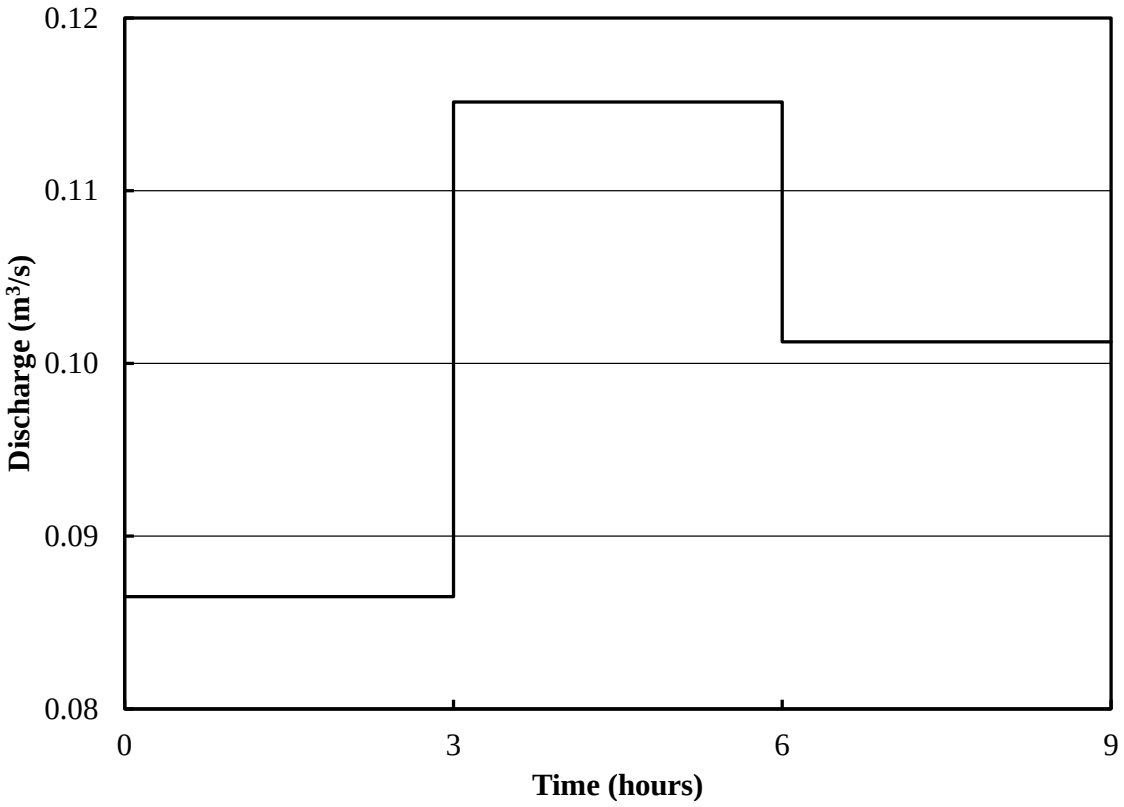

Figure 3.11: Hydrograph No. 3

Table 3.8: Hydrograph No. 4

Step No.	Base Flow	Duration (hours)	Discharge (m^3/s)	Flow Depth (mm)	Velocity (cm/s)	Shear Velocity (cm/s)
1	Q1	3	0.086	254	0.285	2.00
2	Q3	3	0.115	254	0.379	2.85
3	Q1	3	0.087	254	0.286	2.32
4	Q1	71.6	0.087	254	0.286	N/R

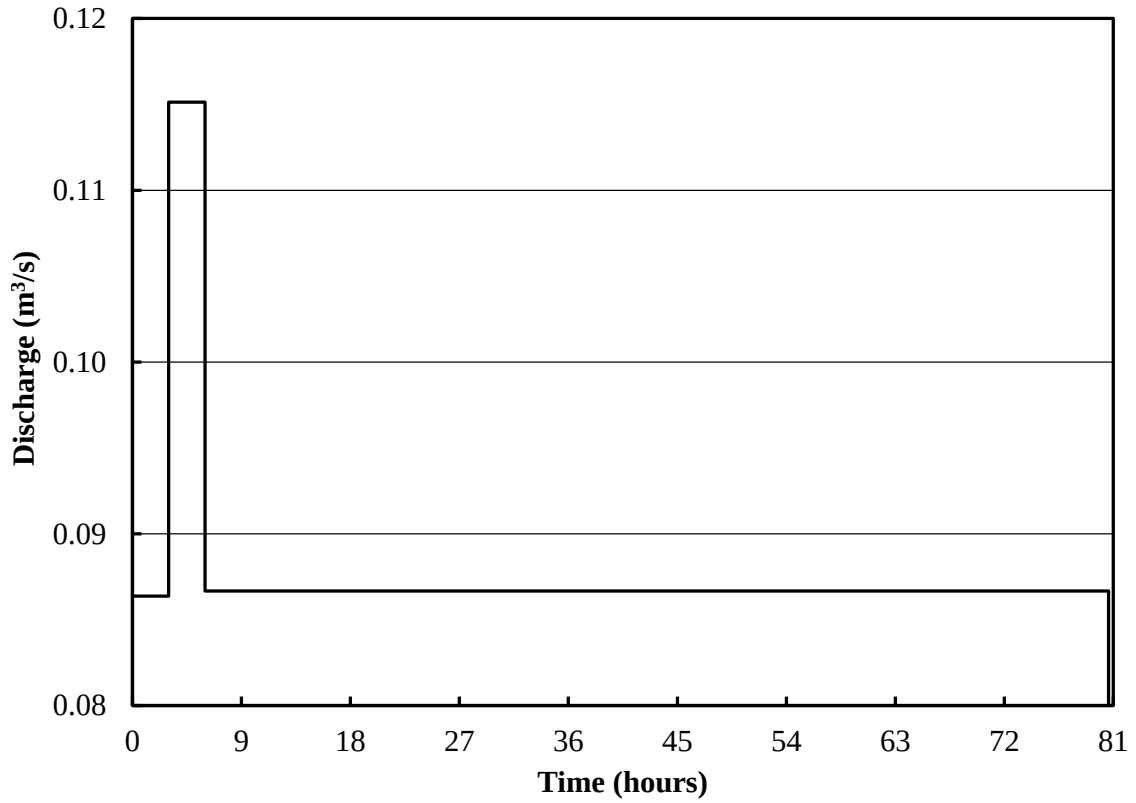

Figure 3.12: Hydrograph No. 4

Table 3.9: Hydrograph No. 5

Step No.	Base Flow	Duration (hours)	Discharge (m^3/s)	Flow Depth (mm)	Velocity (cm/s)	Shear Velocity (cm/s)
1	Q2	3	0.101	254	0.332	1.81
2	Q3	3	0.115	254	0.378	2.98
3	Q2	3	0.101	254	0.334	N/R

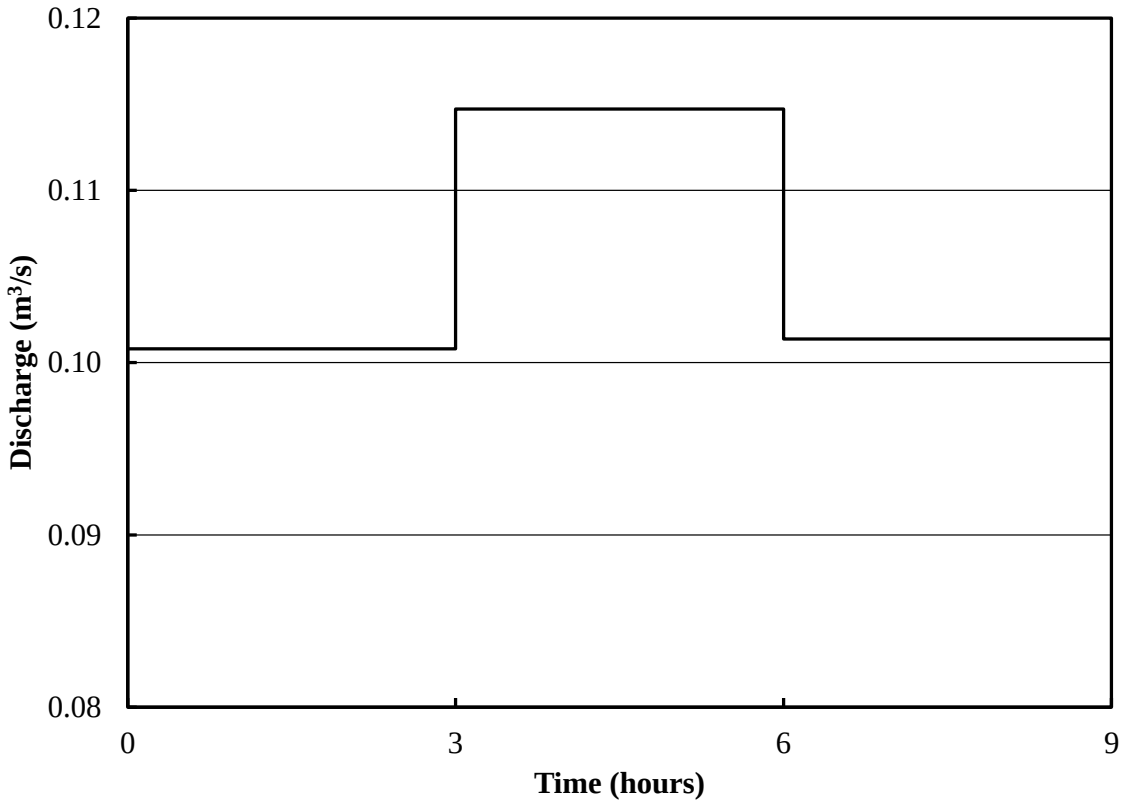

Figure 3.13: Hydrograph No. 5

Table 3.10: Hydrograph No. 6

Step No.	Base Flow	Duration (hours)	Discharge (m^3/s)	Flow Depth (mm)	Velocity (cm/s)	Shear Velocity (cm/s)
1	Q3	3	0.115	254	0.380	N/R
2	Q1	3	0.087	254	0.286	2.19
3	Q3	3	0.115	254	0.379	3.07
4	Q1	16	0.086	254	0.285	N/R
5	Q3	3	0.115	254	0.380	N/R
6	Q1	3	0.087	254	0.286	2.45
7	Q3	3	0.115	254	0.379	3.11

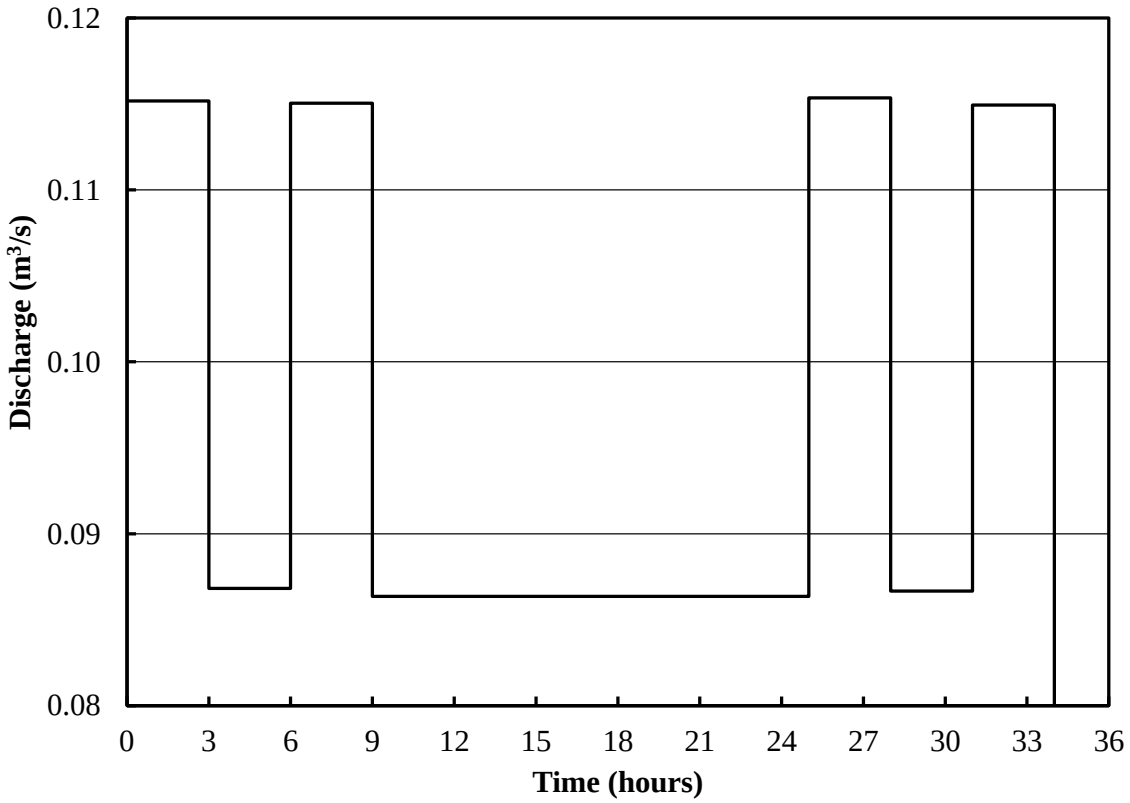

Figure 3.14: Hydrograph No. 6

Table 3.11: Hydrograph No. 7

Step No.	Base Flow	Duration (hours)	Discharge (m^3/s)	Flow Depth (mm)	Velocity (cm/s)	Shear Velocity (cm/s)
1	Q3	3	0.115	254	0.379	N/R
2	Q2	3	0.101	254	0.333	2.57
3	Q3	3	0.115	254	0.379	3.45
4	Q2	15	0.101	254	0.332	N/R
5	Q3	3	0.115	254	0.379	N/R
6	Q2	3	0.101	254	0.334	N/R
7	Q3	3	0.115	254	0.380	N/R

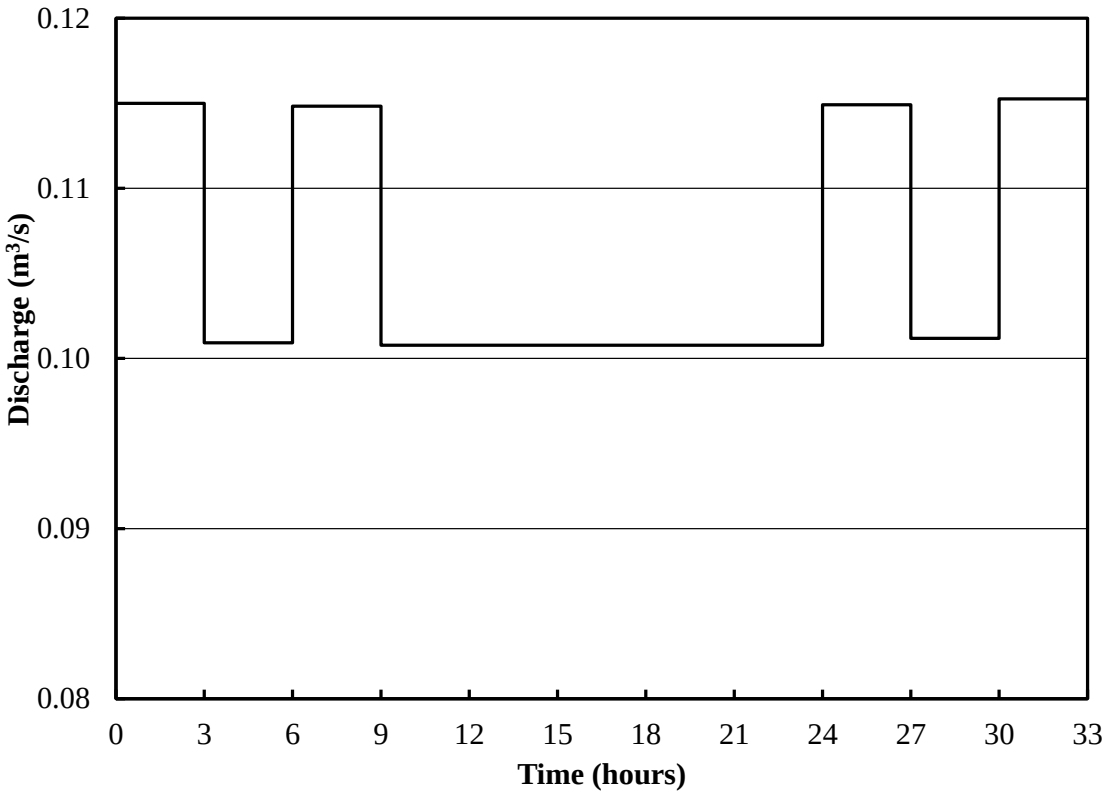

Figure 3.15: Hydrograph No. 7

Table 3.12: Hydrograph No. 8

Step No.	Base Flow	Duration (hours)	Discharge (m^3/s)	Flow Depth (mm)	Velocity (cm/s)	Shear Velocity (cm/s)
1	Q1	3	0.087	254	0.286	2.48
2	Q2	3	0.101	254	0.333	2.69
3	Q3	3	0.115	254	0.380	3.18
4	Q1	15	0.087	254	0.285	N/R
5	Q2	3	0.101	254	0.333	N/R
6	Q3	3	0.115	254	0.379	N/R
7	Q1	3	0.087	254	0.286	N/R
8	Q2	15	0.101	254	0.332	N/R
9	Q3	3	0.115	254	0.380	N/R

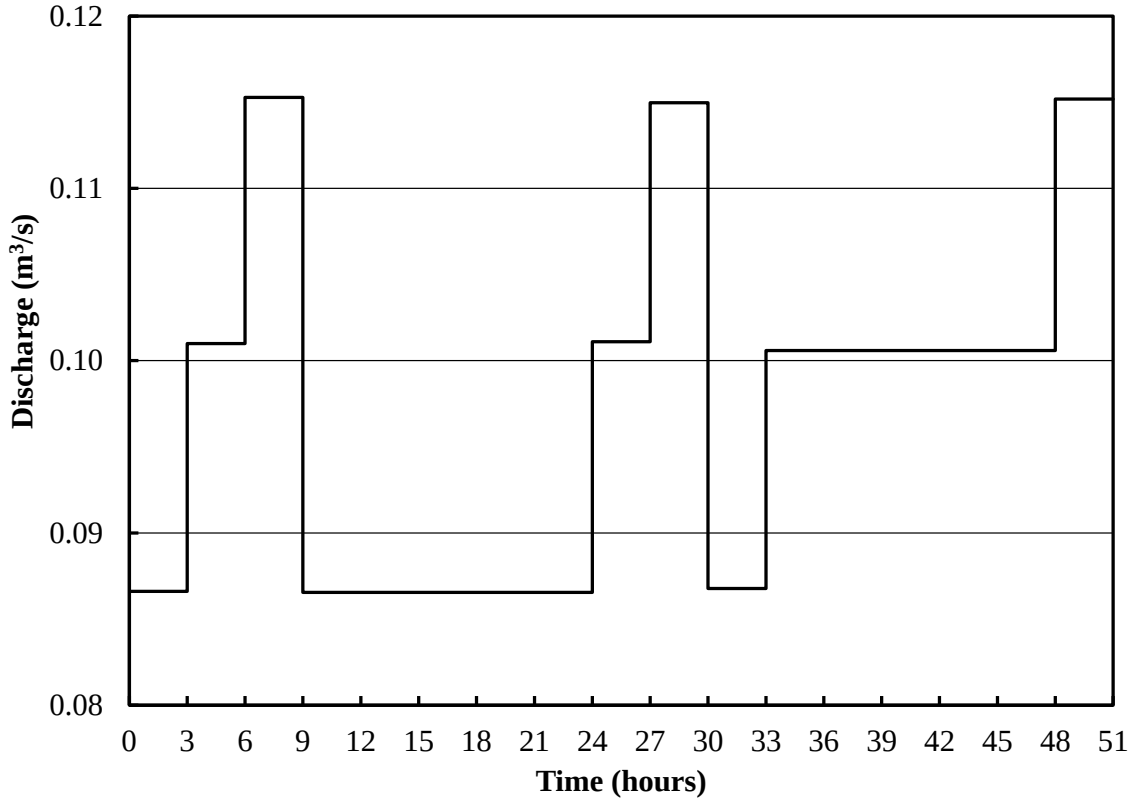

Figure 3.16: Hydrograph No. 8

CHAPTER 4

STEADY FLOW EXPERIMENTS

In this chapter, the steady state experimental results are discussed in detail. The results include the temporal evolution of scour, various equations to predict scour, and the similarity of the scour hole with time and flow conditions. Scour depths were compared with methods recommended by Kothyari et al. (1992), Totapally (1998), Melville and Chiew (1999), FHWA (2001), Oliveto and Hager (2002), and Chang et al. (2004). The steady state experiments were conducted using three different flow rates. The flow depth was always 254 mm and the critical shear velocity for the sediment size tested was 3.42 cm/s. A summary table of the flow conditions is shown below in Table 4.1.

Table 4.1: Summary of Steady Flow Tests

Test No.	t_e (hours)	Discharge (m^3/s)	Flow Depth (mm)	Velocity (m/s)	V/V_c	u_* (cm/s)	d_{se} (mm)
Q1	113.6	0.087	254	0.286	0.49	1.60	92.4
Q2	211.3	0.101	254	0.334	0.57	2.08	140.6
Q3	152.1	0.115	254	0.379	0.65	2.93	188.4

Temporal Evolution of Scour

At the initiation of flow, pier scour is rapid with the greatest rate of scour observed during the initial stages of testing. This is due to the horseshoe vortex being the strongest at this time. As the scour hole develops and expands in three dimensions, vortices are

eventually not strong enough to remove sediment. This has been documented in numerous local scour studies around bridge piers and abutments, for example, Cunha (1975), Franzetti (1989), and Totapally (1998), and this trend was observed in the present study as well. The temporal scour evolution for each test is shown in Figure 4.1 along with the non-dimensionalized scour evolution in Figure 4.2. Power equations were fitted to both Figure 4.1 and 4.2

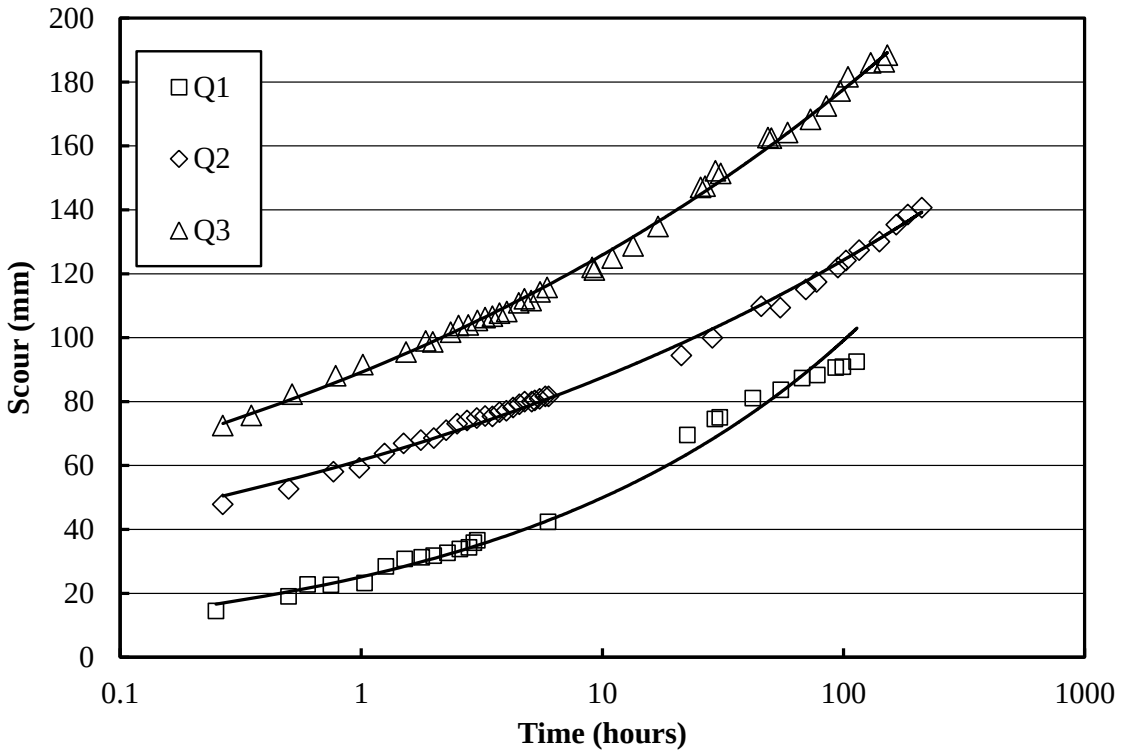

Figure 4.1: Steady Flow Temporal Scour Depth Evolution

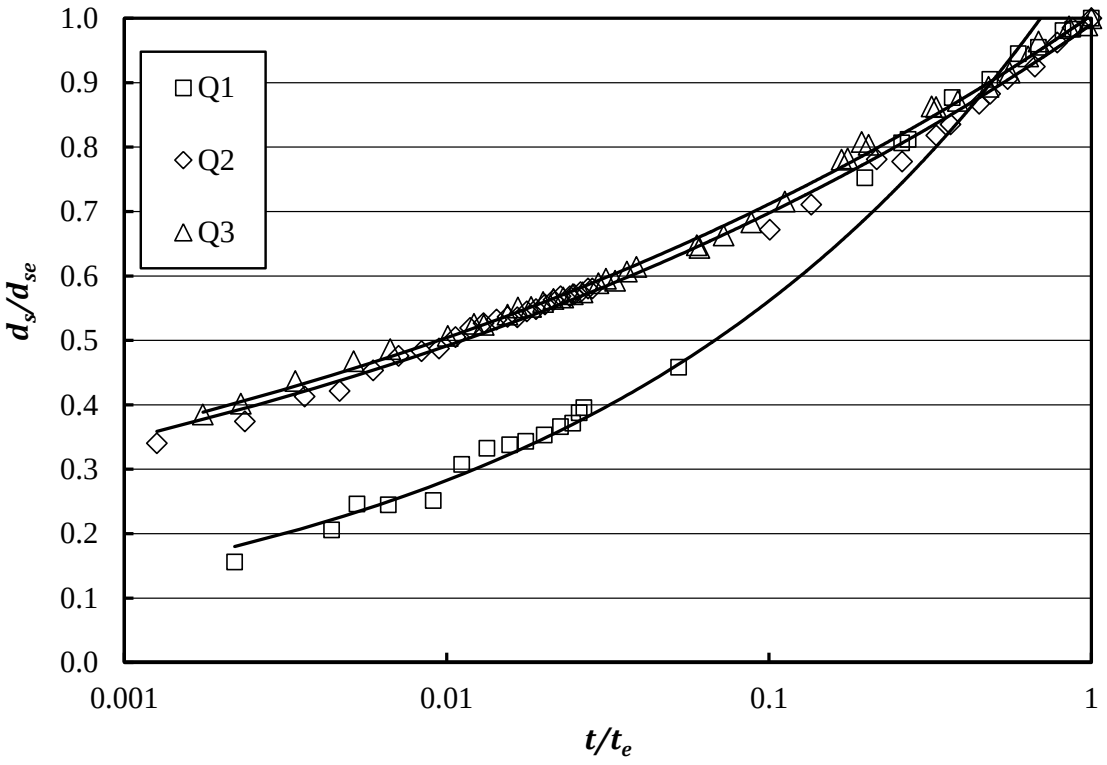

Figure 4.2: Non-Dimensionalized Steady Flow Temporal Scour Depth Evolution

The time to reach the equilibrium scour depth, as defined by Melville and Chiew (1999), ranged from 114 to 211 hours. All three runs reached 50% to 80% of equilibrium scour depth during just 10% of the time it took to reach the equilibrium time ($0.1\,t_e$) as previously documented by Melville and Chiew (1999) and is shown in Figure 4.2. Equilibrium scour depths increased with velocity. For Q1, Q2, and Q3, the equilibrium scour depths were 92.4 mm, 140.6 mm, and 188.4 mm, respectively.

Power equations fit the measured data for all tests very well. The non-dimensionalized scour evolution for tests Q2 and Q3 were very similar as shown in Figure 4.2. Test Q1

followed a different non-dimensional curve but was similar to a low critical velocity ratio test conducted by Melville and Chiew (1999). Currently there is no consensus in whether pier scour evolution is a power or logarithmic function with various researchers using different functions. Many researchers including Rouse (1965), Gill (1972), Dargahi (1990) and Oliveto and Hager (2002) have used a logarithmic function to describe temporal scour. Breusers (1967), Cunha (1975), and others used power laws to describe the process. The equations used in these experiments to describe each flow condition for steady and unsteady flow were the equations with the highest correlation in fitting the measured data. For all three flow conditions, power equations were the best fit to predict temporal scour evolution. Best-fit power and logarithmic equations and their respective correlation coefficients for each flow condition are shown in Table 4.2.

Figures 4.3 to 4.5 demonstrate that either logarithmic or power functions can adequately describe steady state pier scour evolution. Both logarithmic and power curves fit the data well during the early stages of scour evolution; however the logarithmic curve tended to underestimate scour depths during longer flood durations for high flows (Q2 and Q3). For Q2 and Q3, the scour evolution was measured multiple times to ensure repeatability. Figures 4.4 and 4.5 also showed that the experiments were repeatable.

Table 4.2: Comparison of Best-Fit Temporal Scour Equations

Test No.	Range of Data Points	No. of Data Points	Logarithmic[(1)] Equation			Power[(2)] Equation		
			m	c	R^2	m	c	R^2
Q1	All Data	25	14.3	-33.6	0.98	7.4	0.298	0.99
Q2	All Data	37	13.8	2.8	0.98	33.1	0.152	0.99
Q3	All Data	40	18.9	9.1	0.98	48.3	0.150	1.00

Notes:

(1) $d_s = mln(t) + c$

(2) $d_s = mt^c$

(3) d_s in mm and t in minutes

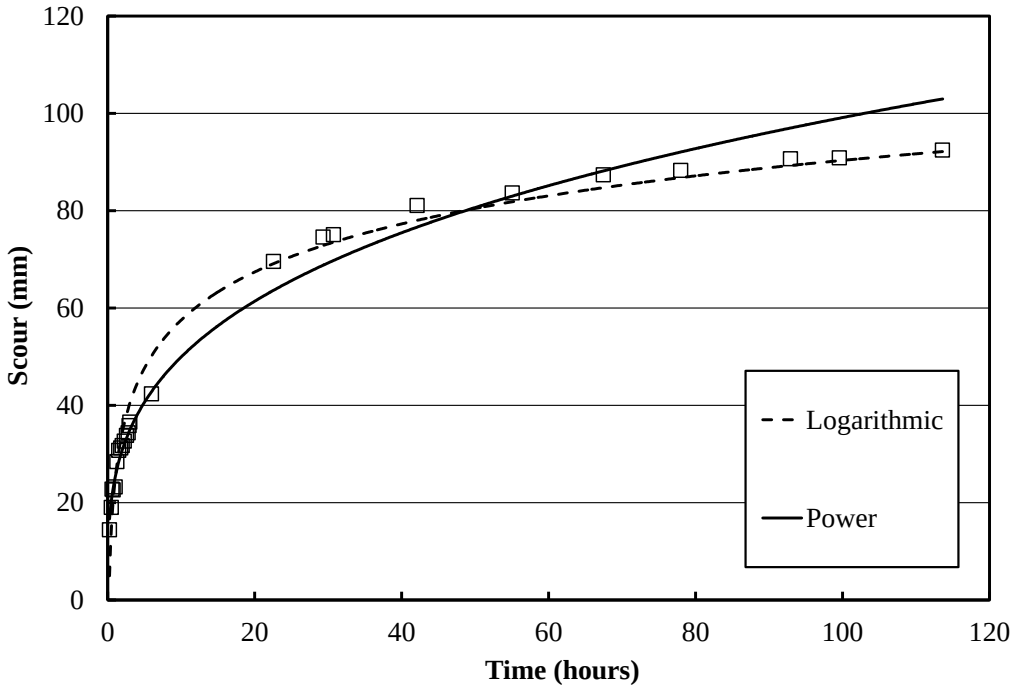

Figure 4.3: Temporal Scour Depth Evolution, Q1

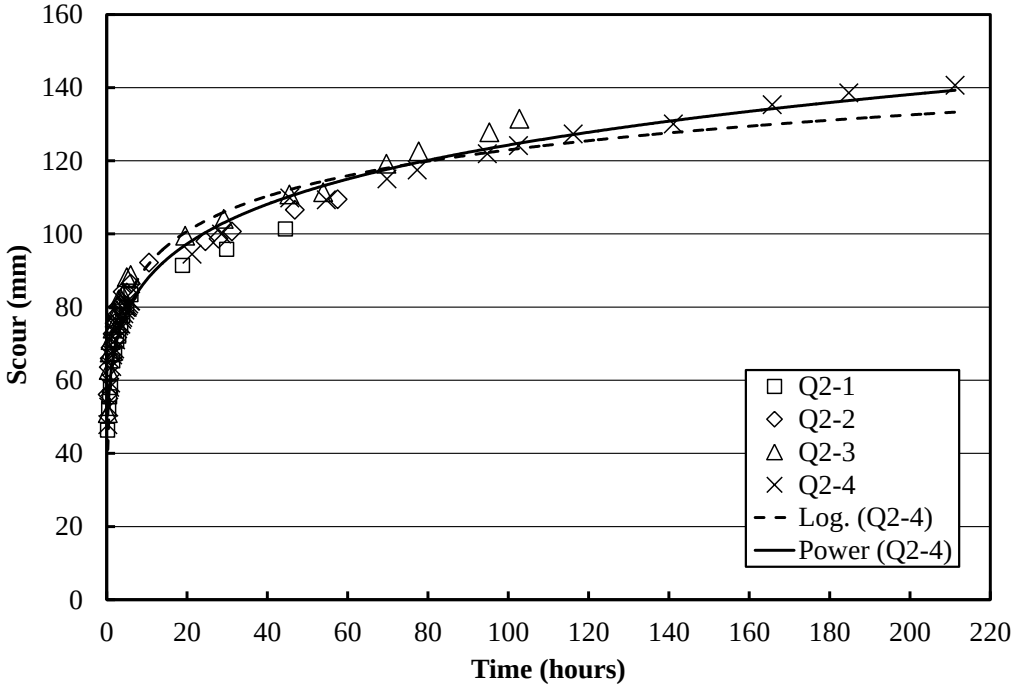

Figure 4.4: Temporal Scour Depth Evolution, Q2

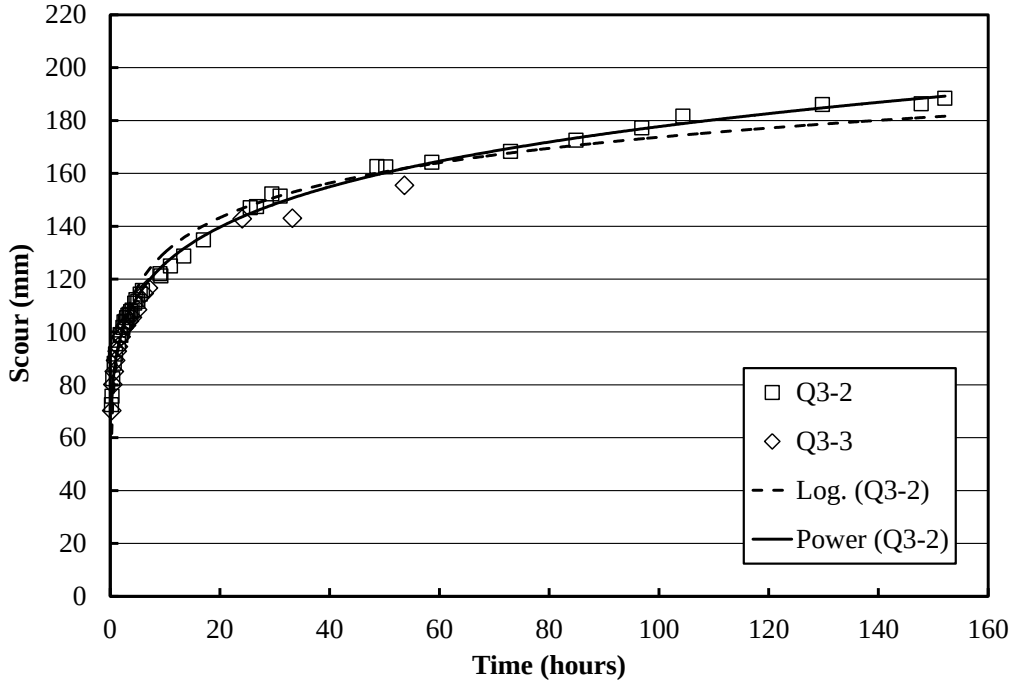

Figure 4.5: Temporal Scour Depth Evolution, Q3

Comparison with Temporal Scour Equations and FHWA (2001) Method

A comparison of measured equilibrium scour depths with calculated equilibrium scour depths from the CSU equation, recommended by the FHWA (2001) in HEC-18, was made and shown in Figure 4.6. Measured values were close to the calculated values for Q2 and Q3 but equilibrium scour depths were slightly under predicted. For flow condition Q1, the scour depth was over predicted by the FHWA equation by 33%. These discrepancies of the CSU equation may be attributed to the fact that the original data set used b/d_{50} ratios from 96 to 633 (Jones and Sheppard, 2000). This was significantly higher than the ratio of 51 used in this study.

Comparisons between the measured and calculated equilibrium scour depth were also made using several temporal scour evolution equations. These methods included Kothyari et al. (1992), Melville and Chiew (1999), Oliveto and Hager (2002), and Chang et al. (2004). The computed versus measured equilibrium scour depths are also shown in Figure 4.6.

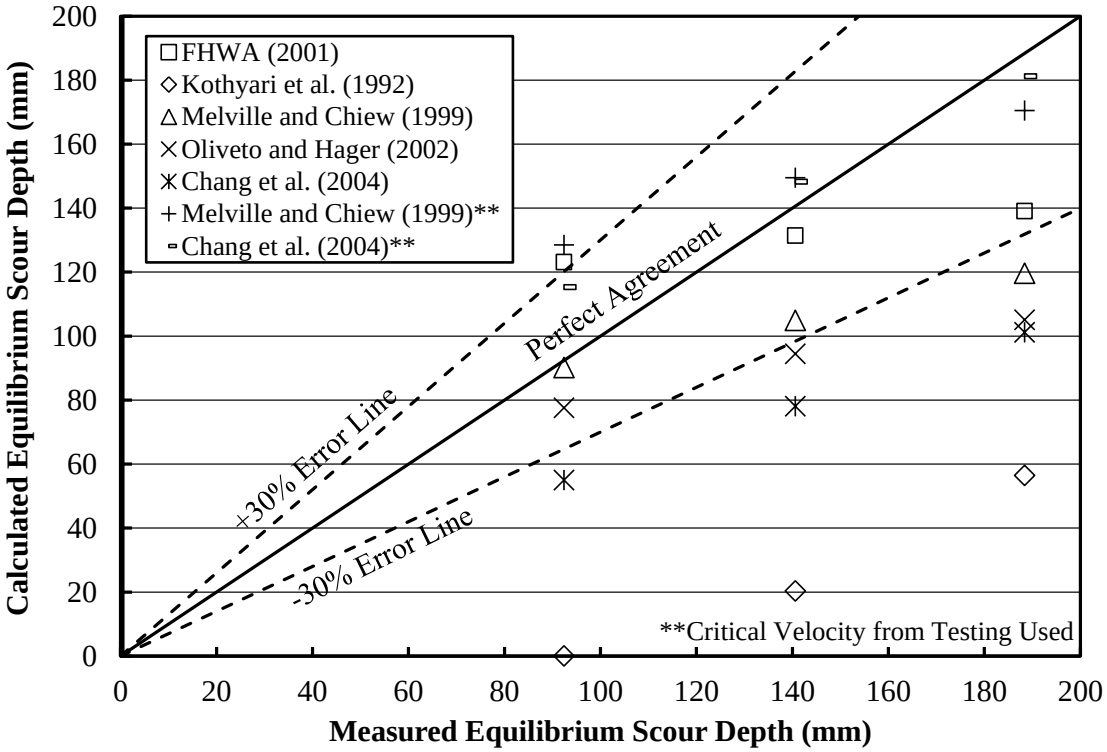

Figure 4.6: Comparison of Equilibrium Scour Depth Predictions

In computing equilibrium scour depth (d_{se}) and time to reach equilibrium scour depth (t_e) using the algorithm by Kothyari et al. (1992), an angle of repose of 30º suggested by Kothyari et al. (1992) and the measured angle of repose (38º) were used for comparison. It was found that the method described by Kothyari et al. (1992) under predicted d_{se} and t_e, regardless of which angle of repose was used. Results from Kothyari et al. (1992) are shown with an angle of repose of 30º in the figures and tables. Dimensionless temporal scour evolution for flow conditions Q1, Q2, and Q3 are shown in Figures 4.7 to 4.9, respectively. The equilibrium time and scour depth used is from the measured data. During flow condition Q1, no scour was computed based on Kothyari et al. (1992) as the

computed shear stress was lower than their definition of the incipient shear stress to cause local scour. Mia and Nago (2003) compared the method by Kothyari et al. (1992) with data from Chabert and Engeldinger (1956), Ettema (1980), Yanmaz and Atlinbilek (1991), and their own. The authors came to a similar conclusion, that the algorithm under predicted both equilibrium scour depth and time.

From preliminary testing the critical velocity was found to be 0.41 m/s. The Melville and Chiew's (1999) method suggested finding the critical velocity using equation 3.1, and a value of 0.58 m/s was found. Temporal scour profiles were computed using both measured and computed critical velocities. Using the calculated critical velocity of 0.58 m/s, the method described by Melville and Chiew (1999) predicted equilibrium scour depths within ±25% of the measured data for Q1 and Q2. For flow condition Q3, scour was under predicted by 37%. The temporal scour depth evolution exhibited similar trends with the measured data for Q2 and Q3, as shown in Figures 4.8 and 4.9, respectively. Equilibrium scour times were substantially lower than the measurements for all three tests.

Using the measured critical velocity of 0.41 m/s, the Melville and Chiew's (1999) method predicted equilibrium scour within ±10% of the measured data for Q2 and Q3. For flow condition Q1, equilibrium scour was over predicted by 39%. The measured critical velocity provided more accurate equilibrium scour depths at higher flow conditions than the computed critical velocity. Using the measured critical velocity, the

Melville and Chiew's (1999) method can be used to predict equilibrium scour depths at higher flow conditions.

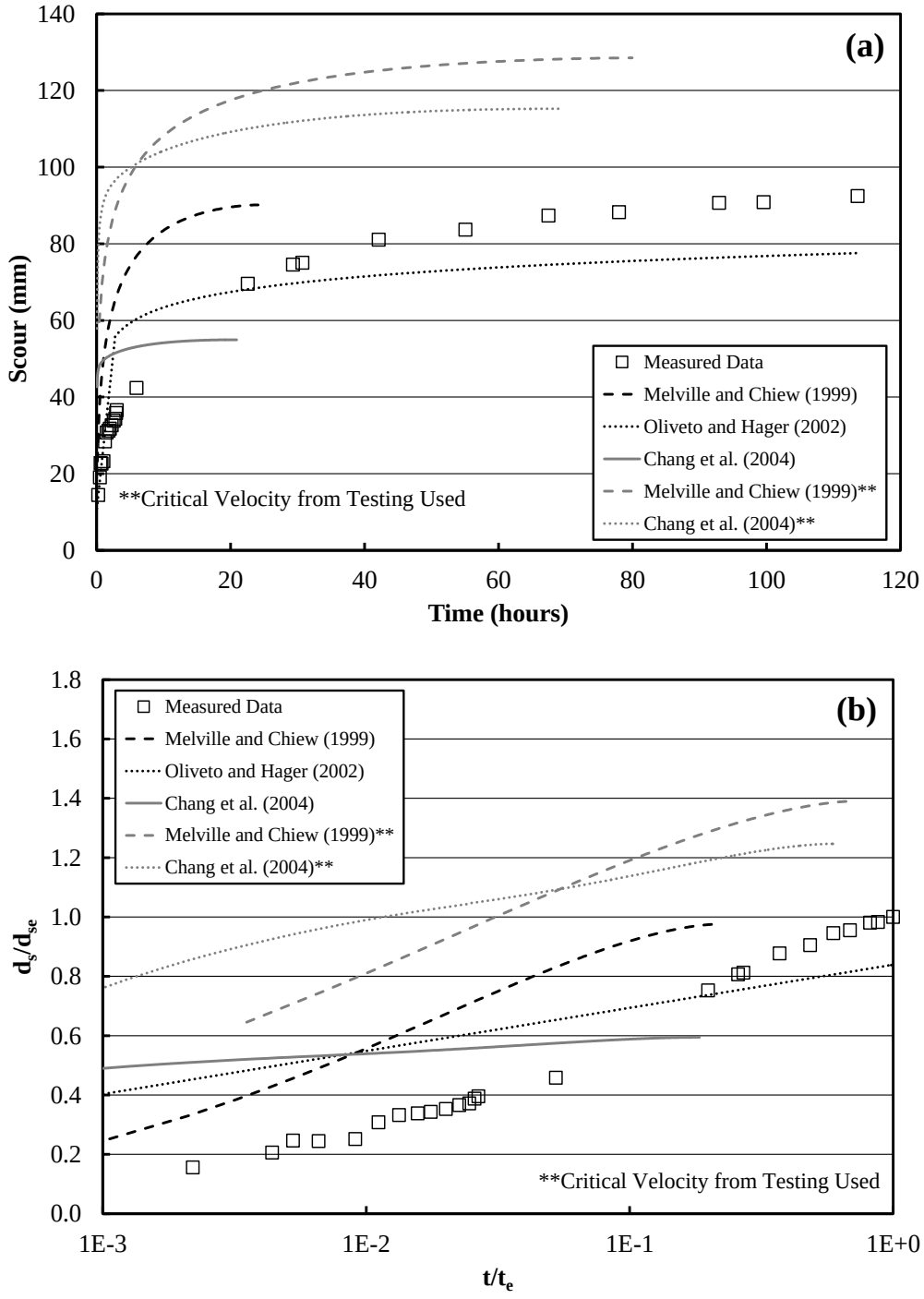

Figure 4.7: Calculated Temporal Scour Evolution, Q1

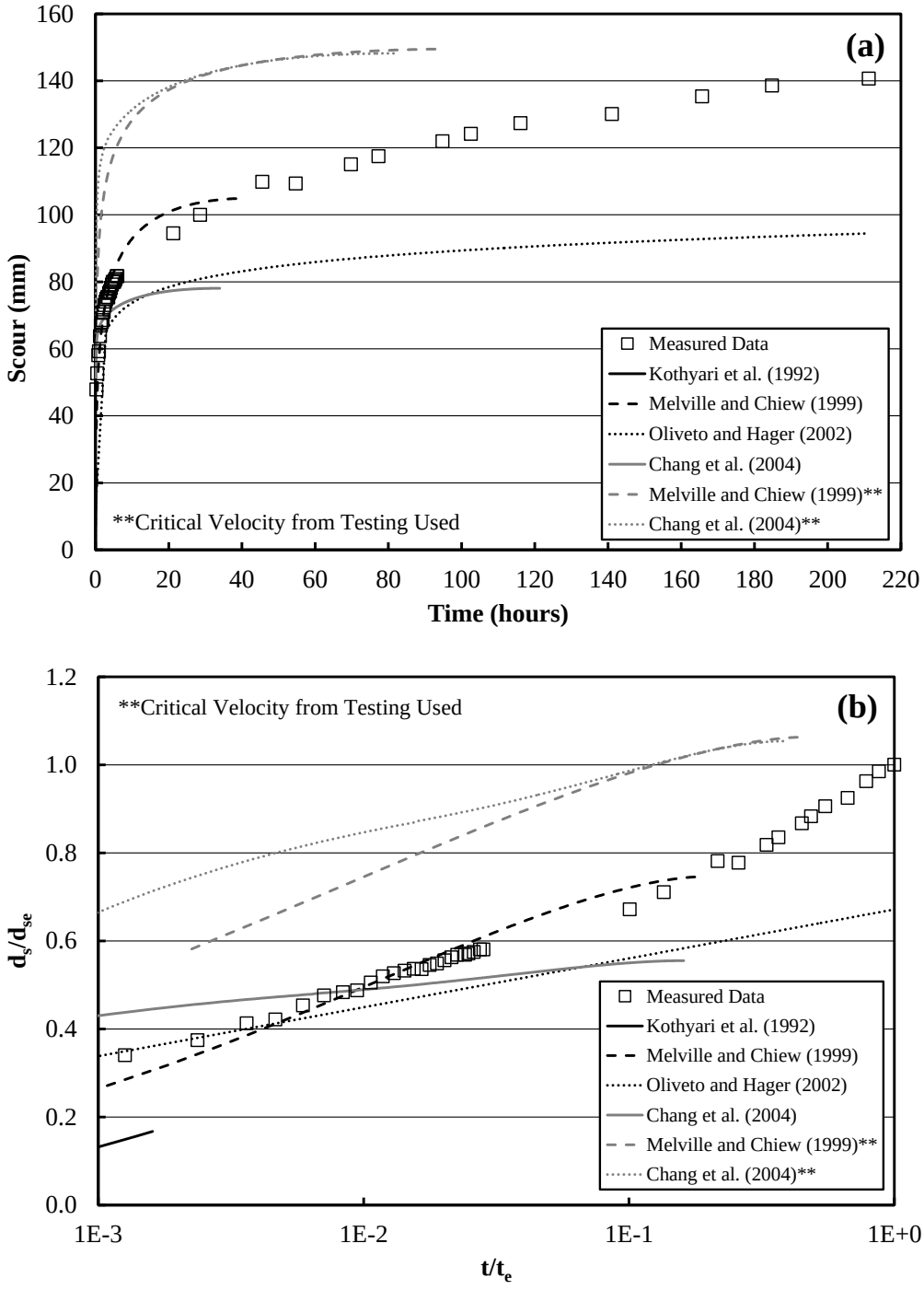

Figure 4.8: Calculated Temporal Scour Evolution, Q2

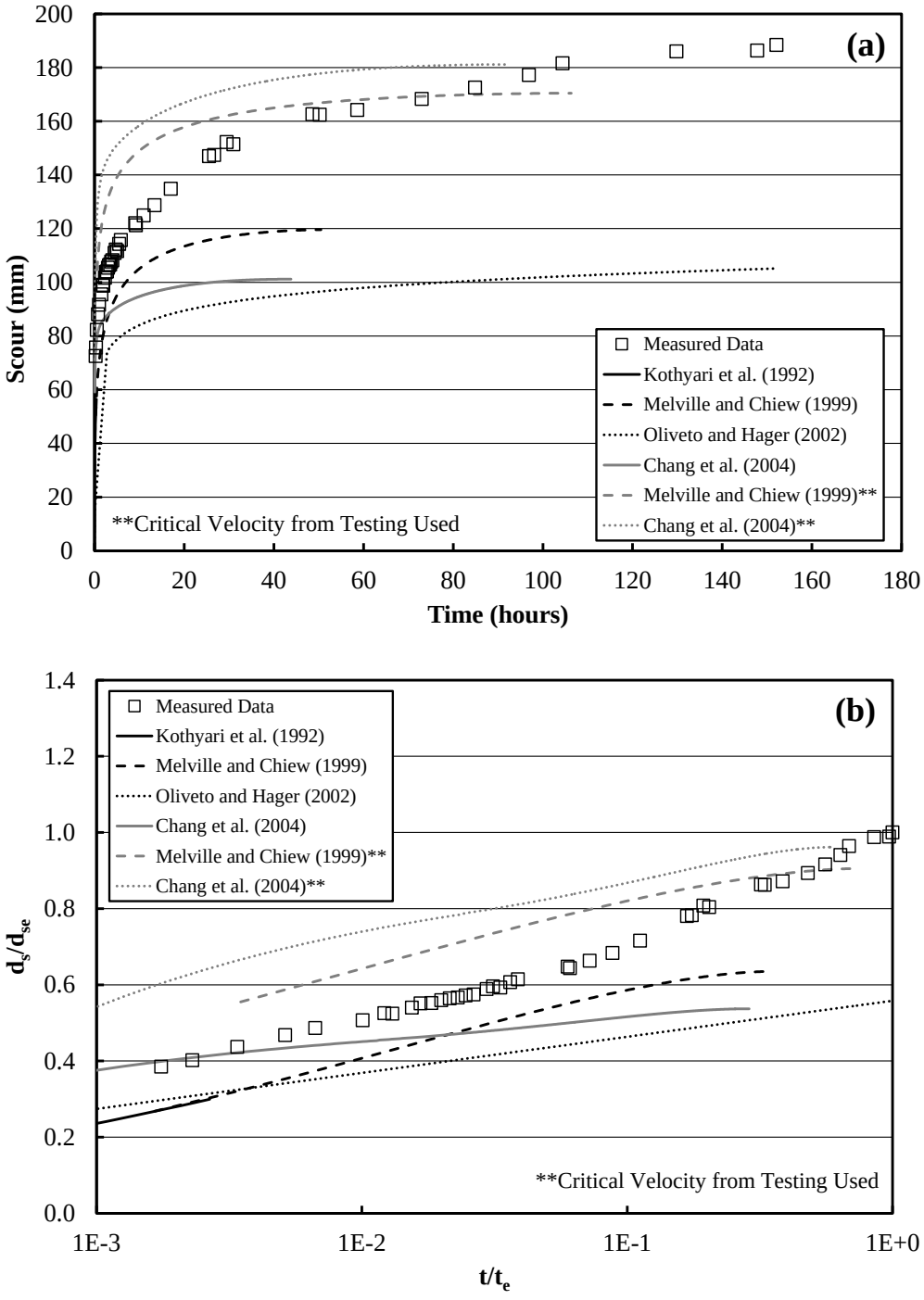

Figure 4.9: Calculated Temporal Scour Evolution, Q3

The scour evolution method proposed by Oliveto and Hager (2002) under predicted equilibrium scour depths for flow conditions Q2 and Q3 by a large margin (≥ 30%). The measured temporal evolution for flow conditions Q2 and Q3 deviated from the logarithmic function proposed by Oliveto and Hager (2002) as time increased. However, this method accurately predicted (<10%) equilibrium scour for flow condition Q1. Since this method did not deploy a time to equilibrium scour, the calculation procedure was repeated until the measured equilibrium time was reached. Due to the generally high margin of error in predicting steady state temporal scour evolution, this method was deemed unsuitable for calculating temporal scour under stepped hydrographs.

For computed critical velocity of 0.58 m/s (based on equation 2.17), the temporal scour method proposed by Chang et al. (2004) under predicted equilibrium scour and time for all three test conditions. The temporal scour evolution deviated from the measured trends as well, with the highest deviations observed at greater times. The predicted equilibrium time increased with greater flow intensities. The authors also proposed another procedure to correct for errors in the critical velocity calculations. Where, if the equilibrium scour depth was known for a flow condition, the critical velocity could be determined using equation 2.18. Using this method, the critical velocity was calculated as 0.46, 0.42, and 0.40 m/s for flow conditions Q1, Q2, and Q3, respectively. Since these calculated critical velocities were very similar to the measured value (0.41 m/s), it was determined that the critical velocity from preliminary testing was sufficiently accurate and could be used instead.

Using the measured critical velocity of 0.41 m/s, predicted equilibrium scour depths from Chang et al. (2004) were within ± 25% of the measured data for all three flow conditions. Equilibrium times were still less than the measured values but were much closer than those found using computed critical velocity. The computed temporal scour evolution for each test is shown in Figures 4.7 to 4.9. The accuracy of the computed equilibrium scour depths improved using the measured critical velocity. The measured equilibrium scour depths and time are summarized in Table 4.3 and compared with several other methods.

By comparing multiple temporal scour evolution methods, it was determined that the methods proposed by Melville and Chiew (1999) and Chang et al. (2004) using the measured critical velocity and the best-fit power equations were the most accurate in predicting temporal scour evolution under steady flows. The logarithmic equations also reasonably fit the data but tended to under predict scour as time increased. Procedures proposed by Kothyari et al. (1992) and Oliveto and Hager (2002) substantially under predicted temporal scour for all three flow conditions and were not used in the following chapter to compute temporal scour evolution under stepped hydrographs. Calculated equilibrium scour using the CSU equation (FHWA, 2001) also predicted equilibrium scour reasonably (±30%) for flow conditions Q2 and Q3 but not as well for Q1.

Table 4.3: Comparison of Scour Predictions

	Test No.					
	Q1		Q2		Q3	
	d_{se} (mm)	t_e (min)	d_{se} (mm)	t_e (min)	d_{se} (mm)	t_e (min)
Measured	92.4	6818	140.6	12675	188.4	9128
Kothyari et al. (1992)	N/A[(1)]	N/A[(1)]	20.3	24	56.4	24
Melville & Chiew (1999, V_c = 0.58 m/s)	90.2	1446	104.9	2349	119.6	3029
Oliveto & Hager (2002)	77.6	6818[(2)]	94.4	12675[(2)]	105.1	8870[(2)]
Chang et al. (2004, V_c = 0.58 m/s)	55.0	1254	78.1	2037	101.2	2628
FHWA (2001)	123.1	N/A[(3)]	131.4	N/A[(3)]	139.0	N/A[(3)]
Melville & Chiew (1999, V_c = 0.41 m/s)	128.5	4797	149.5	5699	170.5	6379
Chang et al. (2004, V_c = 0.41 m/s)	115.2	4165	148.2	4948	181.1	5538

Notes:

(1) The shear velocity was less than the critical value of incipient local pier scour defined by Kothyari et al. (1992)

(2) Equilibrium time was from measured data since this is not defined by Oliveto and Hager (2002)

(3) Equilibrium time is not used in FHWA (2001) method

Scour Hole Similarity under Steady Flows

During steady state testing, the longitudinal scour hole profile was periodically measured to determine how the shape of the scour hole changed with time. Most research had focused on temporal scour depth evolution and not the scour hole geometry. In order to accurately predict scour under various flow conditions, any potential changes in the scour hole geometry might be of importance. Yanmaz and Altinbek (1991) studied bridge pier scour under steady flows and Totapally (1998) measured abutment scour under steady

flows and stepped hydrographs. The scour hole geometry changed with time and flow conditions, however, the non-dimensional scour hole geometry was similar. This is significant, as steady state scour evolution equations may not be accurate when applied to stepped hydrographs if the scour hole geometry is different for various flow conditions.

It was determined that the non-dimensional scour hole geometry remained the same regardless of time or steady state flow condition. The slope of the scour hole was always approximately 38º. Dimensional and non-dimensional scour hole profiles were plotted at various times for each flow condition upstream of the pier. The following six figures (Figure 4.10 to 4.15) show the longitudinal scour profiles and the corresponding non-dimensional scour profile for individual flow conditions Q1, Q2, and Q3, respectively. Figure 4.16 shows the non-dimensional scour profiles for all three flow conditions.

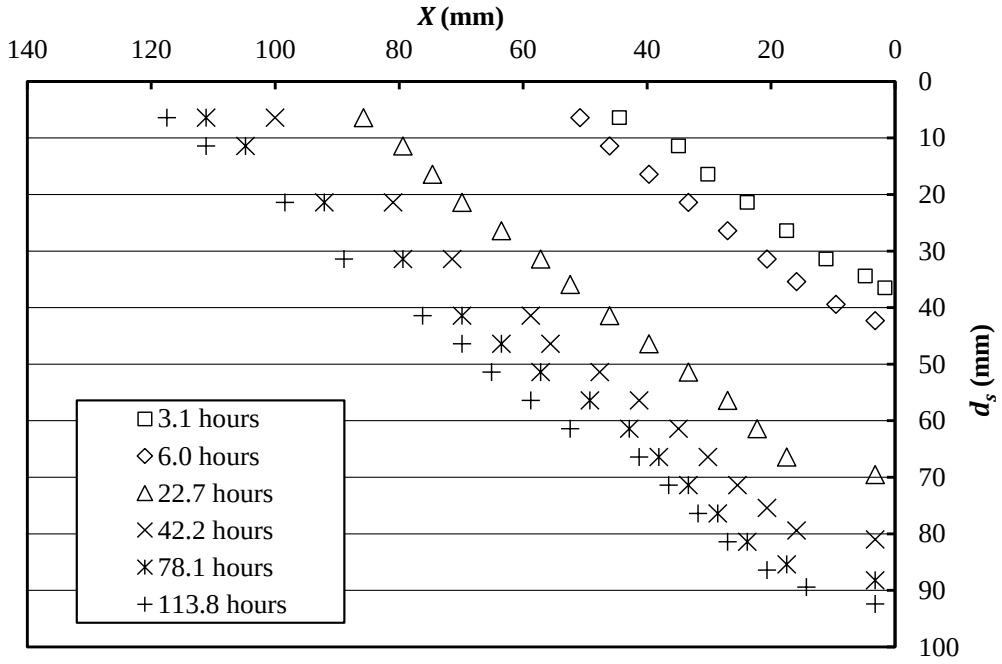

Figure 4.10: Dimensionalized Scour Hole Similarity, Q1

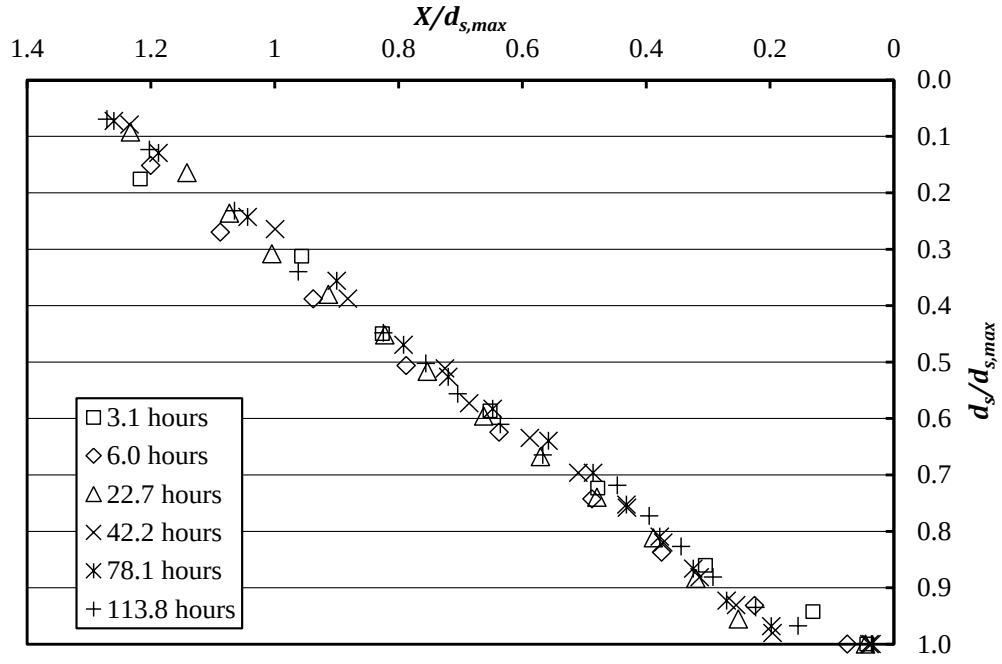

Figure 4.11: Non-Dimensionalized Scour Hole Similarity, Q1

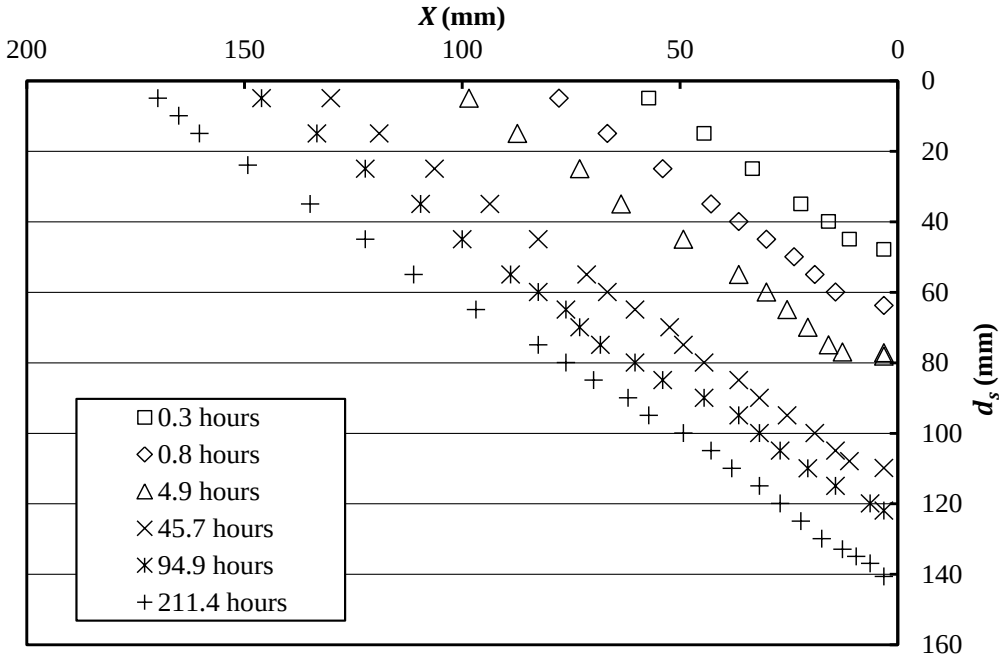

Figure 4.12: Dimensionalized Scour Hole Similarity, Q2

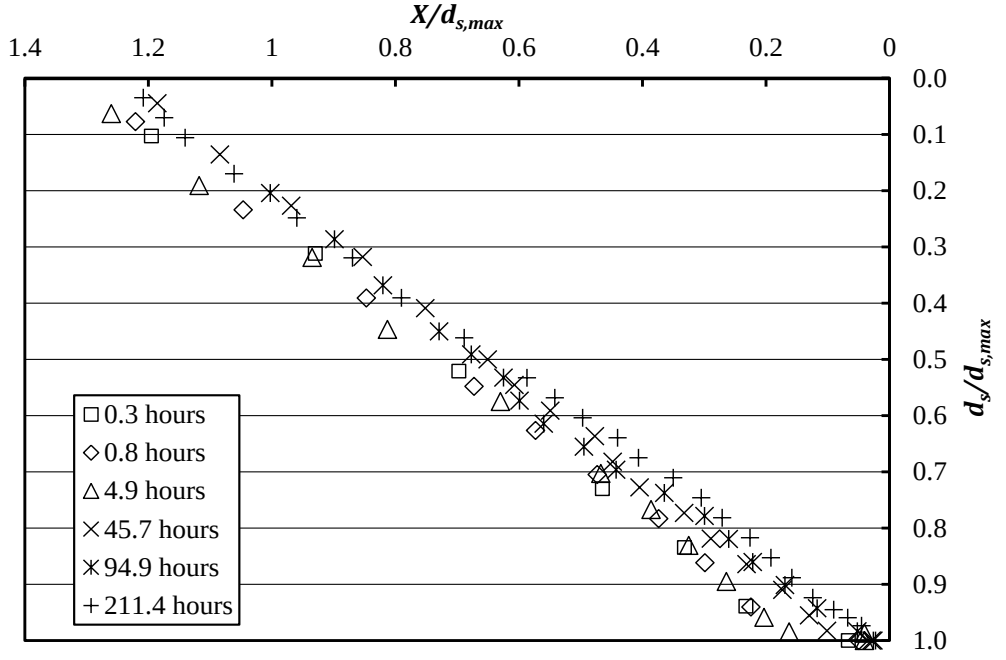

Figure 4.13: Non-Dimensionalized Scour Hole Similarity, Q2

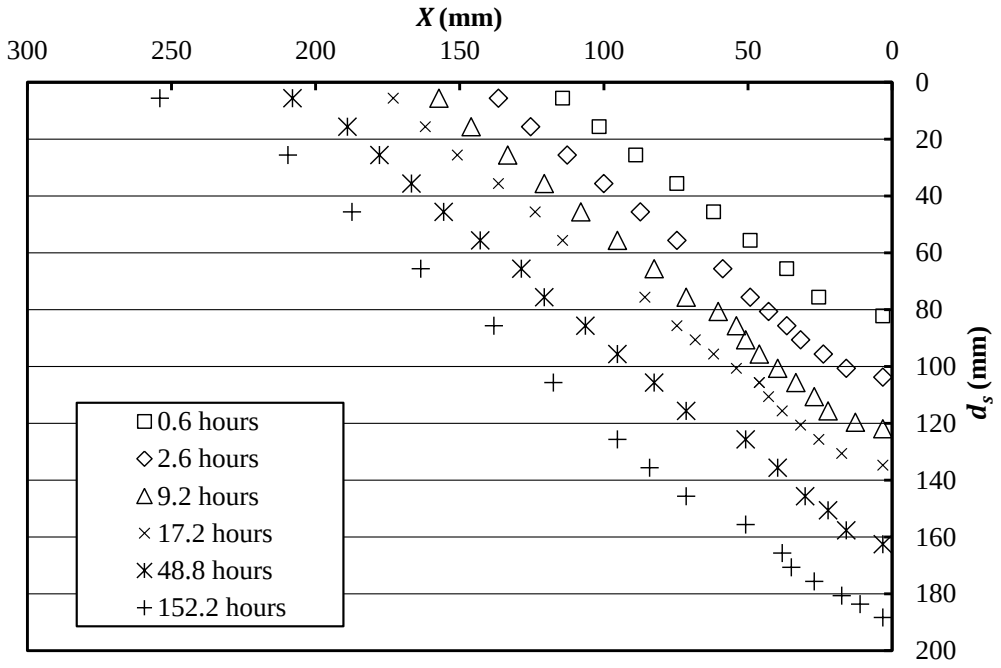

Figure 4.14: Dimensionalized Scour Hole Similarity, Q3

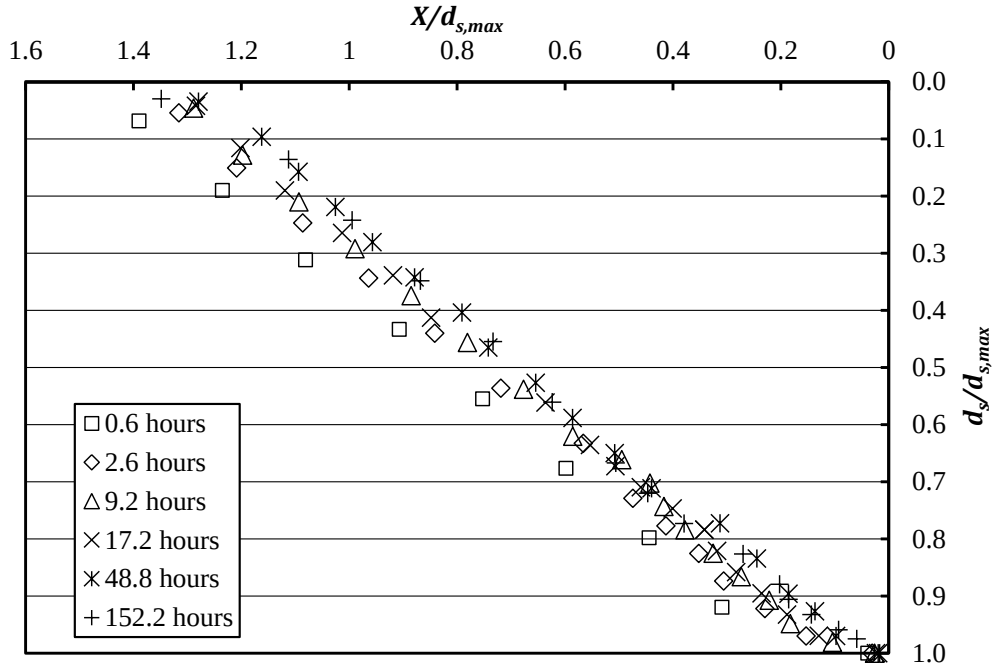

Figure 4.15: Non-Dimensionalized Scour Hole Similarity, Q3

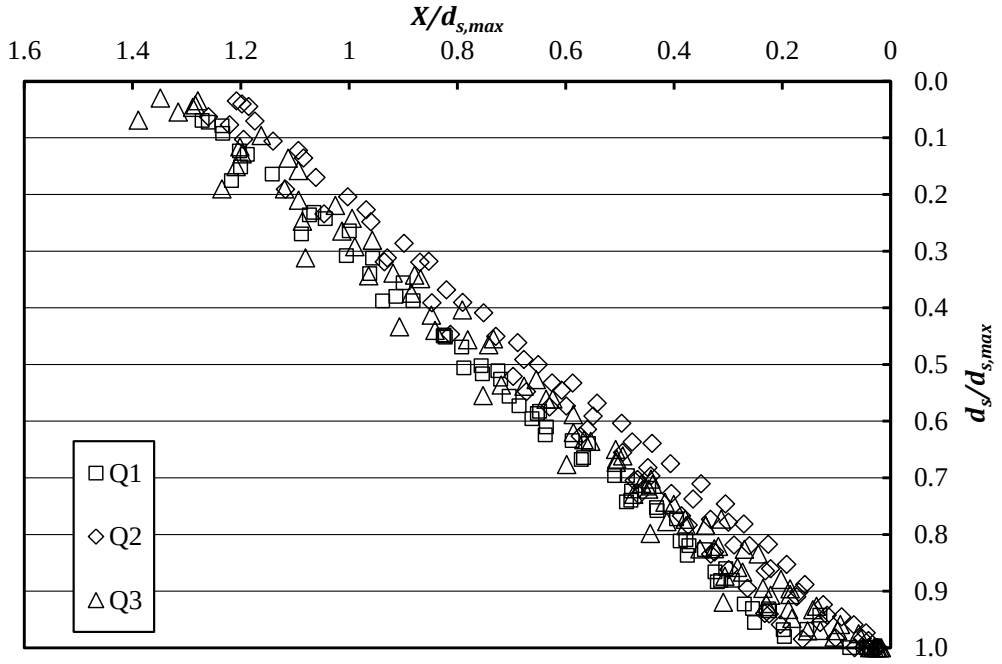

Figure 4.16: Non-Dimensionalized Scour Hole Similarity, All Tests

It is visually apparent from the scour hole profiles, that the scour hole maintained a similar shape regardless of the flow condition or time. From Figures 4.10 to 4.16, it is clear that the top width can be estimated if the bottom width (also called groove) and the angle of repose are known. This method is used by FHWA (2001) and was discussed previously. The bottom width of the scour hole was always small relative to the top width for each test. For practical purposes, the bottom width can be ignored and the slope may be extended up to the face of the pier. This approach was proposed by Carstens (1966) and Shen et al. (1969) to estimate the entire scour hole volume and is discussed in greater detail in Chapter 2. These methods (Carstens, 1966 and Shen et al., 1969) may not allow for a high level of accuracy as it was observed that the longitudinal slope was steeper upstream of the pier compared to downstream.

CHAPTER 5

UNSTEADY FLOW EXPERIMENTS

In this chapter, the unsteady state experimental results are discussed in detail. This chapter includes the temporal evolution of scour under stepped hydrographs. In addition, various equations to predict scour using the method of superposition, the effect of flood order on scour, and the similarity of the scour hole under various hydrographs are evaluated. Temporal scour evolution is compared with various steady state scour equations using the method of superposition. The methods evaluated to predict unsteady scour are the best-fit power and logarithmic functions and procedures described by Melville and Chiew (1999) and Chang et al. (2004) using the measured critical velocity from testing (0.41 m/s). These methods were selected based on their reasonable accuracy in predicting the temporal scour evolution under steady state flows (discussed in Chapter 4).

Eight unsteady tests were conducted using three different flow velocities. The flow depth was always 254 mm and the critical shear velocity for the sediment size tested was 3.42 cm/s. Some tests were repeated to verify data. The unsteady test conditions are shown in Tables 3.5 to 3.12 and Figures 3.9 to 3.16.

Method of Superposition

Using the method of superposition, scour depths under stepped hydrographs can be predicted using best-fit equations from steady state data or steady state temporal evolution models such as those by Melville and Chiew (1999) and Chang et al. (2004). If a flood hydrograph is modeled as multiple steady state hydrographs, the scour can be predicted using these models if the flow conditions and initial scour depth are known.

The concept behind the method of superposition was the same regardless of the type of model used and this was used to predict scour under stepped hydrographs for power, logarithmic, and the steady state methods proposed by Melville and Chiew (1999) and Chang et al. (2004). This method has been used by multiple researchers including Kothyari et al. (1992), Totapally (1998), Chang et al. (2004), and Lu et al. (2011) to predict scour under stepped hydrographs. An example of the method of superposition for temporal scour using power equations is presented below. This process is adopted from Totapally (1998) who used logarithmic equations to calculate temporal scour under simulated hydrographs and is visually shown in Figure 5.1.

(1) Steady state scour depth evolution is estimated as a power equation where m and c are coefficients found using a regression analysis from measured data.

$$d_s = mt^c \tag{5.1}$$

(2) The starting scour depth d_{s1} is measured or calculated from the existing flow conditions (Totapally, 1998).

(3) The time t_{1*} to achieve the scour d_{s1} for the flow condition can be calculated from the temporal scour best fit equation and for the power law fit it can be calculated as follows:

$$t_{1*} = \left(\frac{d_{s1}}{m}\right)^{1/c} \tag{5.2}$$

(4) The scour depth at the end of the time step, Δt_1,can now be calculated as:

$$d_{s2} = m(t_{1*} + \Delta t_1)^c \tag{5.3}$$

Where Δt_1 is the flow duration and $t_2 = t_{1*} + \Delta t_1$.

(5) If the flow condition changes at t_2, the scour evolution will follow the new temporal scour curve. The scour depth, d_{s2}, is the starting scour depth for the new flow condition and the process above is repeated (Totapally, 1998).

(6) If the flow rate in the next time step is lower than the flow rate of the previous time, two possibilities exist (t_4 to t_{4*} in Figure 5.1). The first being where the scour hole depth at the end of the previous time step is lower than the equilibrium scour depth of the next flow condition. In this case, the same procedure as described above is adopted to calculate the scour depth during the next flow condition. However, if the scour depth at the end of the previous time step is higher than the equilibrium scour depth of the next flow condition, there is no change in the scour depth during the next flow condition.

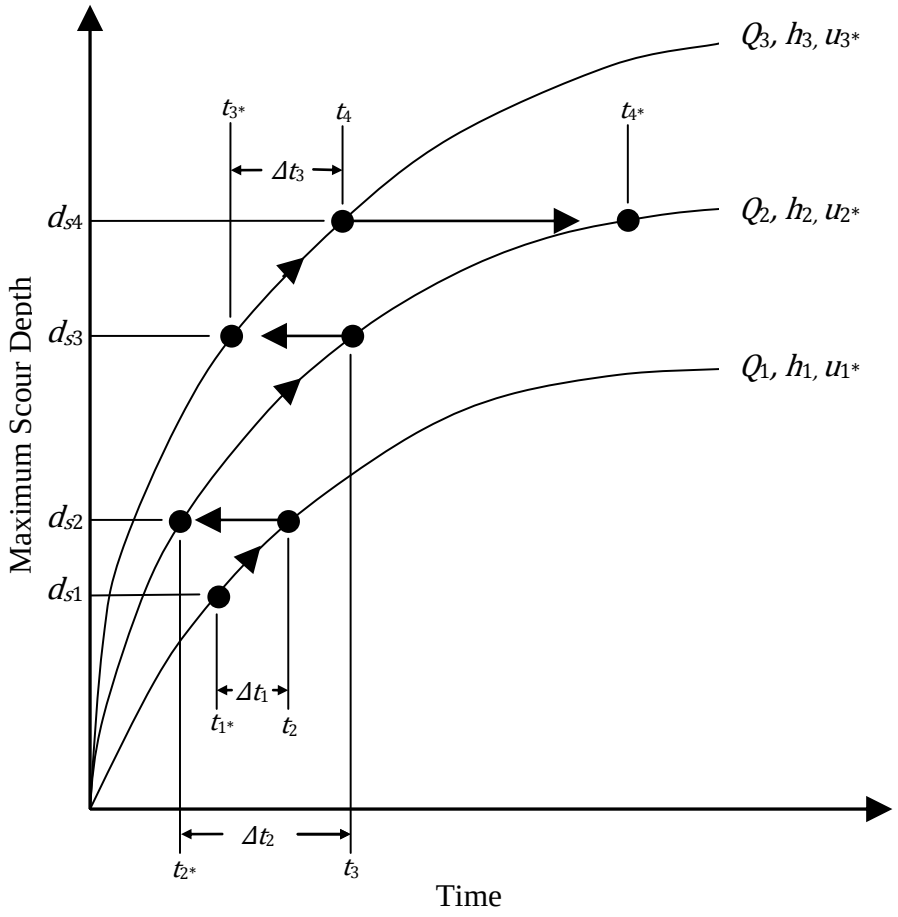

Figure 5.1: Method of Superposition (after Totapally, 1998)

Temporal Scour Predictions under Stepped Hydrographs

Scour depth under stepped hydrographs were predicted using best-fit logarithmic and power equations from measured scour data and from scour models proposed by Melville and Chiew (1999) and Chang et al. (2004) under steady flow conditions. The methods by Melville and Chiew (1999) and Chang et al. (2004) were employed using the measured critical velocity (0.41 m/s) instead of the respective authors' calculated critical velocity (0.58 m/s) as discussed in Chapter 4. All methods were adapted to predict scour under

stepped hydrographs using the method of superposition. The scour depth was assumed not to change during a flow step when the calculated scour depth was greater than the measured (power, logarithmic) or calculated (Melville and Chiew, 1999 and Chang et al., 2004) equilibrium scour depth for that flow condition.

Power equations were found to predict the scour evolution within ± 10% of the final scour depth for all eight unsteady tests. The error in the predicted scour was sometimes greater than 15% for the flow condition Q1. The reason being that the scour depth was small during the early stages of testing, so slight deviations (≤ 5 mm) from the trend was greater than the 15% error range. These deviations did not substantially affect the majority of the scour evolution predictions, as scour depths were relatively small compared to scour under the higher flow conditions (Q2 and Q3). The final scour depth was slightly over predicted for all tests except QU8. The power equations were considered to be accurate in predicting scour under stepped hydrographs.

Best-fit logarithmic equations were also found to reasonably predict temporal scour but not as accurately as the power equations. All tests were within ± 12% of the final scour depth. Slight deviations were sometimes observed during the early stages of testing for flow condition Q1. These deviations were due to the scour depth being small; this was similar to why data deviated from the power trend during the early stages of testing. Generally, the logarithmic equation over predicted scour as time increased.

The method proposed by Melville and Chiew (1999) using the measured critical velocity (0.41 m/s) over predicted scour evolution substantially for all eight unsteady tests. Final scour depths were over predicted by an average of 29%. Scour evolution under flow condition Q1 had the poorest relation between measured and predicted scour. This was also observed during the steady state tests. These over predictions may be attributed to the measured time to reach equilibrium (t_e) being substantially higher than the calculated value for all three steady state flow conditions. Due to the low calculated t_e values, the predicted scour rate was much higher than the observed rate, especially in the beginning part of the test.

The model by Chang et al. (2004) using V_c = 0.41 m/s (> 30%), significantly over predicted scour evolution for all the tests regardless of flow condition. Final scour depths were over predicted by an average of 39%. This is likely due to the predicted equilibrium times under steady state flow being substantially lower than the measured equilibrium times. A comparison of the final scour depth with all four temporal scour methods is shown in Table 5.1. In addition, the predicted equilibrium scour depth for flow condition Q3 (the highest flow encountered) based on the FHWA (2001) procedure is shown in Table 5.1. For QU4, three pulses were used, the first one being Q1 for three hours, the second one being Q3 for three hours, and the last pulse of Q1 discharge was sustained for about 75 hours. The final scour depth for QU4 is shown at 9 hours after the start of the test in the table, as very little change in scour depth was observed after this time.

Table 5.1: Comparison of Final Scour Depth Predictions

Test No.	Final Scour Depth	% Error				
	(mm)	Logarithmic	Power	Melville and Chiew (1999)	Chang et al. (2004)	FHWA (2001)
QU1	102.0	5.6%	9.4%	35.0%	44.7%	36.3%
QU2	99.3	10.9%	7.2%	35.9%	48.4%	40.0%
QU3	103.9	5.0%	2.1%	30.0%	41.4%	33.8%
QU4	99.2 (at 9 hrs)	8.8%	6.0%	33.6%	47.8%	40.2%
QU5	99.4	12.1%	8.4%	37.9%	48.5%	39.9%
QU6	125.3	6.8%	3.2%	20.9%	28.1%	10.9%
QU7	120.5	12.2%	9.8%	27.2%	33.3%	15.3%
QU8	135.1	-3.0%	-5.6%	12.0%	16.8%	2.9%
Avg. of Absolute Error		**8.0%**	**6.5%**	**29.1%**	**38.6%**	**27.4%**

By comparing multiple temporal scour evolution methods, it was determined that the best-fit power equations accurately predicted the temporal evolution of scour when the initial scour depth and flow conditions are known. The majority of measurements were within ± 15% of the predicted scour depth and all final scour depths were within ± 10% of the final scour depth. Logarithmic equations also reasonably predicted scour, with all tests within ± 12% of the final scour depth. The methods proposed by Melville and Chiew (1999) and Chang et al. (2004) did not accurately model temporal scour depths; consistently over predicting the final scour depth by an average of 29% and 39%, respectively. This is likely due to the measured steady state t_e being less than the calculated values of the respective authors' models for all steady state flow conditions. The adapted models by Melville and Chiew (1999) and Chang et al. (2004) predicted the

final scour depth less accurately than the CSU equilibrium scour equation (FHWA, 2001), using flow condition Q3. This shows that unsteady temporal scour models may not give the designer any more confidence in bridge pier scour predictions than simpler equilibrium scour equations.

Maximum scour depths for all eight unsteady tests were less than the equilibrium scour depth for steady state flow condition Q3. During test QU4, no significant increase in maximum scour (0.2 mm over 75 hours) was observed when a low flow condition, Q1, was run after a previous flood had exceeded d_{se} for the low flood condition. This indicates that multiple smaller flood events cannot cause greater scour than larger flood events that reach equilibrium. However, more tests need to be conducted to confirm the finding. The measured and predicted temporal scour depth evolution is shown in Figures 5.2 to 5.9. The scour depths at the end of each flow step are shown below in Table 5.2.

Table 5.2: Scour Depth at the End of Each Flow Step

Scour Depth (mm)								
Unsteady Test No.								
Time (hours)	QU1	QU2	QU3	QU4	QU5	QU6	QU7	QU8
3	36.2	78.7	35.8	42.3	75.9	105.2	94.3	34.5
6	74.5	105.8	102.5	105.1	94.8(1)	103.3	95.3	83.6
9	98.8	99.3	103.9	99.2	99.4	110.6	101.5	106.0
12	101.9	N/A	N/A	N/A	N/A	N/A	N/A	N/A
15	102.0	N/A	N/A	N/A	N/A	N/A	N/A	N/A
24	N/A	N/A	N/A	N/A	N/A	N/A	106.0	108.0
25	N/A	N/A	N/A	N/A	N/A	113.1	N/A	N/A
27	N/A	N/A	N/A	N/A	N/A	N/A	110.3	113.5
28	N/A	N/A	N/A	N/A	N/A	122.2	N/A	N/A
30	N/A	N/A	N/A	N/A	N/A	N/A	113.0	122.7
31	N/A	N/A	N/A	N/A	N/A	119.6(2)	N/A	N/A
33	N/A	N/A	N/A	N/A	N/A	N/A	120.5	120.1
34	N/A	N/A	N/A	N/A	N/A	125.3	N/A	N/A
48	N/A	N/A	N/A	N/A	N/A	N/A	N/A	131.9
51	N/A	N/A	N/A	N/A	N/A	N/A	N/A	135.1
80.6	N/A	N/A	N/A	105.3	N/A	N/A	N/A	N/A

Notes:

(1) Measurement taken at 5 hrs. 45 minutes

(2) Measurement taken at 30 hrs. 51 minutes; scour rate was minimal at this time

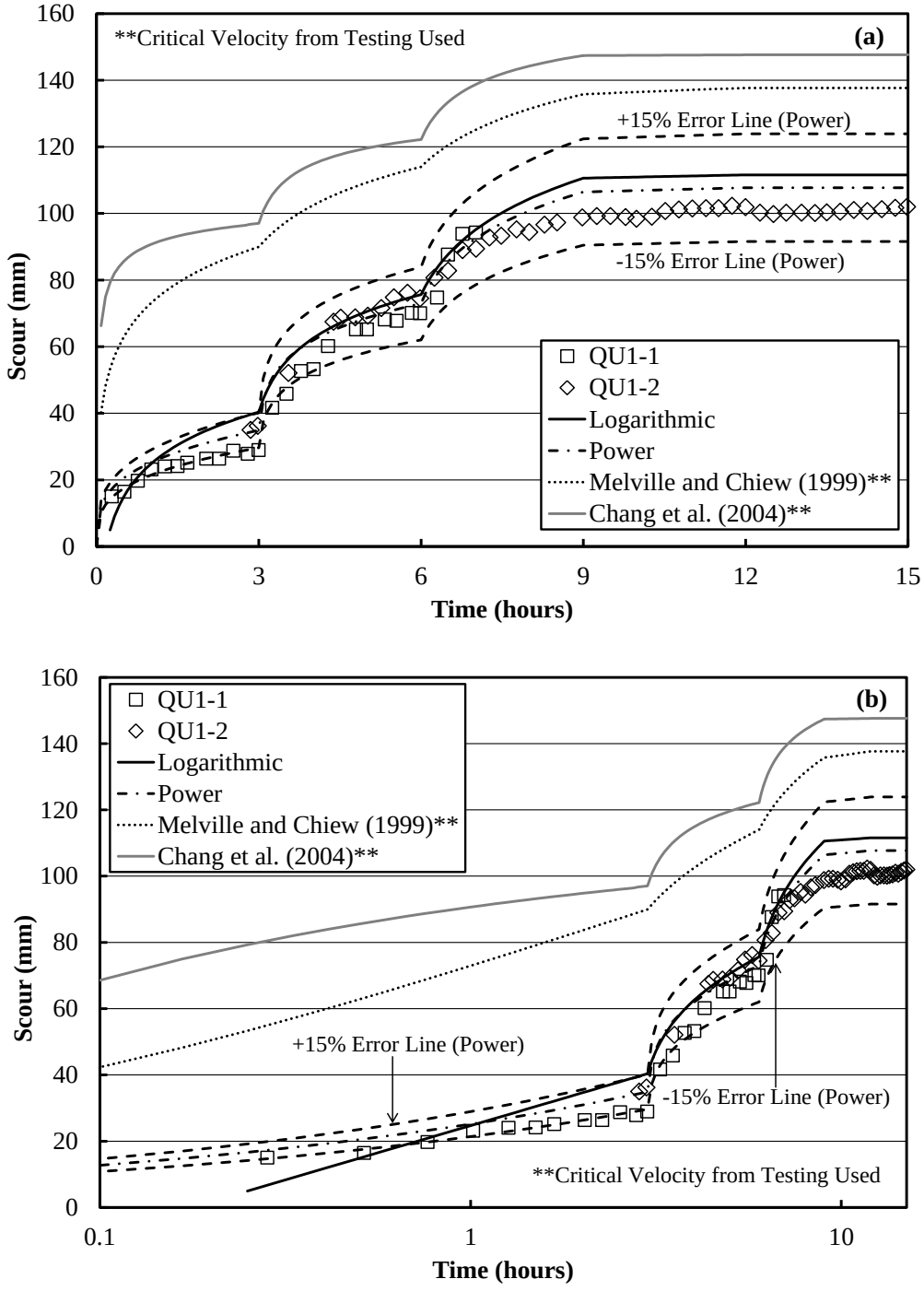

Figure 5.2: Calculated Temporal Scour Evolution, QU1

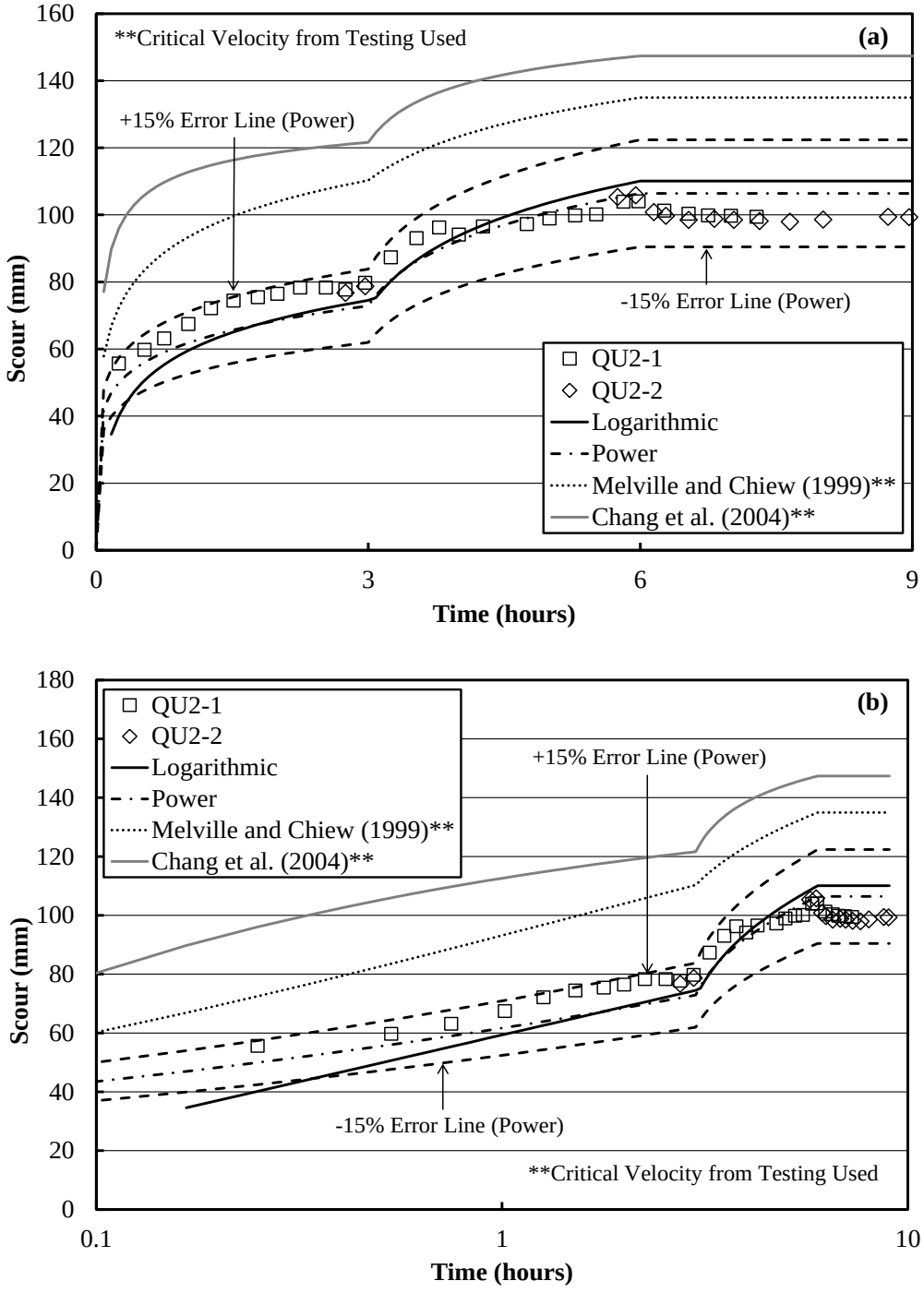

Figure 5.3: Calculated Temporal Scour Evolution, QU2

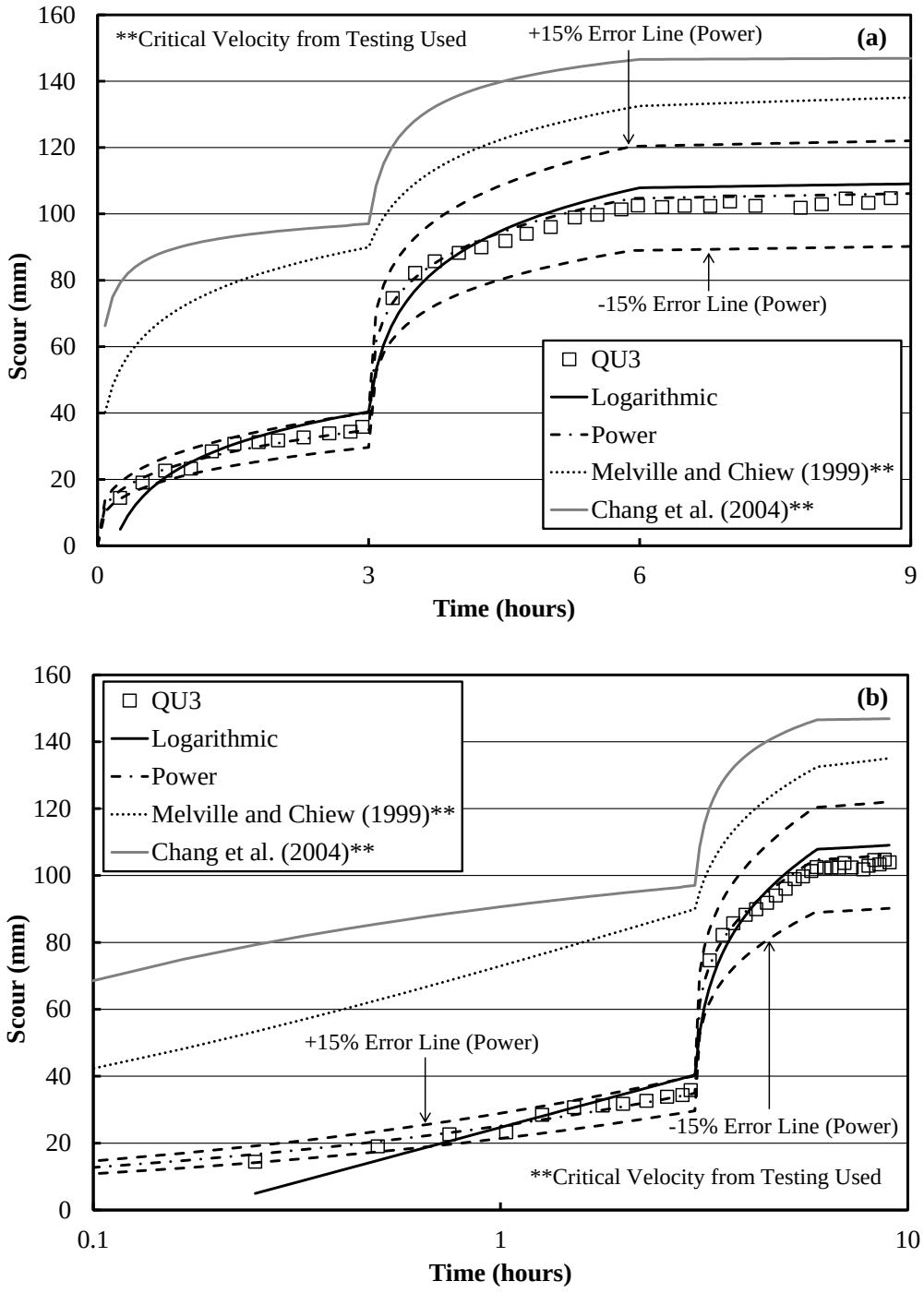

Figure 5.4: Calculated Temporal Scour Evolution, QU3

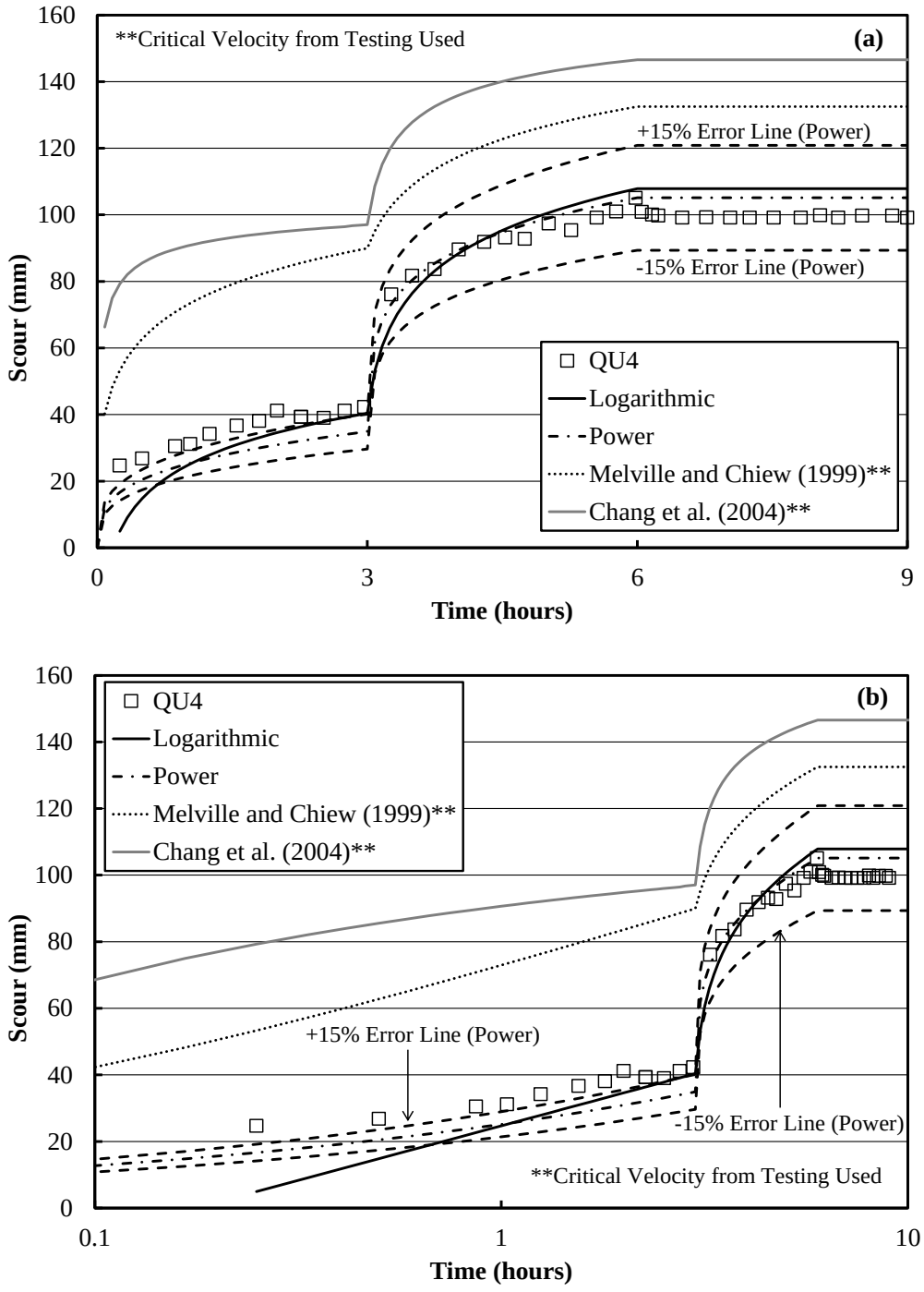

Figure 5.5: Calculated Temporal Scour Evolution, QU4

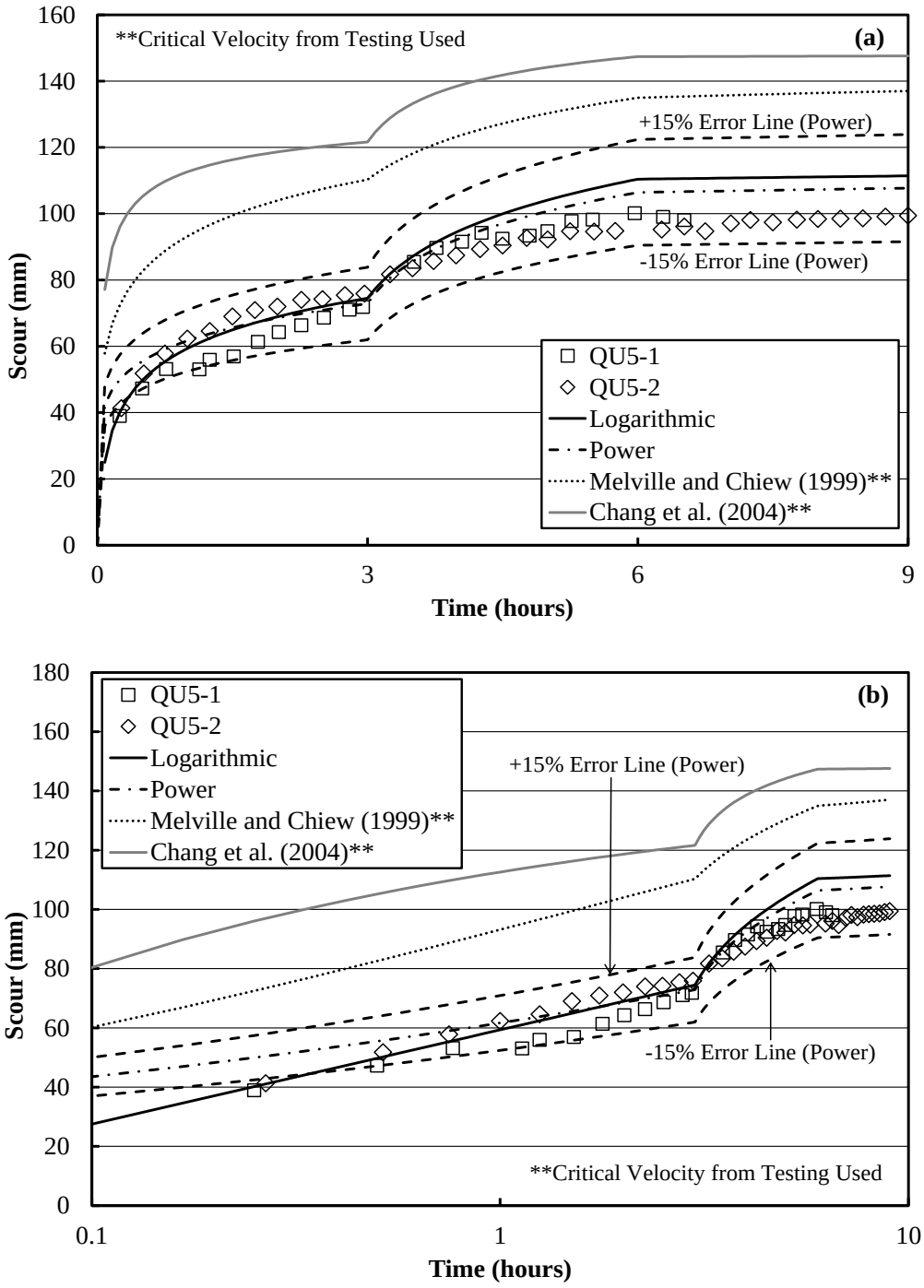

Figure 5.6: Calculated Temporal Scour Evolution, QU5

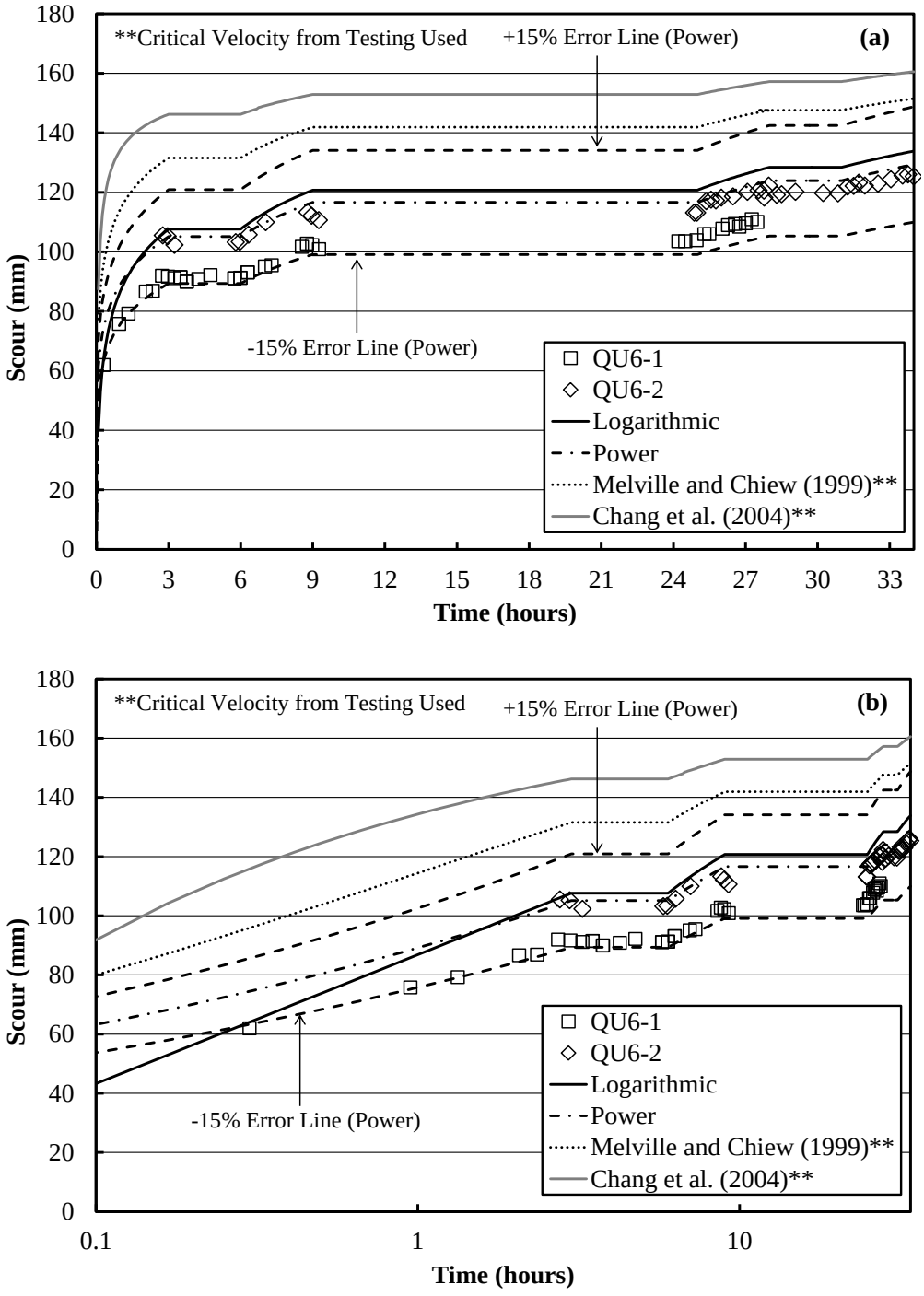

Figure 5.7: Calculated Temporal Scour Evolution, QU6

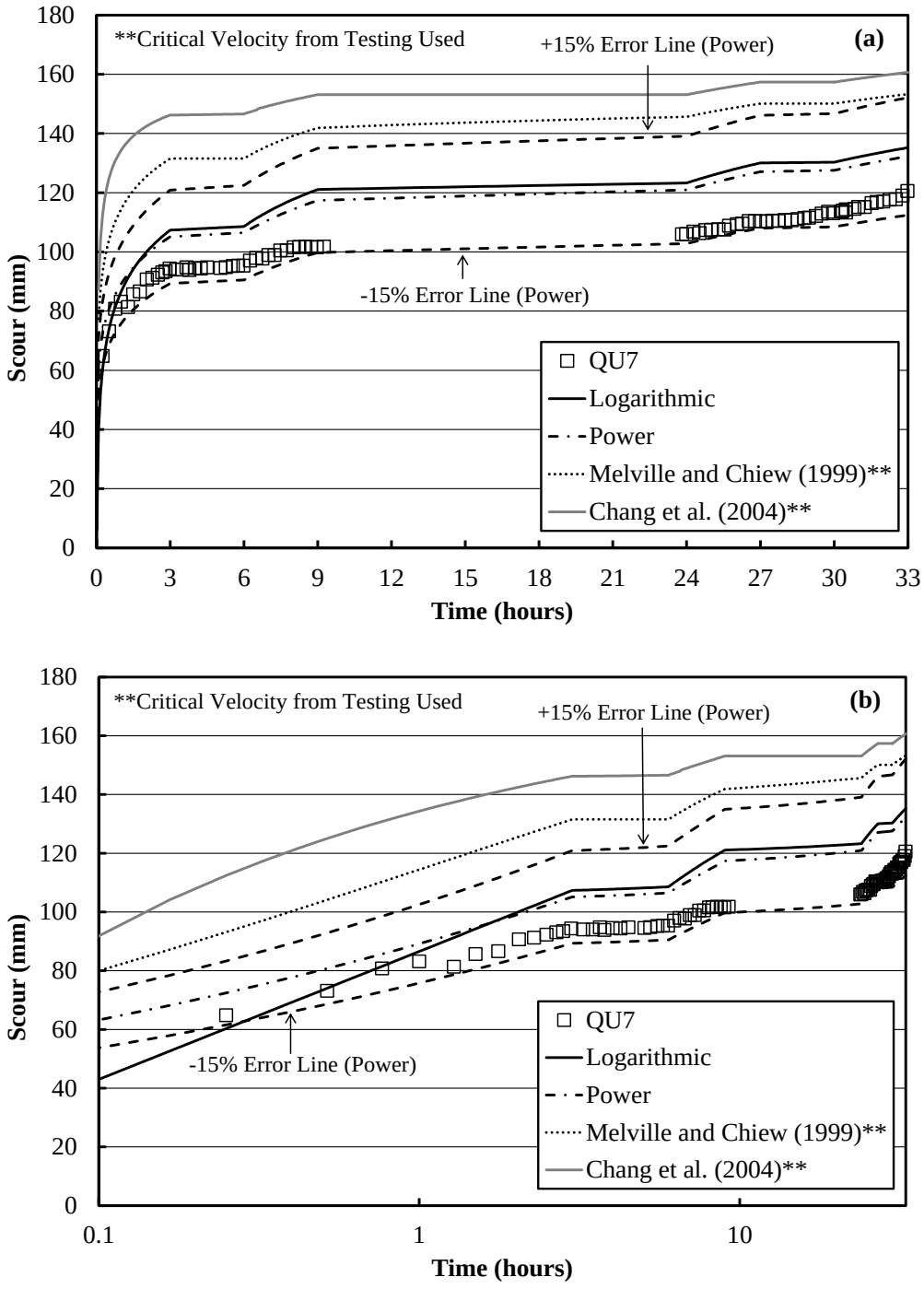

Figure 5.8: Calculated Temporal Scour Evolution, QU7

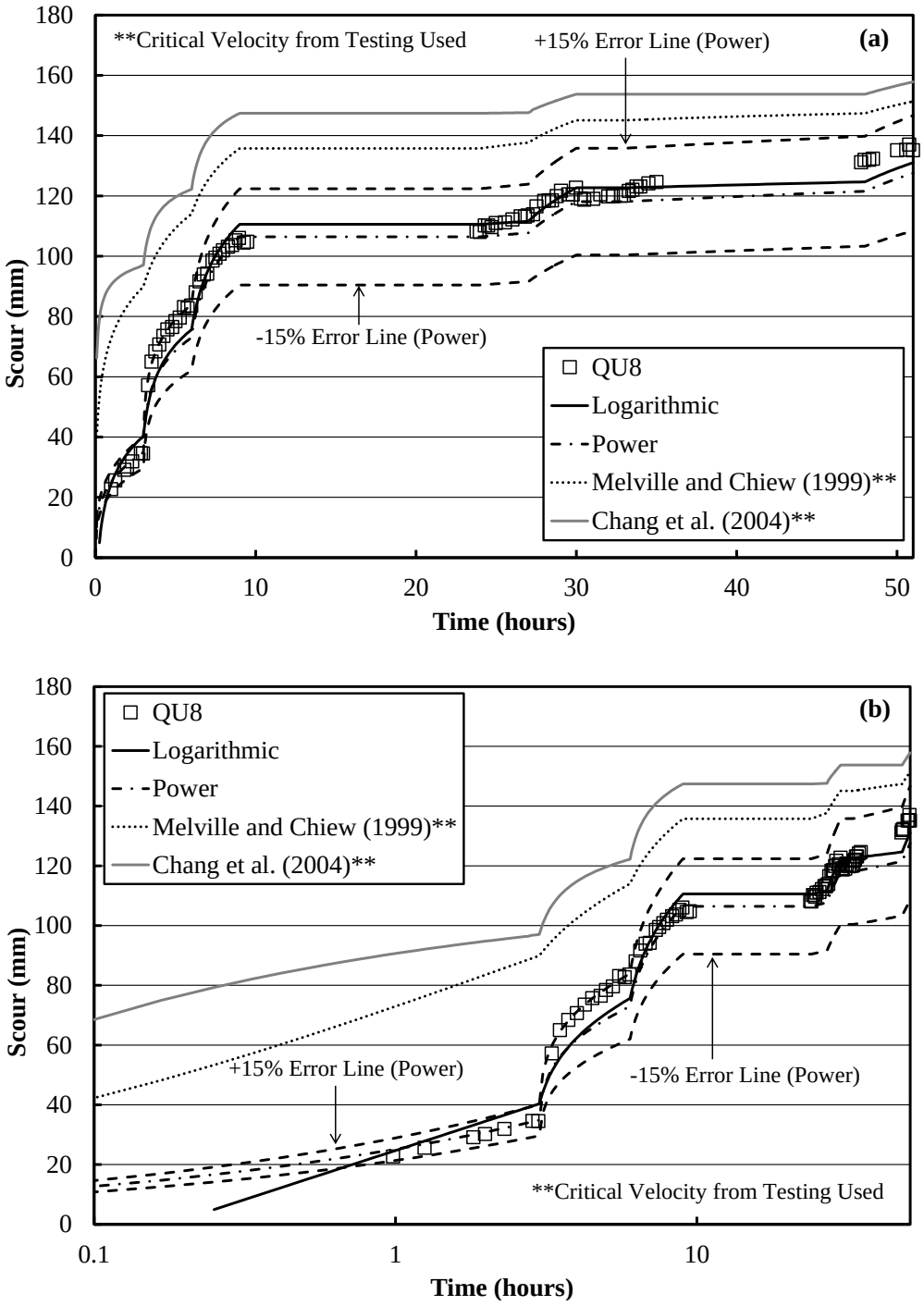

Figure 5.9: Calculated Temporal Scour Evolution, QU8

Scour Hole Similarity under Stepped Hydrographs

During unsteady flow testing, the longitudinal scour hole profile was periodically measured to determine how the shape of the scour hole changed with time and flow history. For steady flows, it was found the non-dimensional scour hole was similar regardless of the flow condition or time (as discussed in Chapter 4). Totapally (1998) measured abutment scour under steady and stepped hydrographs. The author found that the scour hole geometry changed with time and flow conditions, however, the non-dimensional scour hole geometries were similar.

It was determined that the non-dimensional scour hole geometry remained the same regardless of time or flow history. The slope of the scour hole was always approximately 38º. When the hydrograph decreased from a high flow (Q3) to a low flow condition (Q1) and the scour depth was greater than the equilibrium scour depth for the low flow, it was found that the previously suspended sediment within the groove settled on the bed. This decreased the scour depth ($\approx$ 2 to $3d_{50}$) in the groove but the rest of the scour hole retained the same shape. The dimensional and non-dimensional scour hole profiles were plotted at various times for each hydrograph upstream of the pier. The following 16 figures (Figure 5.10 to 5.25) are the longitudinal profiles for each unsteady test. Figure 5.26 compares the non-dimensional scour hole similarity for all eight unsteady tests. This non-dimensional similarity is of importance as it indicates steady state temporal evolution equations can be applied to predict scour depths under stepped hydrographs (as shown previously).

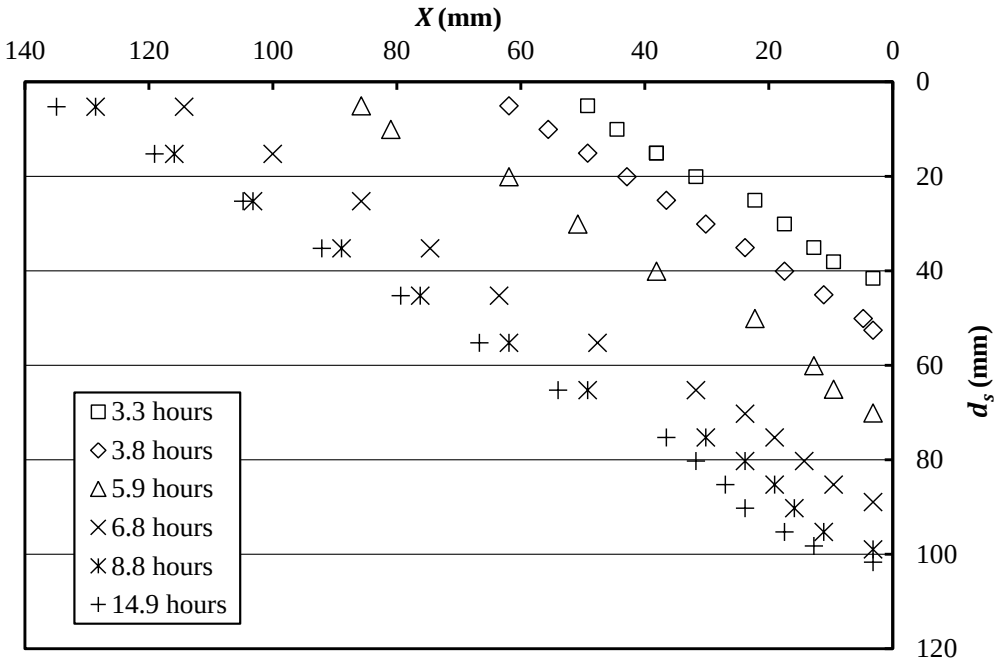

Figure 5.10: Dimensionalized Unsteady Scour Similarity, QU1

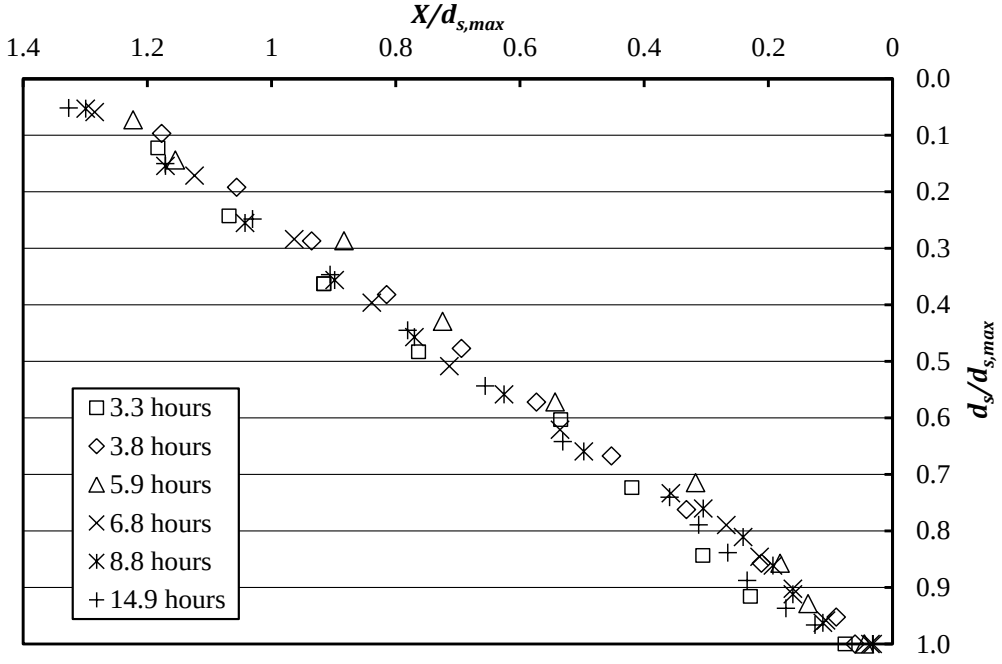

Figure 5.11: Non-Dimensionalized Unsteady Scour Similarity, QU1

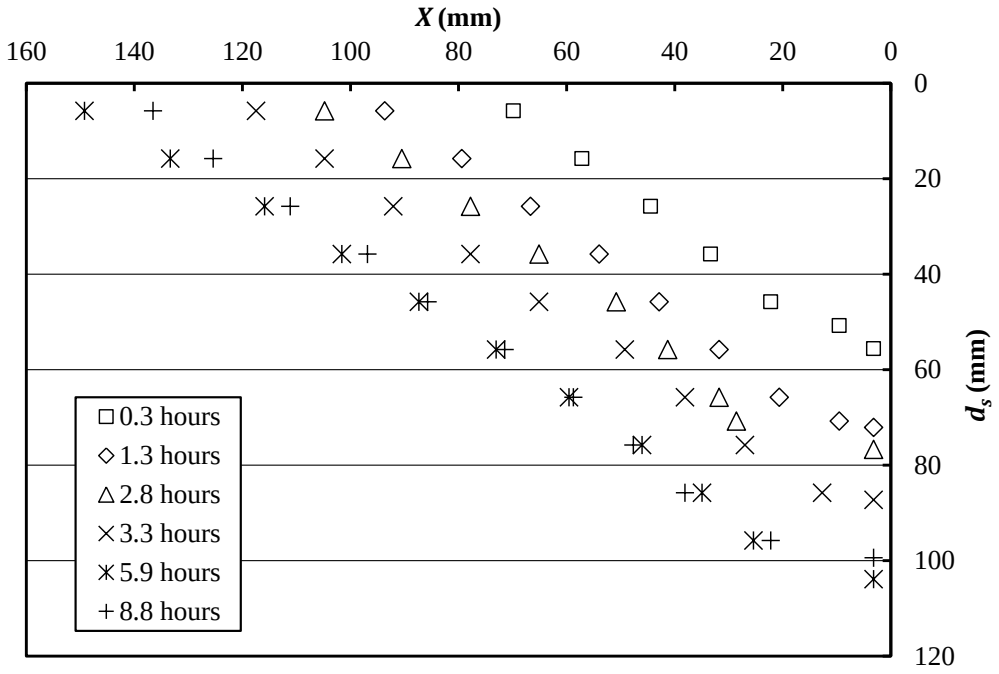

Figure 5.12: Dimensionalized Unsteady Scour Similarity, QU2

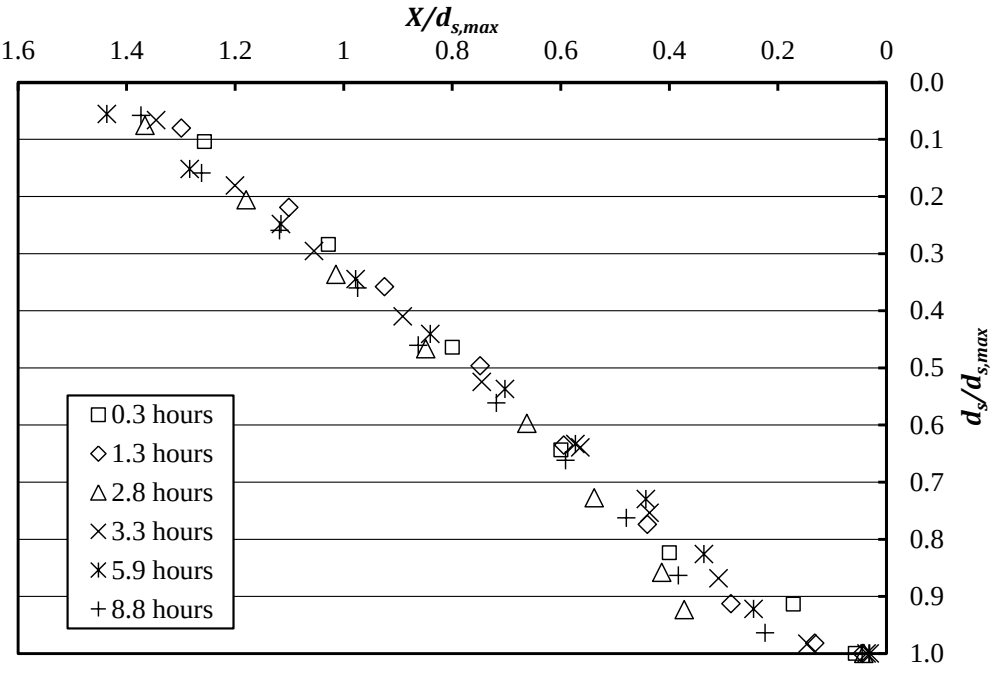

Figure 5.13: Non-Dimensionalized Unsteady Scour Similarity, QU2

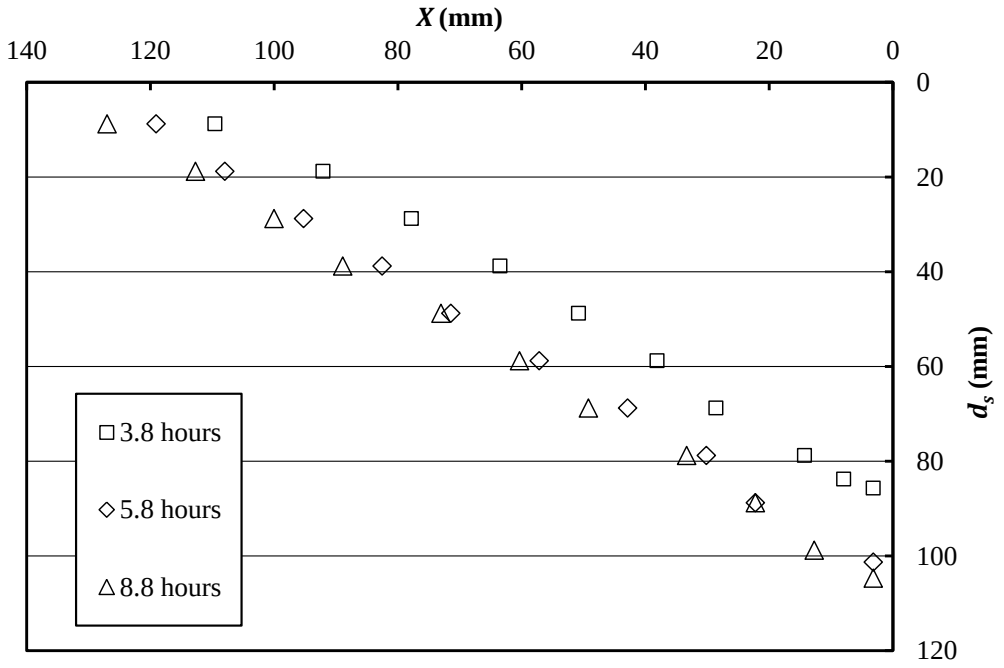

Figure 5.14: Dimensionalized Unsteady Scour Similarity, QU3

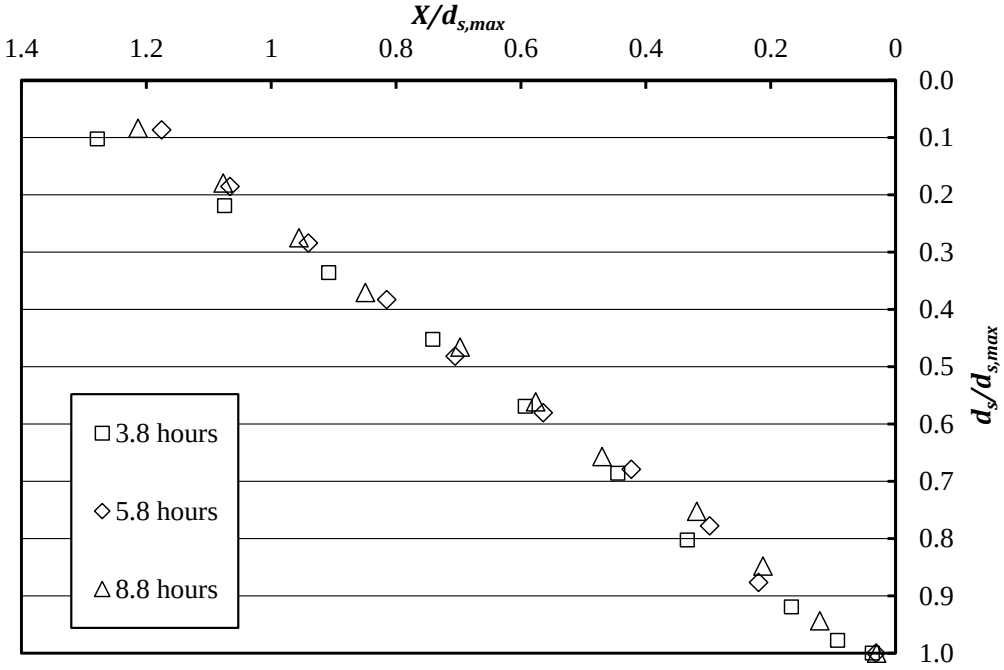

Figure 5.15: Non-Dimensionalized Unsteady Scour Similarity, QU3

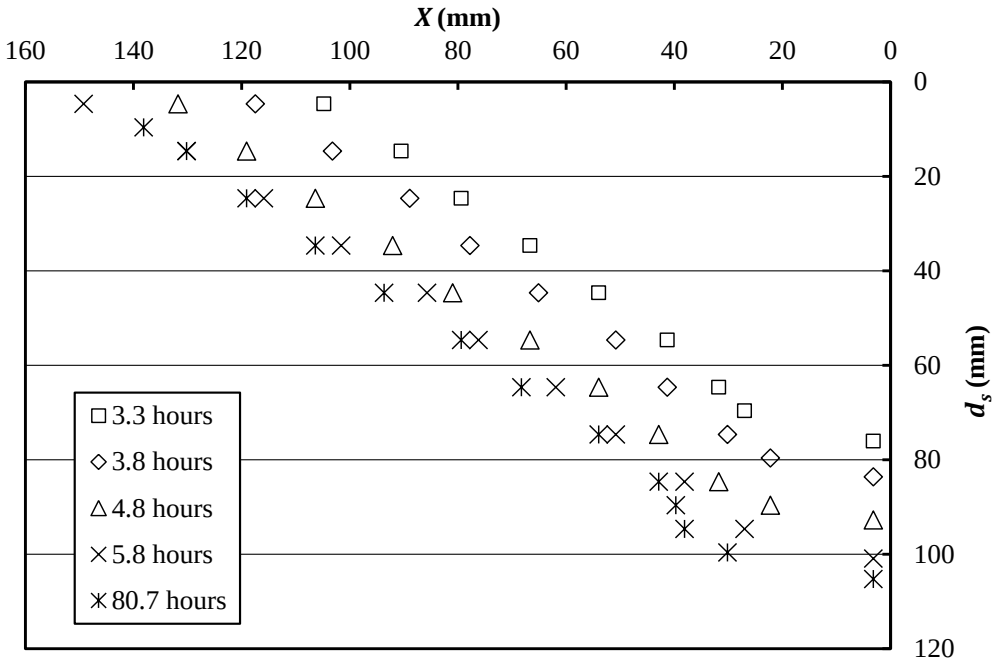

Figure 5.16: Dimensionalized Unsteady Scour Similarity, QU4

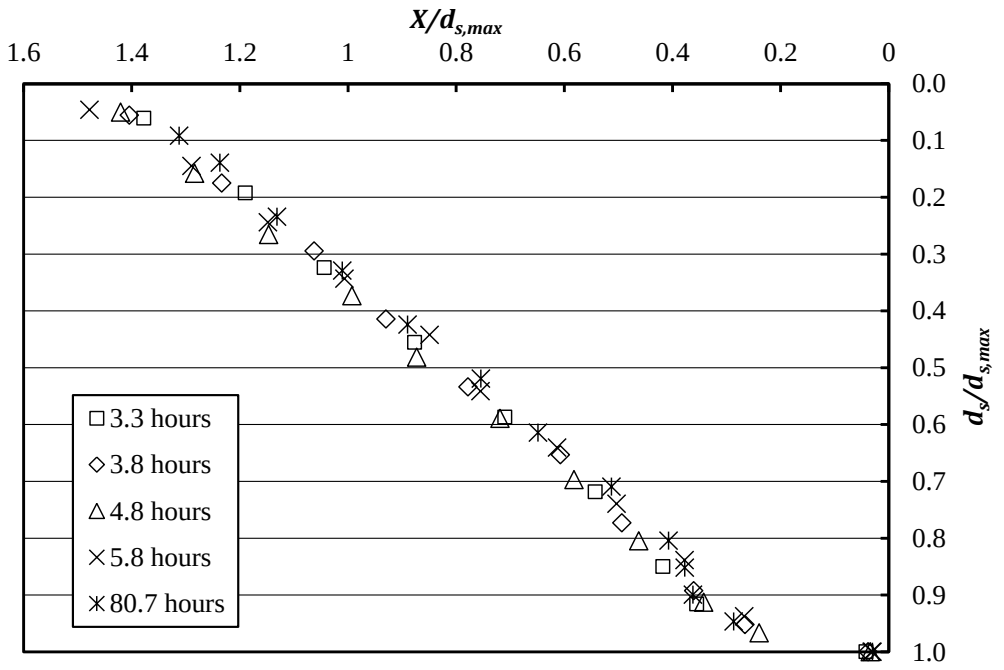

Figure 5.17: Non-Dimensionalized Unsteady Scour Similarity, QU4

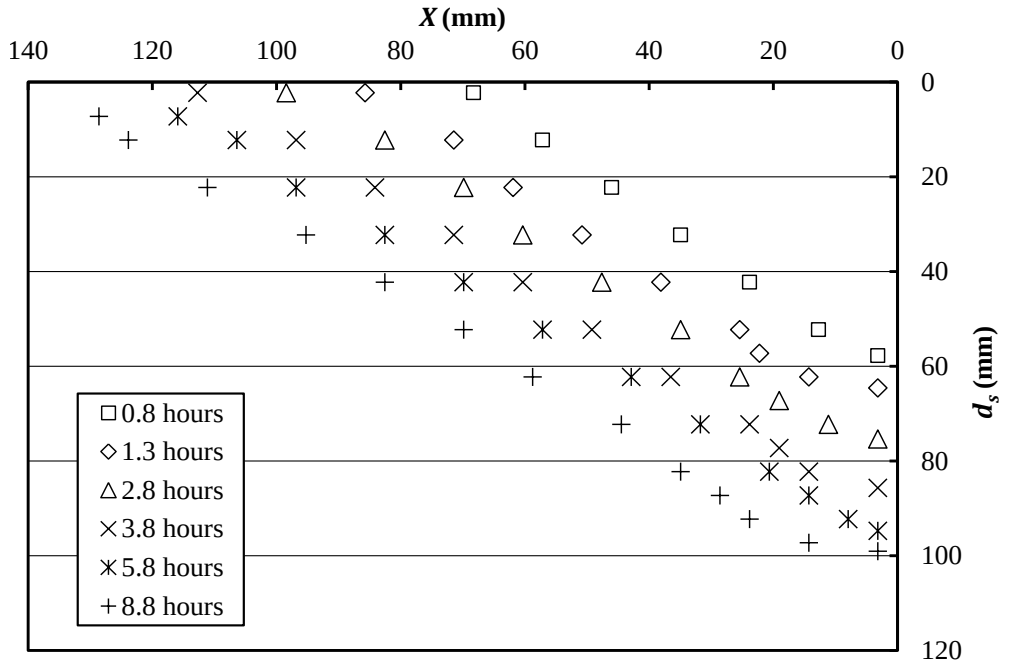

Figure 5.18: Dimensionalized Unsteady Scour Similarity, QU5

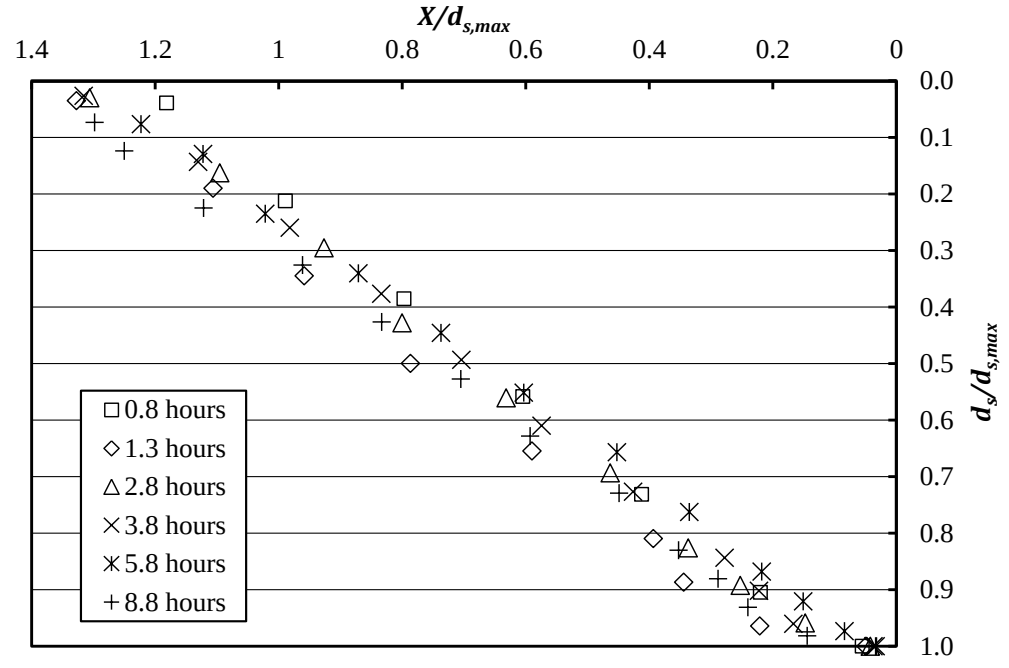

Figure 5.19: Non-Dimensionalized Unsteady Scour Similarity, QU5

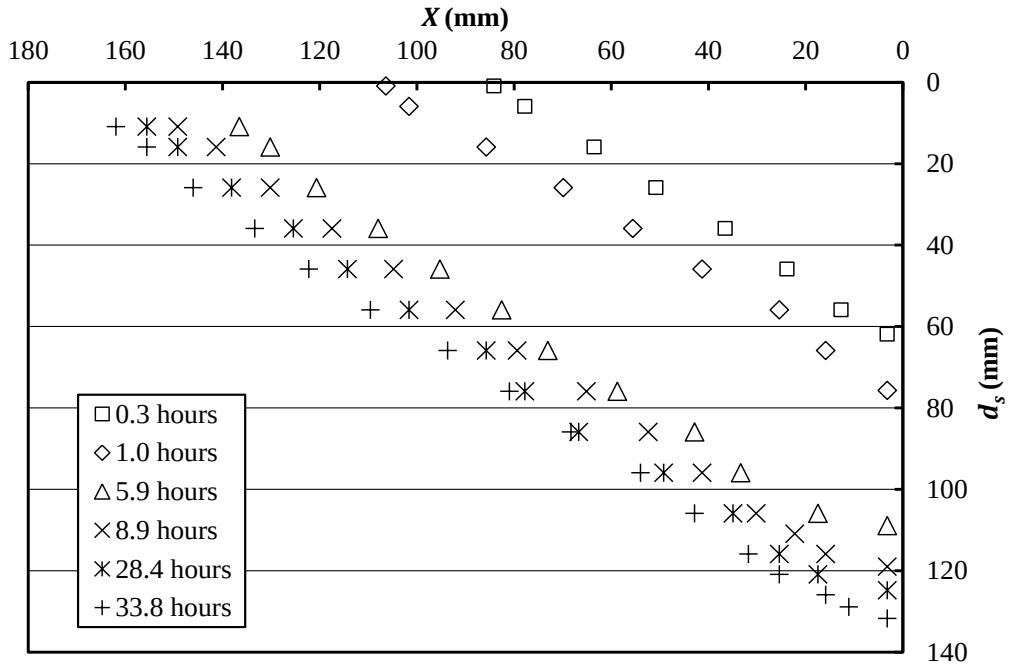

Figure 5.20: Dimensionalized Unsteady Scour Similarity, QU6

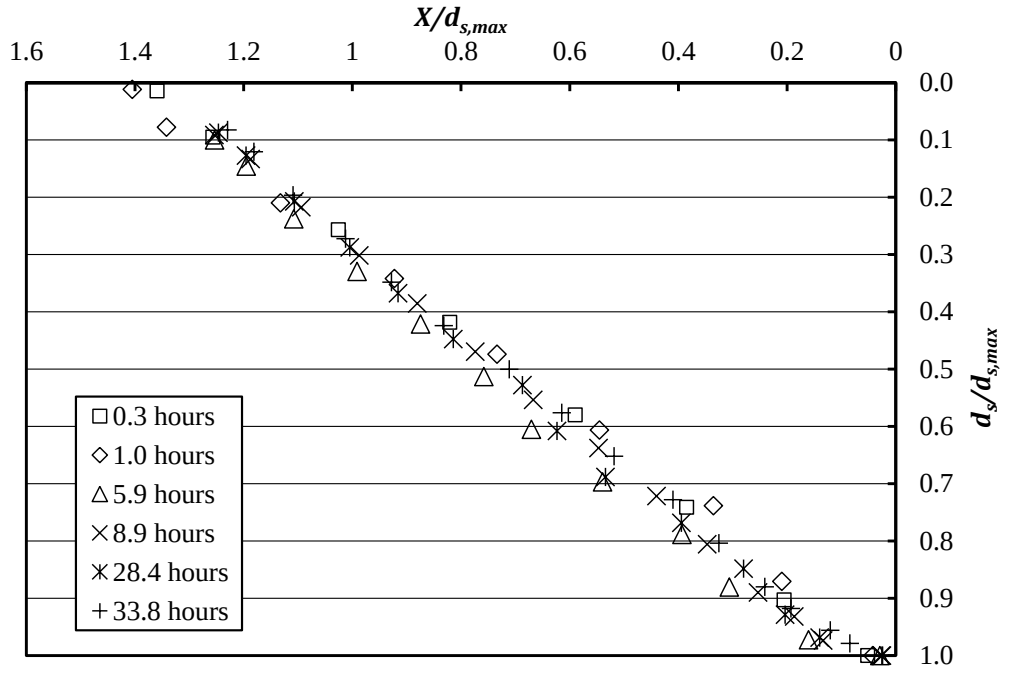

Figure 5.21: Non-Dimensionalized Unsteady Scour Similarity, QU6

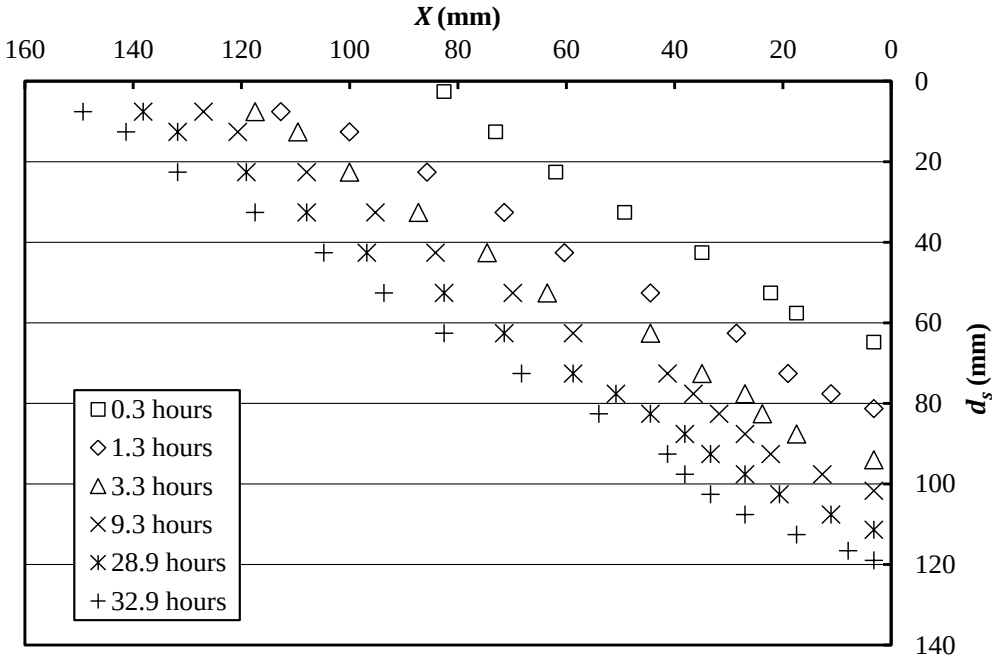

Figure 5.22: Dimensionalized Unsteady Scour Similarity, QU7

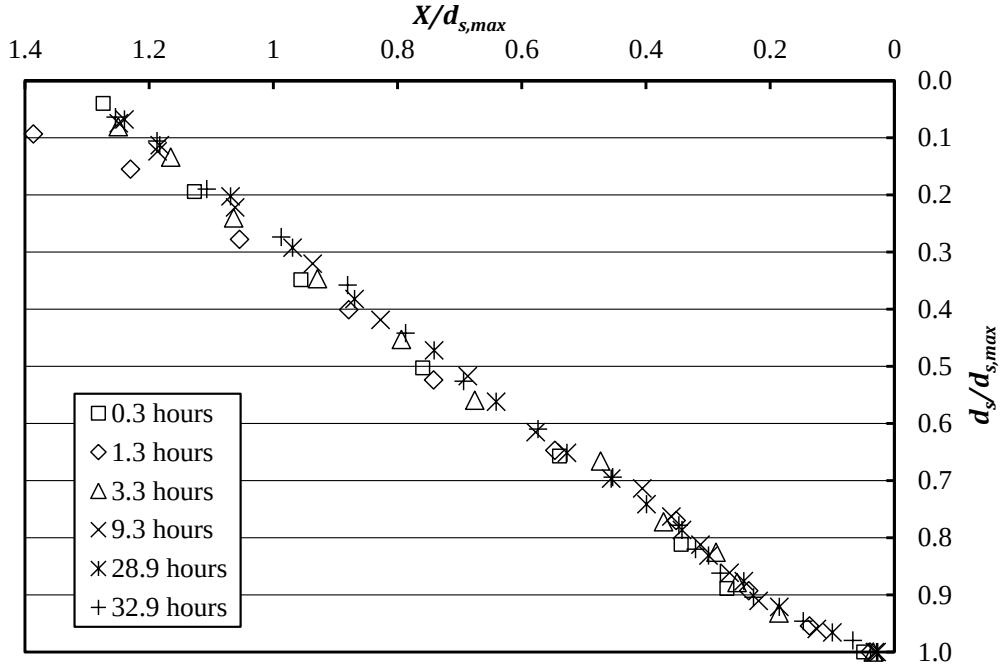

Figure 5.23: Non-Dimensionalized Unsteady Scour Similarity, QU7

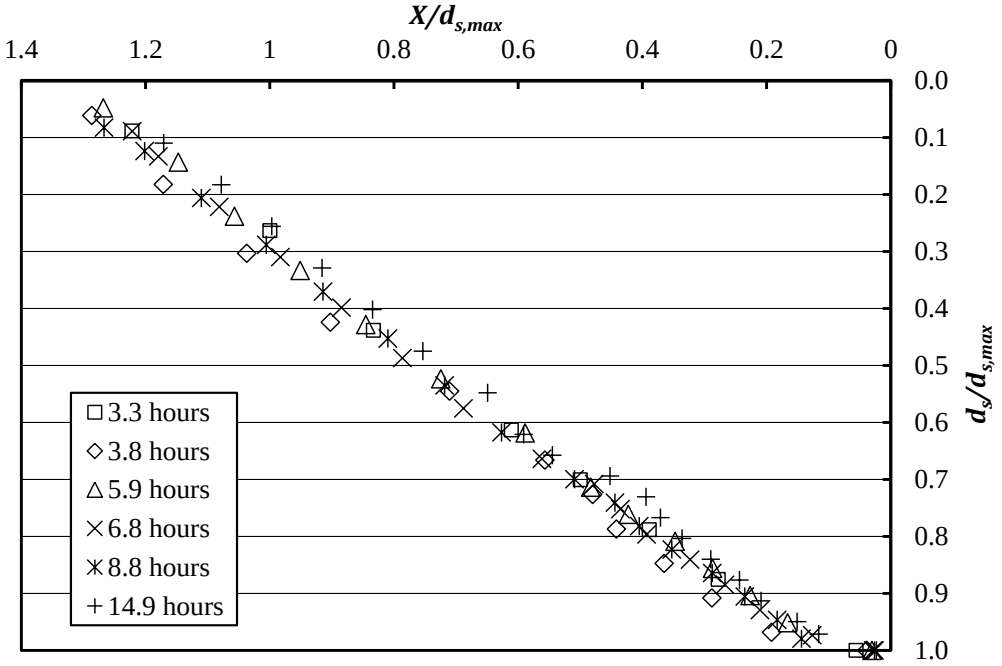

Figure 5.24: Dimensionalized Unsteady Scour Similarity, QU8

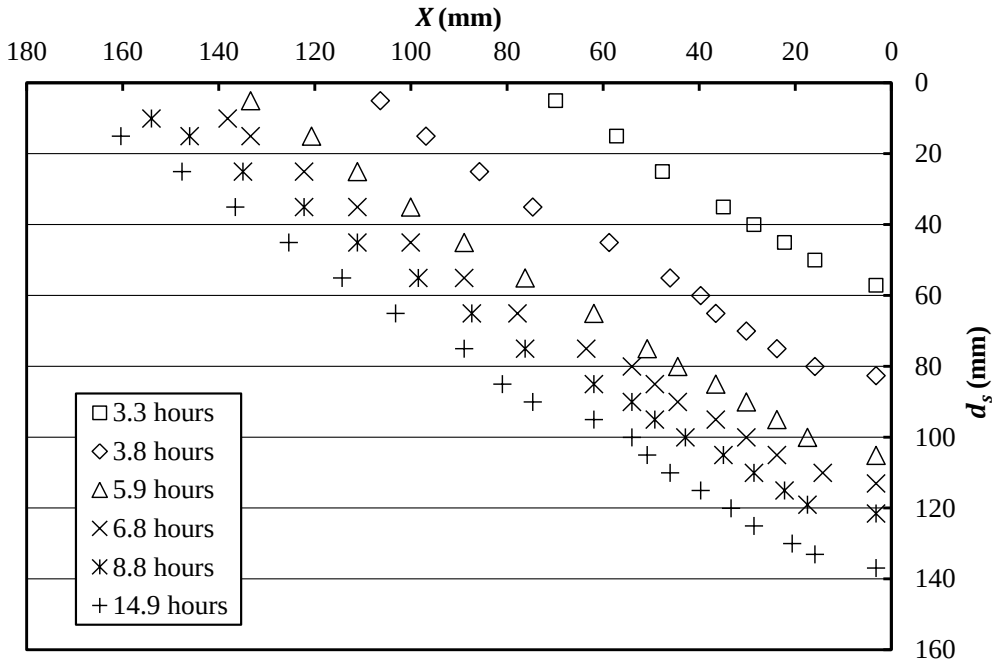

Figure 5.25: Non-Dimensionalized Unsteady Scour Similarity, QU8

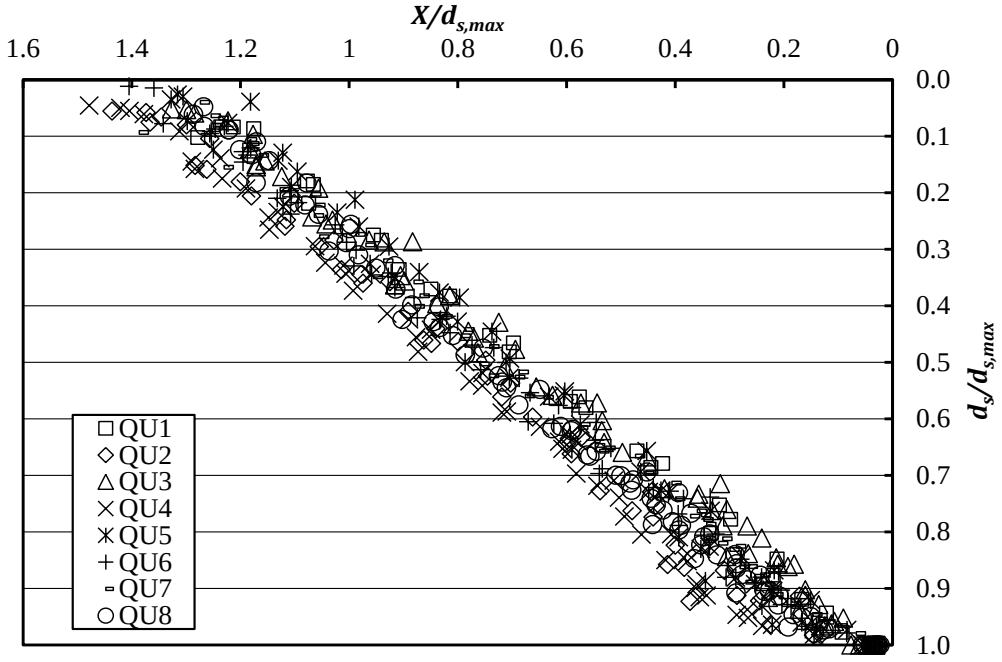

Figure 5.26: Non-Dimensionalized Unsteady Scour Similarity, All Tests

Effect of Flood Event Order

The order of floods events (i.e., 10 yr. flood before 50 yr. or 50 yr. before 10 yr.) was examined in this study. Multiple tests were run to compare how the order of events affected scour hole size and shape. As discussed previously, the non-dimensional scour hole shape remained the same regardless of flow history or time. Table 5.3 compares the first nine hours of various hydrographs (with 3 hour time intervals) to quantitatively show how the flood order affected scour depths.

Table 5.3: Effect of Flood Event Order

	Time (hours)				
	0 to 3	3 to 6	6 to 9	6	9
Test No.	Flow Condition			d_s (mm)	d_s (mm)
QU1	Q1	Q2	Q3	74.5	*98.8*
QU8	Q1	Q2	Q3	83.6	*106.0*
QU2	Q2	Q3	Q1	**105.8**	*99.3*
QU3	Q1	Q3	Q2	102.5	*103.9*
QU4	Q1	Q3	Q1	***105.1***	99.2
QU6	Q3	Q1	Q3	***103.3***	110.6
QU5	Q2	Q3	Q2	**94.8**(1)	99.4
QU7	Q3	Q2	Q3	**95.3**	101.5

Notes:
(1) Measurement taken at 5 hrs. 45 minutes. All other measurements within 5 minutes of stated time

When low flow conditions occurred after high flows, sediment that was previously suspended in the groove settled on the bed. This occurred if the scour depth was greater than the equilibrium scour depth for the low flow condition. The scour depth within the groove only decreased by a few grain sizes ($\approx$ 2 to 3d_{50}) and the rest of the scour hole retained the same size and shape. Non-dimensional scour hole similarity was preserved regardless of the flood order.

CHAPTER 6

CONCLUSIONS AND FUTURE RESEARCH

In this study, the temporal evolution of clear water scour around a circular bridge pier under steady and stepped hydrographs was examined. It was determined that scour hole geometry retained the same shape regardless of flow history or time. This indicated that the best-fit equations from temporal scour evolution data can theoretically be used to model scour under stepped hydrographs. Multiple temporal evolution models and the CSU equation recommended by FHWA (2001) were evaluated and compared. Best-fit power and logarithmic curves from the steady state data were found to accurately predict temporal scour evolution under stepped hydrographs. Recommendations for future research and the conclusions for the steady and unsteady flow conditions are presented below.

Steady Flow

(1) Equilibrium scour depth and scour depth rate increased with flow velocity and bed shear stress.

(2) The temporal evolution of scour depth could best be described as a power equation ($R^2 = 0.99$ to 1.00). Best-fit logarithmic curves ($R^2 = 0.98$) also adequately described the temporal evolution but tended to underestimate scour as time increased for high flow conditions.

(3) The non-dimensional (d_s/d_{se} vs. t/t_e) temporal scour evolution was similar for high flow conditions Q2 and Q3. Flow condition Q1 followed a different trend that was comparable to data from Melville and Chiew (1999) at low V/V_c ratios.

(4) All three runs reached 50% to 80% of equilibrium scour depth during just 10% of the time it took to reach the equilibrium time ($0.1t_e$) as previously documented by Melville and Chiew (1999).

(5) Using the measured critical velocity, methods by Melville and Chiew (1999) and Chang et al. (2004) were the best at predicting temporal scour evolution under steady state flow. Temporal scour methods proposed by Kothyari et al. (1992) and Oliveto and Hager (2002) underestimated scour depths and were found to be less accurate than the CSU equilibrium scour depth equation recommended by the FHWA (2001).

(6) Time to reach equilibrium scour was underestimated by all temporal scour models (Oliveto and Hager, 2002 did not calculate t_e).

(7) The shape of the scour hole was the same regardless of velocity or scour depth. This was indicated by the overlap of all non-dimensional scour hole profiles.

Stepped Hydrographs

(1) Best-fit power and logarithmic equations from steady state tests adequately described the temporal scour evolution under stepped hydrographs using the method of superposition. The final scour depths were predicted within ±10% and ±12% of the measured data for all eight unsteady tests, respectively.

(2) Temporal scour depth models proposed by Melville and Chiew (1999) and Chang et al. (2004) using the measured critical velocity, poorly predicted temporal evolution and final scour depths. The final scour depths were over predicted by an average of 29% and 39%, respectively. These results were slightly less accurate than the CSU equilibrium scour equation (FHWA, 2001), which over predicted final scour depths by an average of 27%.

(3) The scour hole maintained a similar shape regardless of flow history or time as shown by the overlap of all non-dimensional scour hole profiles. However, when the hydrograph decreased from a high flow (Q3) to a low flow condition (Q1) and the scour depth was greater than the equilibrium scour depth for the low flow, it was found that the previously suspended sediment within the groove settled on the bed. This decreased the scour depth minimally ($\approx$ 2 to $3d_{50}$) in the groove but the rest of the scour hole retained the same shape.

(4) Low flow conditions were not able to increase the scour depth after high flows caused greater scour than the equilibrium scour depth of the low flow condition.

(5) Flood order was found to have no substantial effect on scour hole non-dimensional similarity.

Future Research

There are multiple possibilities for extension of the research conducted herein. Since research was only conducted on a single, uniform size sediment, future research should incorporate different sediment sizes. In addition, non-uniform size sediment should be

incorporated in the future research, as natural rivers generally consist of non-uniform sediment. Predicting temporal scour under stepped hydrographs using best-fit steady state scour equations or other models may not be valid if bed armoring occurs. The order of floods and shape of hydrograph may be of more importance as non-uniformity increases.

Scour hole similarity may not be valid if the flow history includes both live-bed and clear water events. No research has yet been conducted on scour under stepped hydrographs with both types of scour. During live-bed scour, the maximum scour depth oscillates around an average depth as material is transported into and out of the scour hole. After a live-bed event, it would be of interest to see if this sediment would be quickly removed from the scour hole by a clear water event.

Due to the relatively limited data on temporal pier scour under stepped hydrographs, future research should incorporate a wider range of parameters (flow depth, velocity ratios, shear velocities, etc.) for clear water or live bed scour. Currently, temporal scour models are not recommended to predict scour in the field and design is still based on single equilibrium scour events. Verification of these models with a wide range of field data has yet to be conducted. Until more temporal unsteady scour data is collected and verified under prototype conditions, scour design will still be based on single equilibrium flood events. These equations do not have a high level of accuracy and are antiquated in the hydraulic engineering community.

REFERENCES

ASCE (2006). "Code of Ethics," Retrieved on July 13th, 2011 from http://www.asce.org/Leadership-and-Management/Ethics/Code-of-Ethics/

Baker, C.J. (1979). "Laminar Horseshoe Vortex," Journal of Fluid Mechanics, Vol. 95, No. 2, 317-367.

Ballio, F. and Orsi, E. (2000). "Time Evolution of Scour Around Bridge Abutments," Water Eng. Res., Vol. 2, No.4, 243-259.

Ballio, F. and Radice, A. (2003). "A Non-Touch Sensor for Local Scour Measurements," Journal of Hydraulic Research, IAHR, Vol. 4, No. 1, 105-108.

Breusers, H.N.C. (1967), "Time Scale of Two-Dimensional Local Scour," Proc. 12th Congress, IAHR, Ft. Collins, Colorado, Vol. 3, 275-282.

Breusers, H.N.C. and Raudkivi, A.J. (1991). "Scouring- Hydraulic Structures Design Manual No. 2," IAHR, A.A. Balkema, Rotterdam/Brookfield.

Brice, J.C. and Blodgett, J.C. (1978). "Countermeasures for Hydraulic Problems at Bridges," Vol. 1 & 2, FHWA/RD-78-162 & 163, Federal Highway Administration, U.S. Department of Transportation, Washington, D.C.

Chabert, J. and Engeldinger, R. (1956). "Etude des Affouillements Autour des Piles de Ponts. Serie A," Laboratoire National d' Hydraulique, 6, Quai Watier, Chatou, France (in French).

Chang, W.Y., Lai, J.S., and Yen, C.L. (2004). "Evolution of Scour Depth at Circular Bridge Piers," Journal of Hydraulic Engineering, ASCE, Vol. 130, No. 9, 905-913.

Cao, Z., Pender, G., and Meng, J. (2006). "Explicit Formulation of the Shields Diagram for Incipient Motion of Sediment," Journal of Hydraulic Engineering, ASCE, Vol. 132, No.10, 1097-1099.

Carstens, M.R. (1966). "Similarity Laws for Localized Scour," Journal of Hydraulics Division, ASCE, Vol. 93, No. 3, 13-36.

Chiew, Y.M. (1995). "Mechanics of Riprap Failure at Bridge Piers," Journal of Hydraulic Engineering, ASCE, Vol. 121, No. 9, 635-643.

Coles, D. (1956). "The Law of the Wake in the Turbulent Boundary Layer," Journal of Fluid Mechanics, Vol. 1, 191-226.

Cunha, L.V. (1975). "Time Evolution of Local Scour." Proc.16th Congress, IAHR, Sao Paulo, Brazil, Vol. 2., 285-299.

Dargahi, B. (1990). "Controlling Mechanism of Local Scouring." Journal of Hydraulic Engineering, ASCE, Vol. 116, No. 10, 1197-1214.

Ettema, R. (1980). "Scour at Bridge Piers," Report No. 216, University of Auckland, School of Engineering, Auckland, New Zealand.

Federal Highway Administration (1993). "Evaluating Scour at Bridges," Hydraulic Engineering Circular No. 18," Publication No. FHWA-IP- 90-017, U.S. Dept. of Transportation, Washington, D.C.

Federal Highway Administration (2001). "Evaluating Scour at Bridges Fourth Edition," Hydraulic Engineering Circular No. 18," Publication No. FHWA-NH-01-001, U.S. Dept. of Transportation, Washington, D.C.

Franzetii, S., Larcan, E., and Mignosa, P. (1982). "Influence of the Test Duration on the Evaluation of Ultimate Scour Around Circular Piers," Proc. Int. Conf. Hydraulics and Modeling of Civil Structures, Coventry, UK, 381-396.

Franzetti, S., Larcan, E., and Mignosa, P. (1989). "Erosione alla base di pile circolari di ponti: Verifica sperimentale dell'ipotes di esistenza di una situazione finale di equilibrio." Idrotecnica, Vol. 16, No.3, 135-141 (in Italian).

Froehlich, D.C. (1989). "Local Scour at Bridge Abutments," Proc. National Conference on Hydraulic Engineering, ASCE, New Orleans, Louisiana, 13-18.

Garde, R.J., Subramanya, A.K., and Nambudripad, K.D. (1961). "Study of Scour Around Spur Dikes," Journal of Hydraulics Division, ASCE, Vol. 87, No. 6., 23-27.

Gee, K.W. (2003). "Action: Compliance with the National Bridge Inspection Standards ;Plan of Action for Scour Critical Bridges," Federal Highway Administration, Washington, D.C., Retrieved on Aug. 5th, 2011 from http://www.fhwa.dot.gov/engineering/hydraulics/policymemo/072403.cfm

Gill, M.A. (1972). "Erosion of Sand Beds Around Spur Dikes," Journal of Hydraulics Division, ASCE, Vol. 98, No. 9, 1587-1602.

Graf, W.H. (1995). "Local Scour Around Piers," Annu. Rep., Laboratoirede Recherches Hydrauliques, Ecole Polytechnique Federale de Lausanne, Switzerland, B.33.1–B.33.8.

Hager, W.H. and Del Giudice, G. (2001). Discussion to "Moveable Bed Roughness in Alluvial Channels," Journal of Hydraulic Engineering, ASCE, Vol. 12, No. 7, 627-628.

Hancu, S. (1971). "Sur le Calcul des Affouillements Locaux dans la Zone des Piles du Pont," Proc. Of 14th Congress, IAHR, No. 3, 299-305 (in French).

Hjorth, P. (1975). "Studies on the Nature of Local Scour." Bulletin Series A, No. 46, Lund Institute of Technology, Lund, Sweden.

Jain, S.C. and Fischer, E.E. (1979). "Scour Around Circular Bridge Piers at High Froude Numbers," Report No. FHWA-RD-79-104, Federal Highway Administration, Washington, D.C.

Johnson, P.A. (1995). "Comparison of Pier-Scour Equations Using Field Data," Journal of Hydraulic Engineering, ASCE, Vol. 121, No. 8, 626-629.

Jones, J.S. and Sheppard, D.M. (2000). "Scour at Wide Bridge Piers." ASCE, US Department of Transportation, Federal Highway Administration, Turner-Fairbanks Highway Research Center, 10 p.

Kohli, A. and Hager, W.H (2001). "Building Scour in Floodplains," Proc. Of the Institution of Civil Engineers – Water and Maritime Engineering, London, UK, Vol. 148, No. 2, 61-80.

Kothyari, U.C. (1989). "Scour Around Bridge Piers," Ph.D. Thesis, University of Roorkee, Roorkee, India.

Kothyari, U.C., Garde, R.J., and Ranga-Raju, K.G. (1992). "Temporal Variation of Scour Around Circular Bridge Piers," Journal of Hydraulic Engineering, ASCE, Vol. 118, No. 8, 1091-1106.

Laursen, E.M. and Toch, A. (1956). "Scour Around Bridge Piers and Abutments." Bulletin No. 4, Iowa Highway Research Board.

Lee, S.O. and Sturm, T.W. (2009). "Effect of Sediment Size Scaling on Physical Modeling of Bridge Pier Scour." Journal of Hydraulic Engineering, ASCE, Vol. 135, No.10, 793-802.

Lu, J., Shi, Z., Hong, J., Lee, J., and Raikar, R.V. (2011). "Temporal Variation of Scour Depth at Nonuniform Cylindrical Piers." Journal of Hydraulic Engineering, ASCE, Vol. 137, No. 1, 45-56.

Melville, B.W. (1975). "Local Scour at Bridge Sites," Report No. 117, University of Auckland, Auckland, New Zealand.

Melville, B.W. (1984). "Live Bed Scour at Bridge Piers." Journal of Hydraulic Engineering, ASCE, Vol. 110, No. 9, 1234-1247.

Melville, B.W. (1997). "Pier and Abutment Scour – Integrated Approach," Journal of Hydraulic Engineering, ASCE, Vol. 123, No. 2, 125-136.

Melville, B.W. and Chiew, Y.M. (1999). "Time Scale for Local Scour at Bridge Piers," Journal of Hydraulic Engineering, ASCE, Vol. 125, No. 1, 59-65.

Melville, B.W. and Sutherland, A.J. (1988). "Design Method for Local Scour at Bridge Piers," Journal of Hydraulic Engineering, ASCE, Vol. 114, No. 10, 1210-1226.

Mia, M.F. and Nago, H. (2003). "Design Method of Time-Dependent Local Scour at Circular Bridge Pier." Journal of Hydraulic Engineering, ASCE, Vol. 129, No. 6, 420-427.

Minnesota Department of Transportation (2008). "Economic Impacts of I-35 W Bridge Collapse," Retrieved July 13th, 2011 from http://www.dot.state.mn.us/i35wbridge/rebuild/municipal-consent/economic-impact.pdf

Morris, J.L. and Pagan-Ortiz, J.E. (1997). "Bridge Scour Evaluation Program in the United States," Proc. 27th Congress, IAHR, San Francisco, California, Vol. 1, 110-116.

Mueller, D.S. (1996). "Local Scour at Bridge Piers in Nonuniform Sediment under Dynamic Conditions," Ph.D. Dissertation, Colorado State University, Fort Collins, Colorado.

Muhamed, T.A., Noor, M.J.M.N., Ghazali, A.H., and Huat, B.B.K. (2005). "Validation of Some Bridge Scour Formulate Using Field and Laboratory Data," American Journal of Environmental Science, Vol. 1, No. 2, 119-125.

Muzzamil, M., Gupta, K., Gangadharaiah, T., and Subramanya, K. (1989), "Vorticity Characteristics of Scouring Horseshoe Vortex," Proc. of 3rd Int. Conference on Alluvial River Problems, Roorkee, India, 14-26.

National Cooperative Highway Research Program (2009). "Monitoring Scour Critical Bridges," NCHRP Synthesis of Highway Practice, Issue 396.

Neill, C.R. (1964). "River Bed Scour, a Review for Bridge Engineers," Contract No. 281, Research Council of Alberta, Calgary, Alberta, Canada.

Nezu, I. and Rodi, W. (1986). "Open-Channel Flow Measurements with a Laser Doppler Anemometer," Journal of Hydraulic Engineering, ASCE, Vol. 112, No. 5, 335-355.

Oliveto, G. and Hager, W.H. (2002). "Temporal Evolution of Clear Water Pier and Abutment Scour," Journal of Hydraulic Engineering, ASCE, Vol. 128, No. 9, 811-820.

Paintal, A.S. (1971). "A Stochastic Model of Bed Load Transport," Journal of Hydraulic Research, IAHR, Vol. 9, No. 4, 527-554.

Rajaratnam, N. and Nwachukwu, B.A. (1983). "Flow Near Groin-like Structures," Journal of Hydraulic Engineering, ASCE, Vol. 109, No. 3, 463-480.

Raudkivi, A.J. and Ettema, R. (1983). "Clear Water Scour at Cylindrical Piers," Journal of Hydraulic Engineering, ASCE, Vol. 109, No. 3, 338-350.

Raudkivi, A.J. (1986). "Functional Trends of Scour at Bridge Piers." Journal of Hydraulic Engineering, ASCE, Vol. 112, No. 1, 1-13.

Rhodes, J. and Trent, R.E. (1993)."Economics of Floods, Scour, and Bridge Failures" *in* Shen, H.W., Su, S.T., and Wen, Feng, eds., Hydraulic Engineering '93, ASCE, New York, 928-933.

Rouse, H. (1965). "Engineering Hydraulics: Sediment Transportation," John Wiley and Sons, New York.

Qadar, A. (1980). "The Vortex Scour Mechanism at Bridge Piers," Ph.D. thesis, Aligarh Muslim University, Aligarh, India.

Shatanawi, K.M., Aziz, N.M., and Khan, A.A. (2008). "Frequency of Discharge Causing Abutment Scour in South Carolina," Journal of Hydraulic Engineering, ASCE, Vol. 134, No. 10, 1507-1512.

Shen, H.W., Schneider, V.R., and Karaki, S.S. (1969). "Local Scour Around Bridge Piers," Journal of Hydraulics Division, ASCE, Vol. 95, No. 6, 1919-1940.

Simmaro, G. ,Teixeira, L., and Cardoso, A.H. (2007). "Flow Intensity Parameter in Pier Scour Experiments," Journal of Hydraulic Engineering, ASCE, Vol. 133, No. 11, 1261-1264.

Totapally, H.G.S. (1998). "Local Scour at Abutments under Simulated Hydrographs," Ph.D. Dissertation, Clemson University, Clemson, South Carolina.

USGS (2011). "Evaluation of Potential Bridge Scour in Missouri," Retrieved on Aug. 12th, 2011 from http://mo.water.usgs.gov/current_studies/Scour/

Yalin, M.S. (1977). "Mechanics of Sediment Transport (2nd Edition)," Pergamon, Oxford, England.

Yanmaz, M. and Altinbilek, D. (1991). "Study of Time Dependent Scour Around Bridge Piers." Journal of Hydraulic Engineering, ASCE, Vol. 117, No. 10, 1247-1268.

Zaghloul, N.A. and McCorquodale, J.A. (1975). "A Stable Numerical Model for Local Scour," Journal of Hydraulic Research, IAHR, Vol. 13, No. 4.

Zaghloul, N.A. (1983). "Local Scour Around Spur Dikes," Journal of Hydrology, ASCE, Vol.60, 123-140.